STATIC AND DYNAMIC ANALYSIS OF PLANE COUPLED SHEAR WALLS

STATIC AND DYNAMIC ANALYSIS OF PLANE COUPLED SHEAR WALLS

By

H. B. CHAN, B. ENG. (CIVIL)

A Thesis

Submitted to the Faculty of Graduate Studies

in Partial Fulfilment of the Requirements

for the Degree

Master of Engineering

McMaster University

April, 1971

MASTER OF ENGINEERING (1971) MCMASTER UNIVERSITY

(Civil Engineering) Hamilton, Ontario

TITLE: Static and Dynamic Analysis of Plane Coupled Shear Walls.

AUTHOR: H.B. Chan, B.Eng. (Civil Engineering), McGill University, Montreal, Canada.

SUPERVISOR: Dr. W. K. Tso.

NUMBER OF PAGES: xii, 144

SCOPE AND CONTENTS:

A general formulation of the analysis of plane coupled shear walls is presented. The "continuous method" of analysis of coupled shear walls is reformulated in terms of deflection variables. The assumption that mid-points of the connecting beams are points of contraflexure is relaxed so that the resulting theory is applicable to the general case where the lateral loading on the piers can be arbitrarily distributed. The governing equation of the structural system under static loading with the appropriate boundary conditions are given. The effect of asymmetry of the structure is discussed. As an application of the derived theory, the problem of shear walls subjected to differential foundation settlement and rotation is studied. Solutions to deflections and internal stresses, under such conditions, are given. Evaluation of the

internal stresses was performed on a practical shear wall structure and the results analysed. Through the use of deflection variables, the formulation is extended into the regime of dynamics. The governing equation of motion with appropriate boundary conditions are given. The free vibration of coupled shear walls is studied and design curves for the fundamental natural frequency are presented. The use of substitutive symmetric systems and its effects on the fundamental frequency of asymmetric systems are examined. Theoretical natural frequencies were verified by dynamic testing on two models to show that the proposed theory is sufficiently accurate to provide information for dynamic analysis in seismic design.

ACKNOWLEDGEMENTS

I am most grateful to Dr. W.K. Tso, my research supervisor, for the inspirations and assistance he rendered in guiding me at every stage of the present work.

I am obliged to Dr. A.C. Heidebrecht, Chairman, for making available to me the departmental teaching assistantship, summer scholarship and the Ontario Graduate Fellowship.

I am very grateful to the National Research Council of Canada for the financial assistance of the present work.

I thankfully acknowledge the use of the Applied Dynamics Laboratory for the experimental work and the assistance offered to me by the technical staff of the laboratory for the same.

I also thank the Computer Centre of McMaster University for making possible the computations involved in this work.

My thanks are due to Mrs. Julie Jarrett who made this thesis presentable.

TABLE OF CONTENTS

LIST OF FIGURES

CHAPTER 1

INTRODUCTION

In modern high-rise structures, commercial and residential, shear wall construction has proven economic value. The high in-plane stiffness of the walls, both external and internal, provides the required stability against lateral forces such as wind or earthquake loading. These walls normally contain a band of regular openings for doors, corridors and windows. Such a structural form is referred to as a coupled shear wall. A planar coupled shear wall may be defined as a structural system composed of shear walls interconnected by a series of spandrel beams, all in the same plane.

A review of previous research in shear wall structures has been done by Coull and Stafford Smith (1). A comprehensive account of the methods of analysis of laterally loaded shear walls is given by MacLeod (2). In this study, discussion shall be confined to the analysis of planar coupled shear walls by the 'equivalent continuous system of laminas' method (henceforth, it shall be referred to as the 'continuous' method).

In this approach, the discrete connecting beams between the piers of the coupled shear wall is replaced by an equivalent continuous medium. This medium can be taken

as consisting of a continuous distribution of small laminas, of infinitesimal thickness dx, capable of independent action and rigidly connected to the piers. By assuming that the connecting beams have a point of contraflexure at midspan, and do not deflect axially, the behaviour of the structure may be expressed in terms of the shear forces at the points of contraflexure along the height of the building.

This formulation was first applied to the analysis of coupled shear walls by Chitty (3) in analysing a cantilever composed of a number of parallel beams interconnected by cross bars. Beck (4) extended the analysis to take into account the pier deformations due to normal forces. The case of coupled symmetric shear walls on rigid foundations, subjected to uniform lateral loading was treated. Rosman (5) further extended the analysis to arrive at solutions for a system with two symmetric bands of openings and various foundation conditions. The case of a concentrated load acting at the top of the wall was studied. Burns (6) studied the case of a triangularly distributed load (such as those specified in many seismic codes) and provided charts for the determination of stresses and maximum deflections. His results also include the effects of parabolically varying pier and beam stiffnesses. Similar charts were also given by Beck (4) (for the case of uniform lateral load). A coupled symmetric

shear wall of variable cross-section, subjected to uniform lateral load, was analysed by Traum (7). Experimental verification of the 'continuous' method of analysis of coupled shear walls was given by Barnard and Schwaighofer (8). To reduce the amount of computations involved in the solution of the governing second-order differential equation, Barnard and Schwaighofer (8) have proposed a simplification of Rosman's theory: using a combination of a straight line and a parabola to approximate the true shear force distribution in the connecting beams. Applying Rosman's theory, Coull and Choudhury (9) (10) presented charts for the evaluation of stresses and maximum deflections for general coupled shear walls subjected to uniform lateral load, triangularly distributed lateral load and a point load at the top. Coull and Puri (11) further developed the 'continuous' method to include shear deformation of piers in the analysis of coupled shear walls. The assumption of constant ratio of shear forces in the piers throughout the height of the building was made. The influence of flexibility of wall-beam connection was also considered, employing Michael's (12) suggestion of equivalent beam length. Michael (12) has shown that the flexibility of the joint may be taken into account of approximately by assuming an effective length of beam to be the clear span plus the depth of the beam. To investigate the relative magnitudes of the influences of shear deformation

and joint flexibility, experiments were performed on models with a single band and double symmetric bands of openings. Coull and Puri have concluded that shear deformation of piers has little effect on stresses and deflections; whereas the flexibility of wall-beam connection has a more significant effect. In his investigation of damaged buildings in the Alaskan Earthquake, Jennings (13) has shown that the damage pattern observed in the spandrel beams is consistent with the dynamic response (approximated by the static response under uniform or triangular loading) of a coupled shear wall vibrating in the fundamental mode.

In all the above analyses, only static loading is considered and the assumption of points of contraflexure at the midspan of connecting beams is specified. In Japan, researchers have carried out the dynamic analysis of core-wall buildings. They are concerned with the vibration of the coupled frame and shear wall system. Using the same 'continuous' method, Osawa (14) has presented a dynamic analysis of this type of building, neglecting the shear deformation of the core-wall and the axial deformation of exterior columns. Tani et al (15) continued the study by making no assumption about the contraflexure points of the exterior columns or beams and by including the two types of deformation. A linear ordinary second-order differential equation was derived

with the distributive moment of the beams as the redundant function. Influences of the shear deformation of the core-wall and of the axial deformation of exterior columns were discussed. Design charts for stresses and deflections were prepared in the static analysis. Natural frequencies and mode shapes were presented in the dynamic analysis by means of examples.

Recently, Tso (16) dismissed the assumption of contraflexure points at the midspan of the connecting beams and analysed a symmetric coupled shear wall using the deflections of the two piers as redundant functions. Through a linear transformation of the deflections, the governing equation of the structural system can then be expressed as a pair of linear ordinary fourth-order uncoupled differential equations in terms of the symmetric and antisymmetric modes of deformation. Analysing an example of a symmetric coupled shear wall laterally loaded at the top by two concentrated loads, Tso has concluded that the previous work by Beck and Rosman essentially neglected the symmetric mode of deformation which might be significant near the top of the piers. His results also show that in as far as the shear distribution along the mid-points of the laminas is concerned, Rosman's expression is valid even without the assumption of contraflexure points. An extension of the analysis to shear walls of unequal piers is given by Tso and Chan (17).

Most lateral loads a building is subjected to are dynamic in nature. Wind loading and seismic loading are typical examples. To investigate the response of a coupled shear wall under such dynamic excitation, knowledge about the dynamic characteristics of the coupled shear wall system becomes essential. Hence it will be useful to derive a general formulation of the analysis of coupled shear walls: a formulation which will lend itself easily to the study of dynamics. Such is the purpose of this study. By adapting Tso's approach to general coupled shear walls and subsequently formulating the problem under dynamic loading conditions, this work also serves to assess the accuracy of the previous analysis (with the assumption of contraflexure points) and to put the 'continuous' approach of analysing coupled shear walls in a firm foundation.

The present work consists of three parts. The first part deals with the formulation of general coupled shear walls under static loading. It includes a discussion on the effect of asymmetry, followed by an evaluation of the stresses of a symmetric wall subjected to differential foundation settlement and rotation. The second part deals with the formulation of general coupled shear walls under dynamic loading, followed by a study of the free vibration aspect. Curves for the fundamental frequency, with due consideration for practical dimensions of the

structural system, are presented in terms of non-dimensional quantities to facilitate design computations. The effect on the fundamental frequency, by averaging the properties of the two piers to arrive at a substitutive symmetric system, is examined. Finally, dynamic tests were performed on a symmetric and an asymmetric model to verify the theory.

CHAPTER 2

ANALYSIS OF PLANE COUPLED SHEAR WALLS UNDER STATIC LOADING

2.1 Introduction

In this chapter, the analysis of coupled shear walls under static external loading is presented. The method of replacing the discrete connecting beams by an equivalent continuous system of laminas is employed. Points of contraflexure at the mid-points of the laminas are not assumed and the deflections of the piers are chosen as redundant functions. The formulation of the governing differential equation and boundary conditions is given in Section 2.2. The governing equation takes the form of a pair of linear ordinary fourth-order coupled differential equations. In Section 2.3, through a linear transformation, the formulation is expressed in terms of the symmetric and antisymmetric modes of deformation. It is shown that the pier deflections are not identical even if the external loading on the piers is proportional to the pier stiffness. In Section 2.4, by reducing the general formulation to the case of a symmetric wall, it is possible to assess the previous work by Beck (4) and Rosman (5) and to establish the circumstances under which the assumption of contraflexure points is justified. The coupling action between the symmetric and antisymmetric modes of deflection is studied in Section 2.5.

Finally, in Section 2.6, the formulation is applied to the problem of differential foundation settlement and rotation for the case of a symmetric coupled shear wall. The governing differential equations remain unchanged but the boundary conditions have to be reformulated. Using a shear wall model without external loading, the internal forces in non-dimensional form are evaluated and presented in graphical form. It is shown that the symmetric mode is not a function of foundation settlement. However, it is significant near the bottom of the structure when rotation of the foundation occurs.

2.2 Derivation of Governing Equation

Ccnsider a general coupled shear wall consisting of two piers connected by beams as shown in Figure 1a. It is assumed that the properties of the walls and beams remain constant throughout the height of the wall. The top and bottom connecting beams are assumed to have a second moment of area and cross-sectional area equal to half of those of the intermediate beams.

The left and right piers are subjected to lateral load distributions $w_1(x)$ and $w_2(x)$ respectively. The bending moments caused by the lateral loadings $w_1(x)$ and $w_2(x)$ are taken to be $M_1(x)$ and $M_2(x)$ respectively. The piers are assumed to be rigidly connected to the foundation.

To analyse such a system, the physical model in Figure 1a is replaced by its equivalent model in Figure 1b. In the equivalent model, the discrete connecting beams are replaced by a continuous distribution of independently acting laminas, rigidly attached to the piers. The laminas have thickness dx, moment of inertia $(I_b dx)/h$ and cross-sectional area $(A_b dx)/h$, where I_b and A_b are the respective properties for the connecting beam.

An imaginary cut is made along the mid-points of the laminas. Unlike the previous analysis of coupled shear walls, the mid-points are not considered as points of

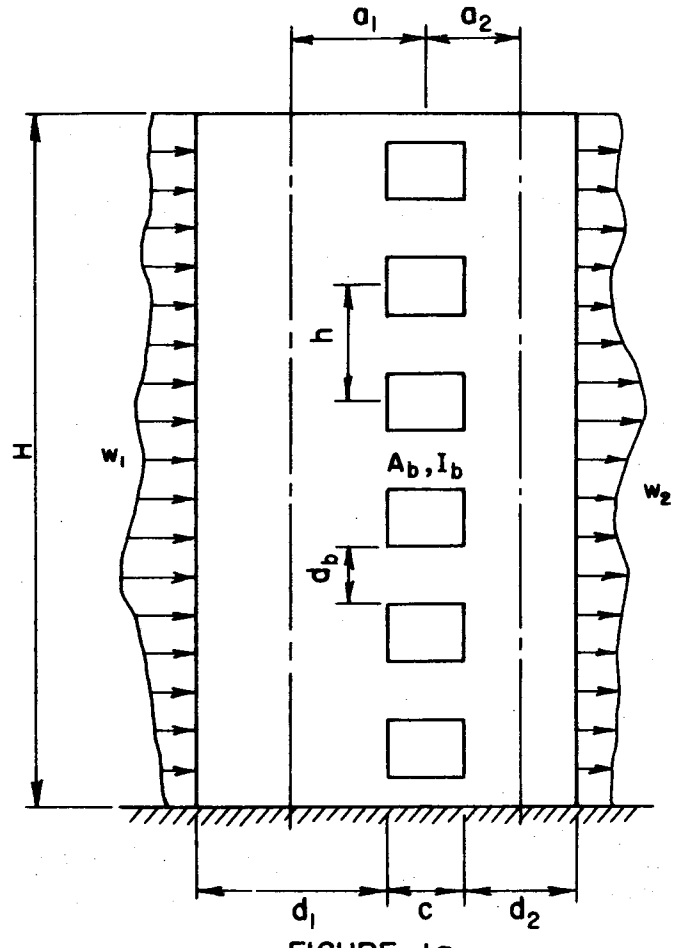

FIGURE 1a

CONFIGURATION OF COUPLED SHEAR WALL

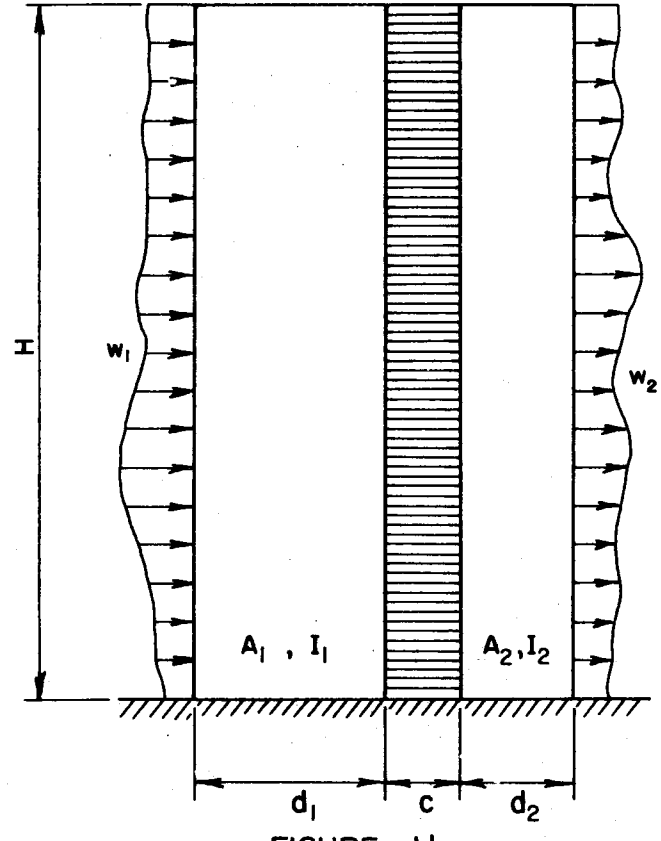

FIGURE 1b

CONFIGURATION OF EQUIVALENT SYSTEM

contraflexure. In making the assumption that mid-points of the connecting beams are points of contraflexure, it is generally taken that the lateral loading on the two piers be distributed in proportion to their respective stiffnesses. Such loading conditions are rarely met in practice. For example, in the case of wind loading, the pressure distribution differs on the windward side and the leeward side. For seismic loading considerations, the inertial loading on the piers is proportional to the respective widths. Since the stiffness of the pier is proportional to the third power of its width, the assumption of lateral load carried by the piers proportional to their respective stiffnesses is not applicable for plane coupled asymmetric shear walls. Even when such an assumption is made, the deflections of the two piers need not be the same because of their coupling action. While one may argue that the difference of the deflections would be sufficiently small to be negligible in many cases, one will not be able to determine the magnitudes of the axial force and moment in the connecting beams which may be significant.

Therefore, along the cut, there is a distribution of bending moment $m(x)$ and axial force $n(x)$ in addition to the shear distribution $q(x)$. This internal force distribution is shown in Figure 2. Since the deflections of the piers are in general different, there results in five unknowns in the problem; namely; (i) the deflection

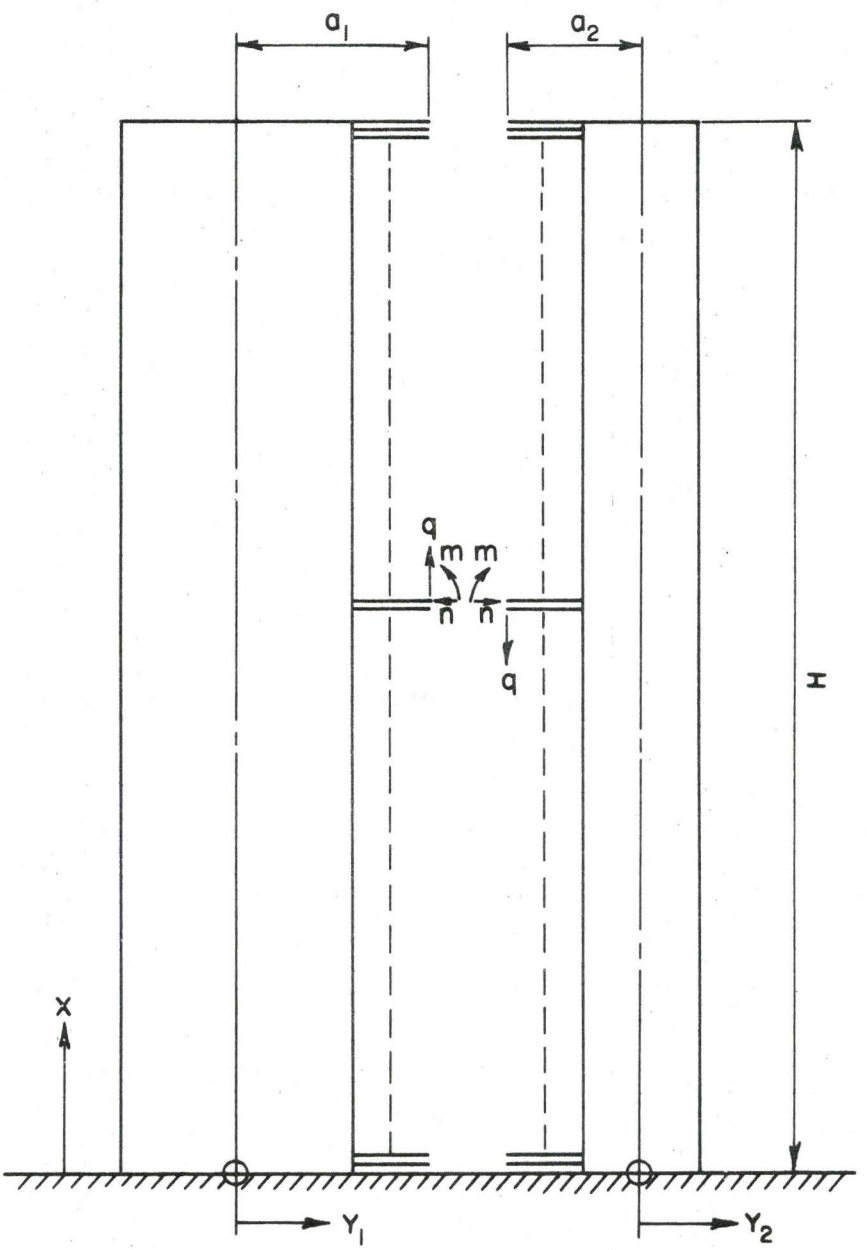

FIGURE 2

INTERNAL FORCE DISTRIBUTION ALONG MID-POINTS OF LAMINAS

of the left pier $y_1(x)$, (ii) the deflection of the right pier $y_2(x)$, (iii) the shear distribution $q(x)$, (iv) the moment distribution $m(x)$ and (v) the axial force distribution $n(x)$.

The first equation relating the five unknown variables can be obtained from the displacement compatibility condition along the imaginary cut. Figure 3 shows the relative vertical displacements at the section along the cut.

Due to bending of the piers, the relative displacement $\delta_1(x)$ is given by

$$\delta_1(x) = a_1\frac{dy_1}{dx} + a_2\frac{dy_2}{dx} \qquad (2.1)$$

where a_1 and a_2 are distances from the imaginary cut to the centroidal axes of pier 1 and pier 2 respectively.

The shear qdx acting at the mid-point of each lamina (having equivalent moment of inertia $(I_b dx)/h$ and equivalent cross-sectional area $(A_b dx)/h$) will cause a relative displacement $\delta_2(x)$ due to bending of the lamina

$$\delta_2(x) = \frac{-qhc^3}{12EI_b} \qquad (2.2)$$

where h denotes the storey height

c denotes the clear span of the connecting beam

E denotes the elastic modulus of the material of the shear wall system

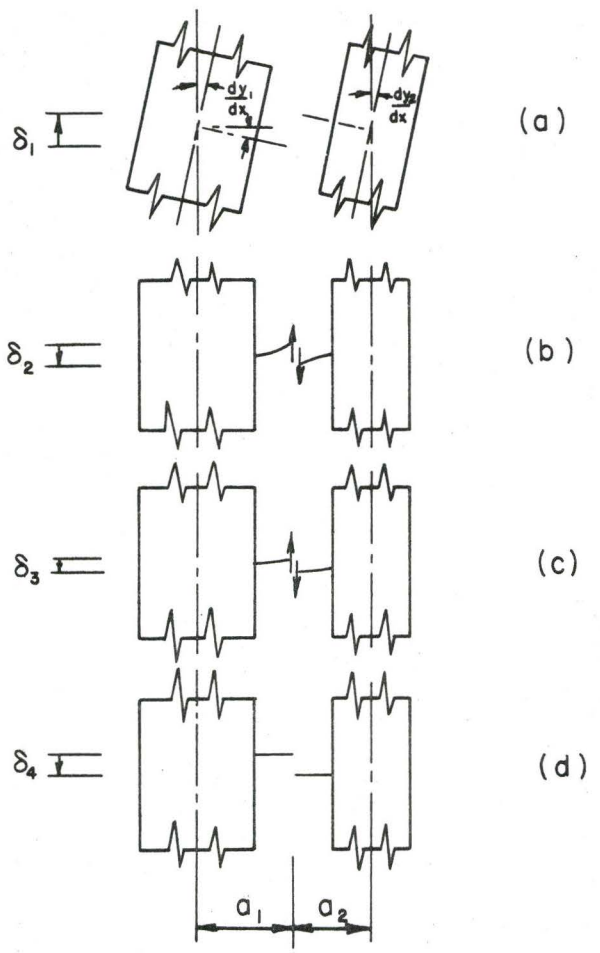

FIGURE 3

RELATIVE VERTICAL DISPLACEMENT AT THE SECTION ALONG THE MID-POINTS OF LAMINAS

(a) DUE TO BENDING OF THE WALL
(b) DUE TO BENDING OF THE CONNECTING BEAM
(c) DUE TO SHEAR DEFORMATION OF THE CONNECTING BEAM
(d) DUE TO AXIAL STRAIN OF THE WALL

The shear deformation of the lamina due to shear qdx gives a relative displacement $\delta_3(x)$ where

$$\delta_3(x) = \frac{-qhc}{GA_b^*} \tag{2.3}$$

where A_b^* is the effective cross-sectional area of the connecting beam to be considered for shear deformation and G is the shear modulus of the beam material.

The relative displacement $\delta_4(x)$ as a result of axial deformation of the piers is given by

$$\delta_4(x) = -\frac{1}{E}\left(\frac{1}{A_1} + \frac{1}{A_2}\right)\int_o^x \int_\eta^H q(\lambda)\,d\lambda\,d\eta \tag{2.4}$$

where A_1 and A_2 are the cross-sectional areas of piers 1 and 2 respectively.

It should be noted that the moment m(x) and axial force n(x) on a lamina do not cause any relative displacement of the lamina at the imaginary cut. The compatibility condition requires that the sum of the above relative displacements must be zero, giving

$$a_1 \frac{dy_1}{dx} + a_2 \frac{dy_2}{dx} - \left(\frac{hc^3}{12EI_b} + \frac{hc}{GA_b^*}\right) q - \frac{1}{E}\left(\frac{1}{A_1} + \frac{1}{A_2}\right)\int_o^x \int_\eta^H q(\lambda)\,d\lambda\,d\eta = 0 \tag{2.5}$$

Considering each pier separately, the moment - curvature relationship gives

$$EI_j \frac{d^2y_j}{dx^2} = M_{Ej} \qquad (j=1,2) \qquad (2.6)$$

where I_j is the moment of inertia of pier j. M_{Ej}, the total moment on pier j, is given by (Figure 2)

$$M_{E1} = M_1 - a_1 \int_x^H q\,d\lambda - \int_x^H m\,d\lambda - \int_x^H n(\lambda-x)\,d\lambda \qquad (2.7)$$

$$M_{E2} = M_2 - a_2 \int_x^H q\,d\lambda + \int_x^H m\,d\lambda + \int_x^H n(\lambda-x)\,d\lambda \qquad (2.8)$$

Substituting equations (2.7) and (2.8) into equation (2.6) results

$$EI_1 \frac{d^2y_1}{dx^2} = M_1 - a_1 \int_x^H q\,d\lambda - \int_x^H m\,d\lambda - \int_x^H n(\lambda-x)\,d\lambda \qquad (2.9)$$

$$EI_2 \frac{d^2y_2}{dx^2} = M_2 - a_2 \int_x^H q\,d\lambda + \int_x^H m\,d\lambda + \int_x^H n(\lambda-x)\,d\lambda \qquad (2.10)$$

In this analysis, it is assumed that the connecting beams are sufficiently stout or the axial forces in the connecting beams are sufficiently low that the effect of axial force on the bending deformation of the connecting beams can be neglected. It is also assumed that the end shortenings of the connecting beams, as a result of their flexural deformation, are of secondary importance. With these assumptions, the moment m(x) and the axial force n(x) can be related to the pier deflections as

$$m = \frac{EI_b}{hc}\left(\frac{dy_1}{dx} - \frac{dy_2}{dx}\right) \tag{2.11}$$

$$n = \frac{EA_b}{hc}(y_1 - y_2) \tag{2.12}$$

Compression is taken as positive in setting up the above equation. Thus, equations (2.5),(2.9),(2.10), (2.11) and (2.12) form the five linear equations relating the five unknown functions.

In order to procure a more meaningful and readily soluble representation of the problem, $q(x)$, $m(x)$ and $n(x)$ are eliminated as follows to result in a pair of equations in terms of the deflections $y_1(x)$ and $y_2(x)$ of the piers.

Differentiating equations (2.9) and (2.10) twice with respect to x and subsequent substitution of equations (2.11) and (2.12), there is obtained

$$EI_1 \frac{d^4y_1}{dx^4} = \frac{d^2M_1}{dx^2} + a_1 \frac{dq}{dx} + \frac{EI_b}{hc}\left(\frac{d^2y_1}{dx^2} - \frac{d^2y_2}{dx^2}\right) - \frac{EA_b}{hc}(y_1 - y_2) \tag{2.13}$$

$$EI_2 \frac{d^4y_2}{dx^4} = \frac{d^2M_2}{dx^2} + a_2 \frac{dq}{dx} - \frac{EI_b}{hc}\left(\frac{d^2y_1}{dx^2} - \frac{d^2y_2}{dx^2}\right) + \frac{EA_b}{hc}(y_1 - y_2) \tag{2.14}$$

The next step is to express $\frac{dq}{dx}$ in terms of $y_1(x)$ and $y_2(x)$. Differentiating equations (2.5) with respect to x gives

$$a_1 \frac{d^2y_1}{dx^2} + a_2 \frac{d^2y_2}{dx^2} - \frac{hc^3\beta^2}{12EI_b} \frac{dq}{dx} - \frac{1}{E}\left(\frac{1}{A_1} + \frac{1}{A_2}\right)\int_x^H q\,d\lambda = 0 \tag{2.15}$$

where $$\beta^2 = 1 + \frac{12EI_b}{c^2GA_b^*} \tag{2.16}$$

β^2 is a measure of the relative flexural and shear stiffnesses of the connecting beams. For instance, $\beta^2 = 1$ implies that the shear deformation of the connecting beams is neglected. Adding equations (2.9) and (2.10) results in

$$EI_1 \frac{d^2y_1}{dx^2} + EI_2 \frac{d^2y_2}{dx^2} = M_1 + M_2 - (a_1+a_2) \int_x^H q d\lambda \tag{2.17}$$

From equations (2.15) and (2.17), $\frac{dq}{dx}$ can be expressed in terms of $y_1(x)$ and $y_2(x)$ by eliminating $\int_x^H q d\lambda$ obtaining

$$\frac{hc^3\beta^2}{12EI_b} \frac{dq}{dx} = \frac{d^2y_1}{dx^2}\left(a_1 + \frac{I_1}{aA}\right) + \frac{d^2y_2}{dx^2}\left(a_2 + \frac{I_2}{aA}\right) - \frac{M}{EaA} \tag{2.18}$$

where $$a = a_1 + a_2 \tag{2.19}$$

$$\frac{1}{A} = \frac{1}{A_1} + \frac{1}{A_2} \tag{2.20}$$

$$M = M_1 + M_2 \tag{2.21}$$

Substituting equation (2.18) into equations (2.13) and (2.14), and writing the resulting pair of equations in matrix form yields

$$E \begin{bmatrix} I_1 & 0 \\ 0 & I_2 \end{bmatrix} \frac{d^4}{dx^4} \begin{Bmatrix} y_1 \\ y_2 \end{Bmatrix} - \frac{EI_b}{hc} \begin{bmatrix} p_{11} & p_{12} \\ p_{21} & p_{22} \end{bmatrix} \frac{d^2}{dx^2} \begin{Bmatrix} y_1 \\ y_2 \end{Bmatrix} + \frac{EA_b}{hc} \begin{bmatrix} 1 & -1 \\ -1 & 1 \end{bmatrix} \begin{Bmatrix} y_1 \\ y_2 \end{Bmatrix} = \begin{Bmatrix} f_1 \\ f_2 \end{Bmatrix} \tag{2.22}$$

where $$p_{11} = \frac{12a_1^2}{c^2\beta^2}\ \gamma_1 + 1 \qquad (2.23)$$

$$p_{12} = \frac{12a_1a_2}{c^2\beta^2}\ \gamma_2 - 1 \qquad (2.24)$$

$$p_{21} = \frac{12a_1a_2}{c^2\beta^2}\ \gamma_1 - 1 \qquad (2.25)$$

$$p_{22} = \frac{12a_2^2}{c^2\beta^2}\ \gamma_2 + 1 \qquad (2.26)$$

$$\gamma_j = 1 + \frac{I_j}{a_j aA} \qquad (j = 1,2) \qquad (2.27)$$

$$f_j = \frac{d^2M_j}{dx^2} - \frac{12a_jI_b}{hc^3\beta^2aA}\,M \quad (j = 1,2) \qquad (2.28)$$

It is noted that γ_j is a measure of the axial deformation of pier j. For instance, neglecting the axial deformation of pier j means $\gamma_j = 1$.

Equation (2.22) is the governing equation of the structural system under static loading, expressed in terms of pier deflections $y_1(x)$ and $y_2(x)$. The first term on the left hand side of the equation is the bending term involving the flexural stiffness of the individual pier. The second term is a function of the pier curvatures; it represents the effect of axial force on the lateral equili-

brium of the shear wall. The third term is the elastic foundation term since it is proportional to the deflection vector. It should be noted that the properties of the connecting beams are reflected in the latter two terms. The right hand side of the equation represents the forcing function due to external lateral loading. This forcing function can be readily calculated once the external loading is defined. Thus, the governing equation takes the form of a pair of beams on elastic foundation and under 'axial' loading.

By using displacement variables rather than force variables as unknowns, this formulation lends itself easily to include the inertial effect of the piers, as is required in the dynamic study of coupled shear walls. It also simplifies the formulation of boundary conditions.

Equation (2.22) is a pair of linear, ordinary fourth-order differential equations. To completely define the behaviour of the shear wall system, eight boundary conditions, four at the top and four at the base of the piers are required to complement the governing equation. Assuming that the piers are rigidly connected to the foundation, the boundary conditions at the base are

$$\text{at } x = 0 \qquad y_j = 0 \quad (j = 1,2) \tag{2.29}$$

$$\frac{dy_j}{dx} = 0 \quad (j = 1,2) \tag{2.30}$$

The boundary conditions at the top require more consideration. From equations (2.9) and (2.10), putting x = H (where H is the height of the shear wall) gives

$$\text{at } x = H \quad EI_j \frac{d^2y_j}{dx^2} = M_j \quad (j = 1,2) \tag{2.31}$$

Differentiating equations (2.9) and (2.10) with respect to x gives

$$EI_1 \frac{d^3y_1}{dx^3} = \frac{dM_1}{dx} + a_1 q + m + \int_x^H n\,d\lambda \tag{2.32}$$

$$EI_2 \frac{d^3y_2}{dx^3} = \frac{dM_2}{dx} + a_2 q - m - \int_x^H n\,d\lambda \tag{2.33}$$

To express q(x) in terms of functions of $y_1(x)$ and $y_2(x)$, equation (2.18) is integrated with respect to x, resulting in

$$\frac{hc^3\beta^2}{12EI_b} q = \frac{dy_1}{dx}\left(a_1 + \frac{I_1}{aA}\right) + \frac{dy_2}{dx}\left(a_2 + \frac{I_2}{aA}\right) - \frac{1}{EaA}\int_o^x M d\bar{x} \tag{2.34}$$

Substituting equations (2.34) and (2.11) into equations (2.32) and (2.33) and evaluating at x = H yields the final set of boundary conditions. In matrix form, they are

$$E \begin{bmatrix} I_1 & 0 \\ 0 & I_2 \end{bmatrix} \frac{d^3}{dx^3} \begin{Bmatrix} y_1 \\ y_2 \end{Bmatrix} - \frac{EI_b}{hc} \begin{bmatrix} p_{11} & p_{12} \\ p_{21} & p_{22} \end{bmatrix} \frac{d}{dx} \begin{Bmatrix} y_1 \\ y_2 \end{Bmatrix} = \begin{Bmatrix} g_1 \\ g_2 \end{Bmatrix} \tag{2.35}$$

where

$$g_j = \frac{dM_j}{dx} - \frac{12a_jI_b}{hc^3\beta^2aA}\int_o^H Mdx \quad (j = 1,2) \tag{2.36}$$

Equation (2.35) is the condition relating to the shear forces at the top of the piers. Thus, the analysis of an asymmetric coupled shear wall subjected to arbitrary distributed lateral loading on the piers reduces to the solution of equation (2.22) stipulated by boundary conditions (2.29),(2.30),(2.31) and (2.35).

2.3 Symmetric and Antisymmetric Deformation

To provide better physical insight of the problem, it is convenient to recast equations (2.22),(2.29),(2.30) (2.31) and (2.35) in terms of variables which represent the antisymmetric and symmetric deformation of the piers. This is achieved by using new variables z_1 and z_2 defined by the linear transformation

$$\begin{Bmatrix} y_1 \\ y_2 \end{Bmatrix} = \begin{bmatrix} 1 & 1 \\ 1 & -1 \end{bmatrix} \begin{Bmatrix} z_1 \\ z_2 \end{Bmatrix} \tag{2.37}$$

or

$$\begin{Bmatrix} z_1 \\ z_2 \end{Bmatrix} = \frac{1}{2} \begin{bmatrix} 1 & 1 \\ 1 & -1 \end{bmatrix} \begin{Bmatrix} y_1 \\ y_2 \end{Bmatrix} \tag{2.38}$$

From the transformation, it is readily seen that if both piers deflect equally, i.e. $y_1 = y_2$, then z_2 is identically zero and z_1 represents the antisymmetric mode of deflection of the system. On the other hand, if the piers deflect equally but in opposite directions, i.e. $y_1 = -y_2$, then z_1 is identically zero and z_2 represents the symmetric mode of deflection. Thus, the deflection of the piers is represented by a linear combination of anti-symmetric and symmetric modes of deformation z_1 and z_2 respectively.

Substituting equation (2.37) into equation (2.22) and premultiplying the subsequent equation by the transpose of the transformation matrix, one obtains

$$E \begin{bmatrix} I & \tilde{I} \\ \tilde{I} & I \end{bmatrix} \frac{d^4}{dx^4} \begin{Bmatrix} z_1 \\ z_2 \end{Bmatrix} - \frac{12EI_b}{hc^3\beta^2} \begin{bmatrix} a(a_1\gamma_1 + a_2\gamma_2) & a(a_1\gamma_1 - a_2\gamma_2) \\ \tilde{a}(a_1\gamma_1 + a_2\gamma_2) & \tilde{a}(a_1\gamma_1 - a_2\gamma_2) + \frac{c^2\beta^2}{3} \end{bmatrix}$$

$$\frac{d^2}{dx^2} \begin{Bmatrix} z_1 \\ z_2 \end{Bmatrix} + \frac{EA_b}{hc} \begin{bmatrix} 0 & 0 \\ 0 & 4 \end{bmatrix} \begin{Bmatrix} z_1 \\ z_2 \end{Bmatrix} = \begin{Bmatrix} \frac{d^2M}{dx^2} - \frac{12I_bM}{hc^3\beta^2A} \\ \frac{d^2\tilde{M}}{dx^2} - \frac{12I_b\tilde{a}M}{hc^3\beta^2aA} \end{Bmatrix} \qquad (2.39)$$

where

$$I = I_1 + I_2 \qquad (2.40)$$

$$\tilde{I} = I_1 - I_2 \qquad (2.41)$$

$$\tilde{a} = a_1 - a_2 \qquad (2.42)$$

$$\tilde{M} = M_1 - M_2 \qquad (2.43)$$

Writing equation (2.39) in terms of the non-dimensional spatial coordinate ξ defined by

$$x = \xi H \qquad (2.44)$$

the governing equation becomes

$$[L]\ \{Z\}' + \frac{H^4 A_b}{hc}\begin{bmatrix}0 & 0\\ 0 & 4\end{bmatrix}\{Z\} = \frac{H^2}{E}\begin{Bmatrix} M'' - \frac{\alpha^2 M}{A} \\ \tilde{M}'' - \frac{\alpha^2 \tilde{a} M}{aA}\end{Bmatrix} \quad (2.45)$$

where

$$\{Z\} = \begin{Bmatrix} z_1(\xi) \\ z_2(\xi)\end{Bmatrix} \quad (2.46)$$

$$\alpha^2 = \frac{12H^2 I_b}{hc^3\beta^2} \quad (2.47)$$

and [L] is an operator matrix with elements

$$L_{11} = I(\ )''' - \alpha^2 a(a_1\gamma_1 + a_2\gamma_2)(\ )' \quad (2.48)$$

$$L_{12} = \tilde{I}(\ )''' - \alpha^2 a(a_1\gamma_1 - a_2\gamma_2)(\ )' \quad (2.49)$$

$$L_{21} = \tilde{I}(\ )''' - \alpha^2 \tilde{a}(a_1\gamma_1 + a_2\gamma_2)(\ )' \quad (2.50)$$

$$L_{22} = I(\ )''' - \alpha^2 [\tilde{a}(a_1\gamma_1 - a_2\gamma_2) + \frac{c^2\beta^2}{3}]\ (\ )' \quad (2.51)$$

It is noted that α^2 has a dimension of [length^2] and that $(\ )'$ denotes differentiation with respect to variable ξ.

Applying the same procedure to equations (2.29), (2.30), (2.31) and (2.35), the boundary conditions become

$$\text{at } \xi = 0 \quad \{Z\} = \{0\} \quad (2.52)$$

$$\{Z\}' = \{0\} \quad (2.53)$$

$$\text{at } \xi = 1 \begin{bmatrix} I & \tilde{I} \\ \tilde{I} & I\end{bmatrix} \{Z\}'' = \frac{H^2}{E}\begin{Bmatrix} M \\ \tilde{M}\end{Bmatrix} \quad (2.54)$$

$$[L]\{Z\} = \frac{H^2}{E}\begin{Bmatrix} M' - \frac{\alpha^2}{A}\int_o^1 M d\xi \\ \tilde{M}' - \frac{\alpha^2 \tilde{a}}{aA}\int_o^1 M d\xi \end{Bmatrix} \tag{2.55}$$

Thus, in terms of the antisymmetric and symmetric modes of deflection, the problem of coupled shear walls subjected to arbitrarily distributed lateral loading on the piers reduces to the solution of equation (2.45) subjected to boundary conditions (2.52) through (2.55). Once z_1 and z_2 are solved, the other physical quantities of interest in the problem can be obtained as follows:

deflections
$$\begin{Bmatrix} y_1(\xi) \\ y_2(\xi) \end{Bmatrix} = \begin{bmatrix} 1 & 1 \\ 1 & -1 \end{bmatrix} \begin{Bmatrix} z_1 \\ z_2 \end{Bmatrix} \tag{2.37}$$

moment (from equations (2.11) and (2.38))
$$m(\xi) = \frac{2EI_b}{Hhc}\, z_2' \tag{2.56}$$

axial force (from equations (2.12) and (2.38))
$$n(\xi) = \frac{2EA_b}{hc}\, z_2 \tag{2.57}$$

shear (from differentiating equation (2.17) and using equation (2.38))
$$q(\xi) = \frac{E}{aH^3}\left[I z_1''' + \tilde{I} z_2''' - \frac{H^2}{E} M'\right] \tag{2.58}$$

moment on pier 1 (from equations (2.6) and (2.37))

$$M_{E1}(\xi) = \frac{EI_1}{H^2}(z_1'' + z_2'') \tag{2.59}$$

moment on pier 2 (from equations (2.6) and (2.37))

$$M_{E2}(\xi) = \frac{EI_2}{H^2}(z_1'' - z_2'') \tag{2.60}$$

For a coupled shear wall with unequal piers, the antisymmetric deflection z_1 and the symmetric deflection z_2 are coupled. The coupling occurs in both equations (2.45) and (2.55). It appears, at first glance, that equation (2.54) is also coupled, but with some mathematical manipulation, it can be uncoupled, reading as

$$\text{at } \xi = 1 \qquad \{Z\}'' = \frac{H^2}{2EI_1I_2}\begin{Bmatrix} I_2M_1 + I_1M_2 \\ I_2M_1 - I_1M_2 \end{Bmatrix} \tag{2.61}$$

From equations (2.56) and (2.57), it can be seen that so long as the deflections of the two piers are not identical, the moment $m(\xi)$ and the axial force $n(\xi)$ in the connecting beams will not vanish. In the case that the deflections are identical, the shear $q(\xi)$ and the total moments on the piers $M_{E1}(\xi)$ and $M_{E2}(\xi)$ are functions of the antisymmetric deformation z_1. It is pointed out in Section 2.1 that a proportional distribution of the lateral load according to the pier stiffnesses does not necessarily imply equal deflections of the piers. This fact can be

seen by putting $I_2M_1 = I_1M_2$ into equations (2.45) and (2.52) through (2.55). The resulting set of equations does not admit a solution $z_2 \equiv 0$.

2.4 Reduction to Wall of Equal Piers

In this section, the general formulation is reduced to the particular case of a coupled shear wall with equal piers.

Symmetry of the shear wall system implies that

$$a_1 = a_2 = a_s/2 \tag{2.62}$$

$$A_1 = A_2 = A_s \tag{2.63}$$

$$I_1 = I_2 = I_s \tag{2.64}$$

$$\gamma_1 = \gamma_2 = \gamma_s \tag{2.65}$$

$$d_1 = d_2 = d_s \tag{2.66}$$

where the subscript s refers to the symmetric wall. Substituting equations (2.62) through (2.66) in equation (2.45), the governing differential equation takes the form of a pair of uncoupled equations, namely,

$$z_1^{iv} - \frac{6H^2 I_b a_s^2 \gamma_s}{hc^3\beta^2 I_s} z_1'' = \frac{H^2}{2EI_s} M'' - \frac{12H^4 I_b}{EA_s hc^3\beta^2 I_s} M \tag{2.67}$$

$$z_2^{iv} - \frac{2H^2 I_b}{hcI_s} z_2'' + \frac{2H^4 A_b}{hcI_s} z_2 = \frac{H^2}{2EI_s} \tilde{M}'' \tag{2.68}$$

By a similar substitution, the boundary conditions (from equations (2.52) through (2.55)) become

$$\text{at } \xi = 0 \qquad z_1 = 0 \tag{2.69}$$

$$z_2 = 0 \tag{2.73}$$

$$z_1' = 0 \tag{2.70}$$

$$z_2' = 0 \tag{2.74}$$

$$\text{at } \xi = 1 \qquad z_1'' = \frac{H^2}{2EI_s} M \tag{2.71}$$

$$z_2'' = \frac{H^2}{2EI_s} \tilde{M} \tag{2.75}$$

$$z_1''' - \frac{6H^2 I_b a_s^2 \gamma_s}{hc^3 \beta^2 I_s} z_1' = \frac{H^2}{2EI_s} M' - \frac{12H^4 I_b}{EA_s hc^3 \beta^2 I_s} \int_o^1 M d\xi \tag{2.72}$$

$$z_2''' - \frac{2H^2 I_b}{hcI_s} z_2' = \frac{H^2}{2EI_s} \tilde{M}' \tag{2.76}$$

which are consistent with those given by Tso (16).

Therefore, the analysis of a coupled symmetric shear wall fixed at the base and subjected to static loading reduces to the solution of equations (2.67) and (2.68) with boundary conditions (2.69) through (2.72) and (2.73) through (2.76) respectively. From equations (2.56) through (2.60), the internal forces of the symmetric structure can be expressed as

moment $$m(\xi) = \frac{2EI_b}{Hhc} z_2' \tag{2.77}$$

axial force $$n(\xi) = \frac{2EA_b}{hc} z_2 \tag{2.78}$$

shear $$q(\xi) = \frac{2EI_s}{a_s H^3} z_1''' - \frac{M'}{a_s H} \tag{2.79}$$

moment on pier 1 $$M_{E1}(\xi) = \frac{EI_s}{H^2} (z_1'' + z_2'') \tag{2.80}$$

moment on pier 2 $$M_{E2}(\xi) = \frac{EI_s}{H^2} (z_1'' - z_2'') \tag{2.81}$$

Hence, in the case of a coupled shear wall with equal piers, the antisymmetric and symmetric modes of deformation are uncoupled. From equation (2.79), it is seen that the unit shear is independent of the symmetric deflection and of the lateral load distribution on individual piers. It should be noted that equation (2.79) is obtained without the assumption of points of contraflexure at the mid-points of the connecting beams. Also, no assumption of equal load distribution on the piers is made. Equation (2.79) can be shown to be identical to the results obtained by Beck (4), Rosman (5) and Traum (7) for the corresponding external loadings. Thus, as far as the unit shear force is concerned, the results by Beck, Rosman and Traum are applicable to a more general situation than they indicate.

If it is assumed that the lateral loading is equally shared by the piers, i.e. $M_1 = M_2$, then a solution $z_2 \equiv 0$ will satisfy the governing differential equation (2.68) and associated boundary conditions (2.73) through (2.76). In this case, $n(\xi) = m(\xi) = 0$ and the mid-points of the connecting laminas are indeed the points of contraflexure. Since Beck, Rosman and Traum are concerned with equal proportioning of the lateral loading on the piers, their solution is correct for the case of a coupled symmetric shear wall fixed at the base and the assumption of points of contraflexure at the mid-points of the laminas is fully justified.

2.5 Effect of Asymmetry

Structural designers tend to favour the concept of symmetry because of simplicity in computations and sometimes economy in construction. However, asymmetry may occur as a result of architectural or functional requirements. In the case of coupled shear walls, a study of the effect of asymmetry on the formulation of the problem is useful. From the design viewpoint, it may provide justification for a simplification of the design procedure. From the academic viewpoint, it may promote further insight into the problem.

Mathematically, asymmetry is usually manifested in the off-diagonal terms of a matrix formulation. It is seen from equations (2.39) or (2.45) that the main coupling terms (coupling between the antisymmetric and symmetric modes of deflection) are the off-diagonal elements in the matrix associated with the curvatures of the pier deflections. Neglecting the common factor $(EI_b)/(hc\beta^2)$, the matrix [C], with non-dimensional elements, can be written as

$$[C] = \frac{12}{c^2} \begin{bmatrix} a(a_1\gamma_1 + a_2\gamma_2) & a(a_1\gamma_1 - a_2\gamma_2) \\ \tilde{a}(a_1\gamma_1 + a_2\gamma_2) & \tilde{a}(a_1\gamma_1 - a_2\gamma_2) + c^2\beta^2/3 \end{bmatrix} \tag{2.82}$$

The coupling terms C_{12} and C_{21} can be expanded to read as

$$C_{12} = F_1 + F_2 \tag{2.83}$$

$$C_{21} = F_1 - F_2 \tag{2.84}$$

where $$F_1 = \frac{12}{c^2} (a_1^2\gamma_1 - a_2^2\gamma_2) \tag{2.85}$$

$$F_2 = \frac{12}{c^2} a_1a_2 (\gamma_1 - \gamma_2) \tag{2.86}$$

F_1 and F_2, which are non-dimensional, can further be expressed in terms of the pier width (d_j, j = 1,2) to beam span ratios as follows

$$F_1 = 3\left[(\frac{d_1}{c}+1)^2-(\frac{d_2}{c}+1)^2\right]+\frac{\left[(\frac{d_1}{c}+1)(\frac{d_1}{c})^3-(\frac{d_2}{c}+1)(\frac{d_2}{c})^3\right]\left[\frac{c}{d_1}+\frac{c}{d_2}\right]}{(\frac{d_1}{c}+\frac{d_2}{c}+2)} \tag{2.87}$$

$$F_2 = \frac{\left[(\frac{d_2}{c}+1)(\frac{d_1}{c})^3-(\frac{d_1}{c}+1)(\frac{d_2}{c})^3\right]\left[\frac{c}{d_1}+\frac{c}{d_2}\right]}{(\frac{d_1}{c}+\frac{d_2}{c}+2)} \tag{2.88}$$

In a similar manner, the diagonal elements C_{11} and C_{22} can be expressed as

$$C_{11} = F_3 + F_4 \tag{2.89}$$

$$C_{22} = F_3 - F_4 + 4\beta^2 \tag{2.90}$$

where $$F_3 = \frac{12}{c^2} (a_1^2\gamma_1 + a_2^2\gamma_2) \tag{2.91}$$

$$F_4 = \frac{12}{c^2} a_1a_2 (\gamma_1 + \gamma_2) \tag{2.92}$$

In terms of the basic geometry of the shear wall, the quantities F_3, F_4 and β^2 become

$$F_3 = 3\left[\left(\frac{d_1}{c}+1\right)^2+\left(\frac{d_2}{c}+1\right)^2\right] + \frac{\left[\left(\frac{d_1}{c}+1\right)\left(\frac{d_1}{c}\right)^3+\left(\frac{d_2}{c}+1\right)\left(\frac{d_2}{c}\right)^3\right]\left[\frac{c}{d_1}+\frac{c}{d_2}\right]}{\left(\frac{d_1}{c}+\frac{d_2}{c}+2\right)} \qquad (2.93)$$

$$F_4 = 6\left(\frac{d_1}{c}+1\right)\left(\frac{d_2}{c}+1\right) + \frac{\left[\left(\frac{d_2}{c}+1\right)\left(\frac{d_1}{c}\right)^3+\left(\frac{d_1}{c}+1\right)\left(\frac{d_2}{c}\right)^3\right]\left[\frac{c}{d_1}+\frac{c}{d_2}\right]}{\left(\frac{d_1}{c}+\frac{d_2}{c}+2\right)} \qquad (2.94)$$

$$\beta^2 = 1 + 1.2\left(\frac{E}{G}\right)\left(\frac{d_b}{c}\right)^2 \qquad (2.95)$$

where in the last expression, A_b^* the effective cross-sectional area of the connecting beam to be considered for shear deformation is taken as $A_b/1.2$; and d_b is the depth of the connecting beam.

The variations of the coupling terms C_{12} and C_{21} with the pier width ratio d_1/d_2, for various width of pier 1 to beam span ratios d_1/c, are shown in Figures 4 and 5 respectively. Without loss of generality, pier 1 is assumed to be wider than or equal to pier 2, i.e. $d_1 \geq d_2$. The width of pier 1 ranges from one-half to two times the connecting beam span. It is seen that the coupling terms are monotonic increasing functions of the pier width ratio, with the major increase occurring between $\frac{d_1}{d_2} = 1$ and 2, and that they both vanish at $d_1 = d_2$ which is to be expected of a symmetric system. In a similar fashion, Figure 6 shows the variation of C_{12}/C_{11}, the off-diagonal element to the

diagonal element. This is, indirectly, the influence on the antisymmetric mode of deflection by the symmetric mode as a result of coupling. The same comments as in Figures 4 and 5 apply here. However, there is one difference in the trend. At a particular $\frac{d_1}{d_2}$ ratio, the variation of C_{12} or C_{21} with $\frac{d_1}{c}$ has a positive curvature, whereas the corresponding variation of C_{12}/C_{11} has a negative curvature. This implies that when the piers are sufficiently close, the coupling action tends to approach a constant value. As C_{21}/C_{22} is a function of the depth to span of beam ratio $\frac{d_b}{c}$, Figures 7a-d show its variation with $\frac{d_b}{c} = \frac{1}{4}, \frac{1}{8}, \frac{1}{12}, \frac{1}{16}$ respectively. This variation is, indirectly, the influence on the symmetric mode of deflection by the antisymmetric mode. Without loss of generality, $\frac{E}{G}$ is assumed to be 2.60 corresponding to a Poisson's ratio of 0.30. It is seen that higher magnitudes are obtained in Figures 7a-d than in Figure 6. One noticeable feature in Figures 7a-d is the occurrence of peaks for $\frac{d_1}{c} = 1.5$ and 2.0 in the neighbourhood of $\frac{d_1}{d_2} = 2$. This implies that when the width of pier 1 is sufficiently large compared to the beam span ($\frac{d_1}{c} \geq 1.5$), the coupling action is most prominent in the neighbourhood of a pier width ratio of 2. It is also noted that as the depth to span of beam ratio decreases, i.e. as the connecting beams become less stiff, there is more coupling action.

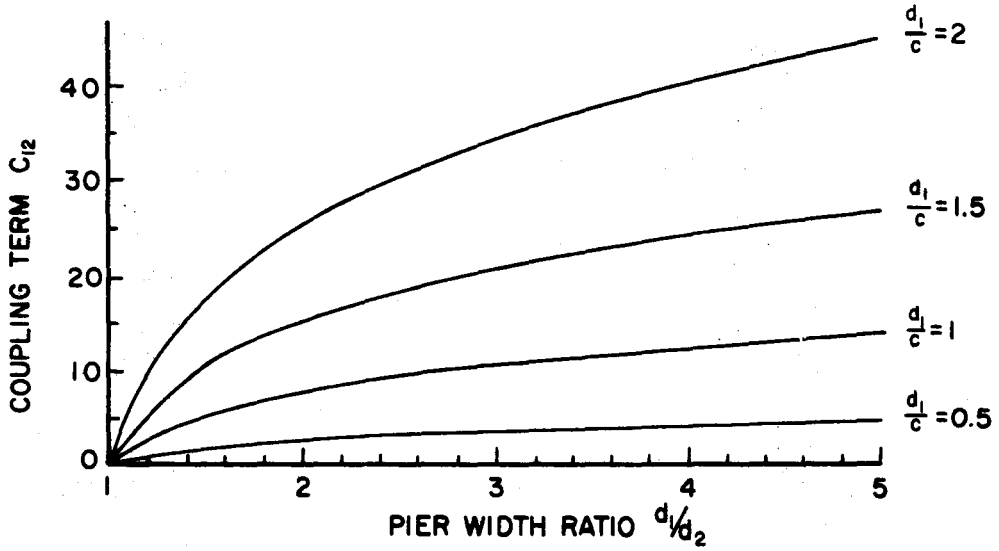

FIGURE 4. VARIATION OF COUPLING TERM C_{12} WITH PIER WIDTH RATIO

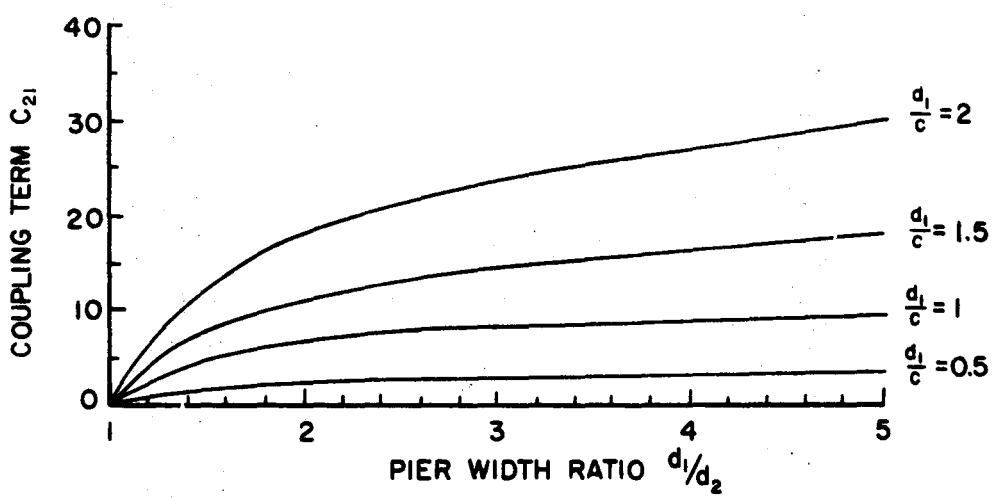

FIGURE 5. VARIATION OF COUPLING TERM C_{21} WITH PIER WIDTH RATIO

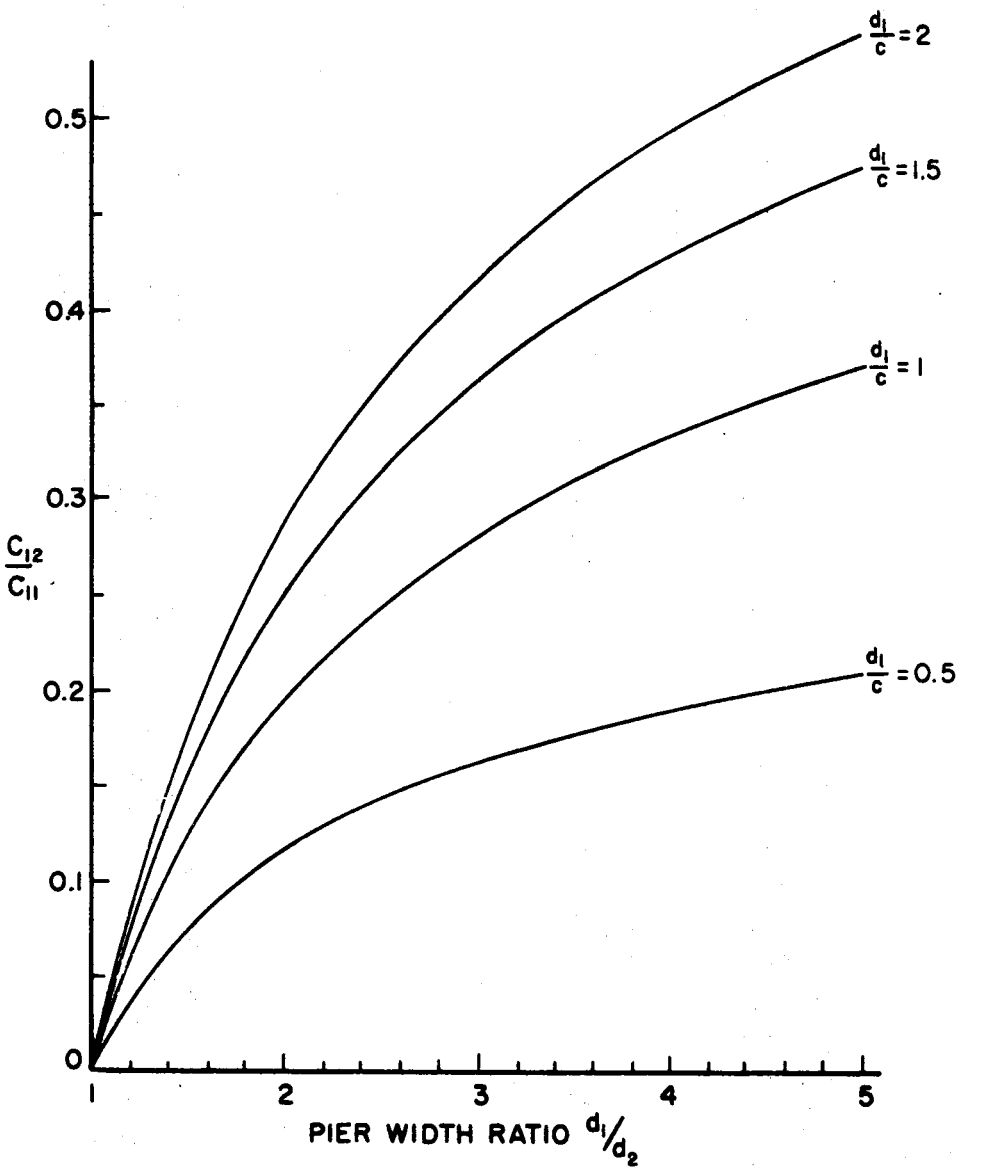

FIGURE 6. VARIATION OF OFF-DIAGONAL TO DIAGONAL ELEMENT C_{12}/C_{11} WITH PIER WIDTH RATIO (FOR ALL d_b/c)

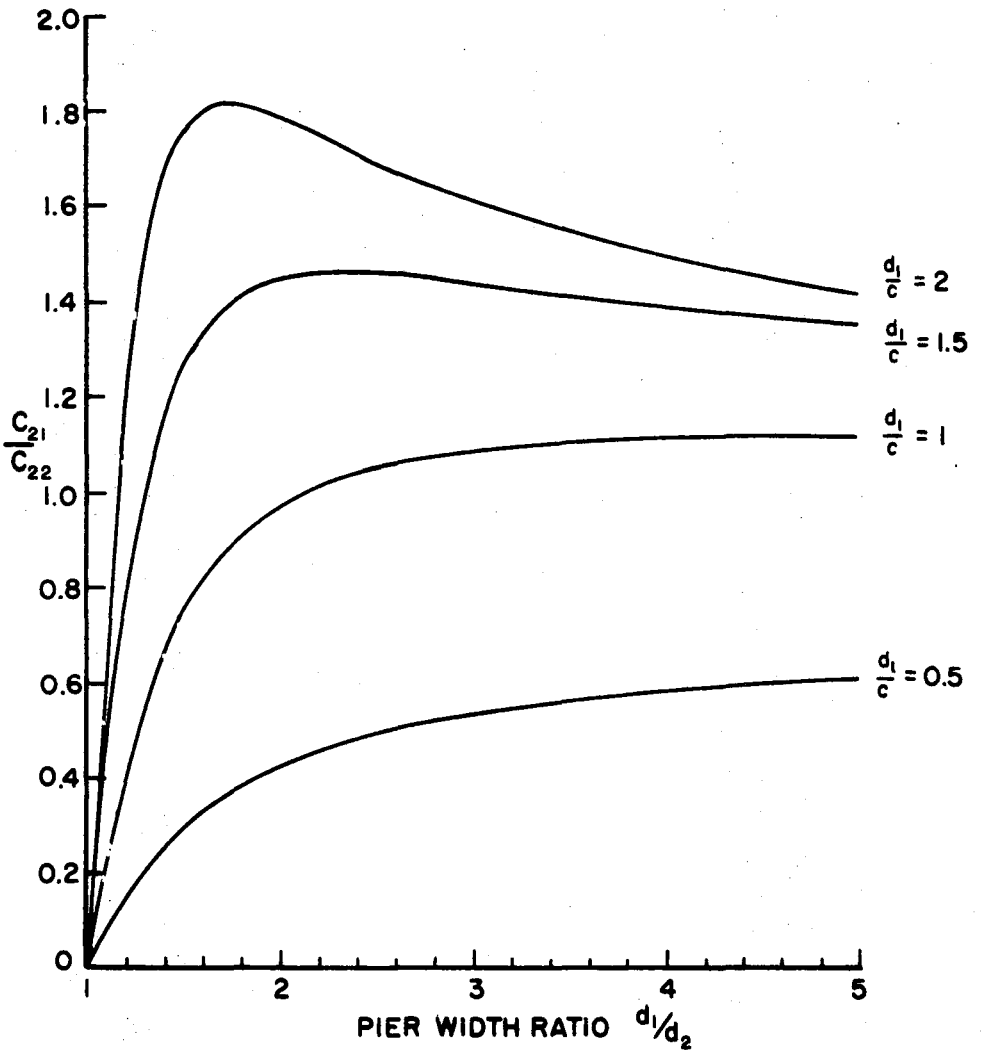

FIGURE 7a. VARIATION OF OFF-DIAGONAL TO DIAGONAL ELEMENT C_{21}/C_{22} WITH PIER WIDTH RATIO, FOR $d_b/c = 1/4$

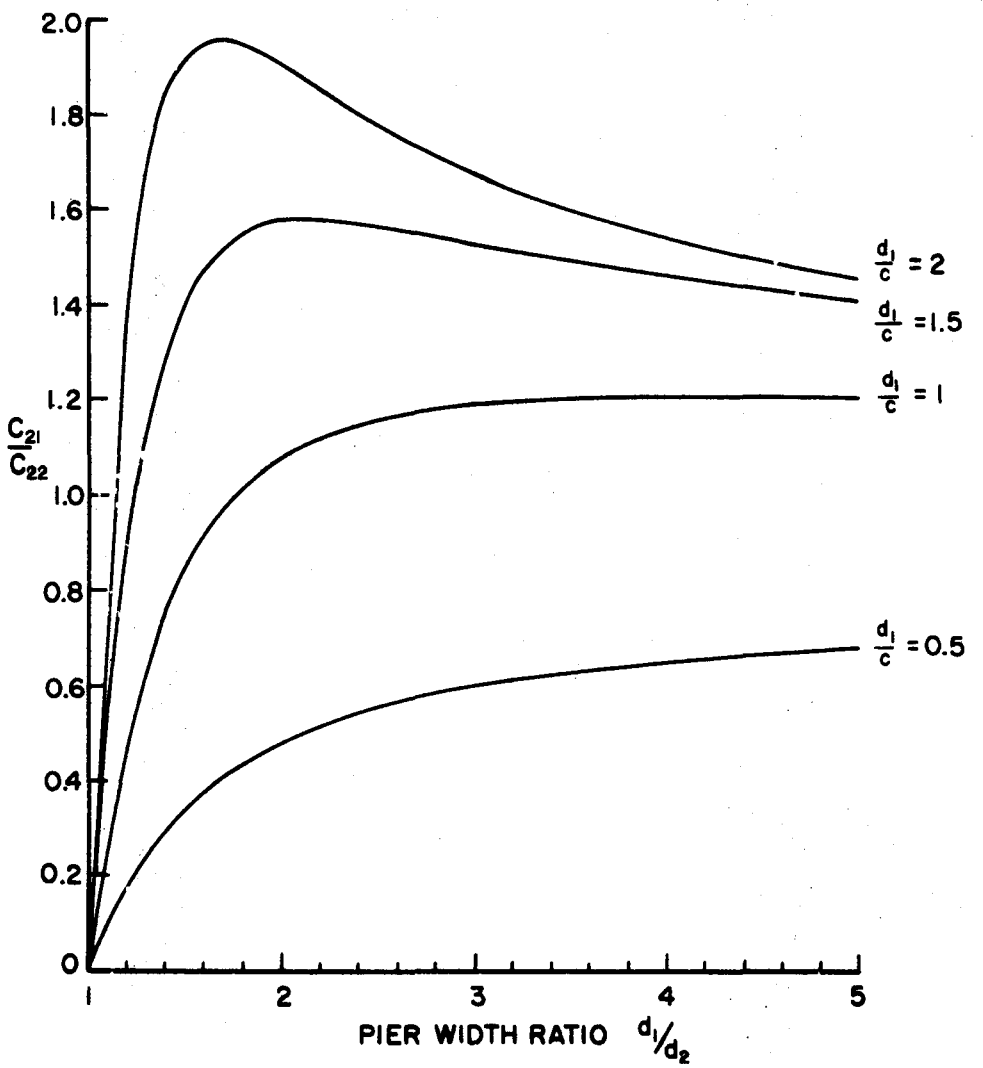

FIGURE 7b. VARIATION OF OFF-DIAGONAL TO DIAGONAL ELEMENT C_{21}/C_{22} WITH PIER WIDTH RATIO, FOR $d_b/c = 1/8$

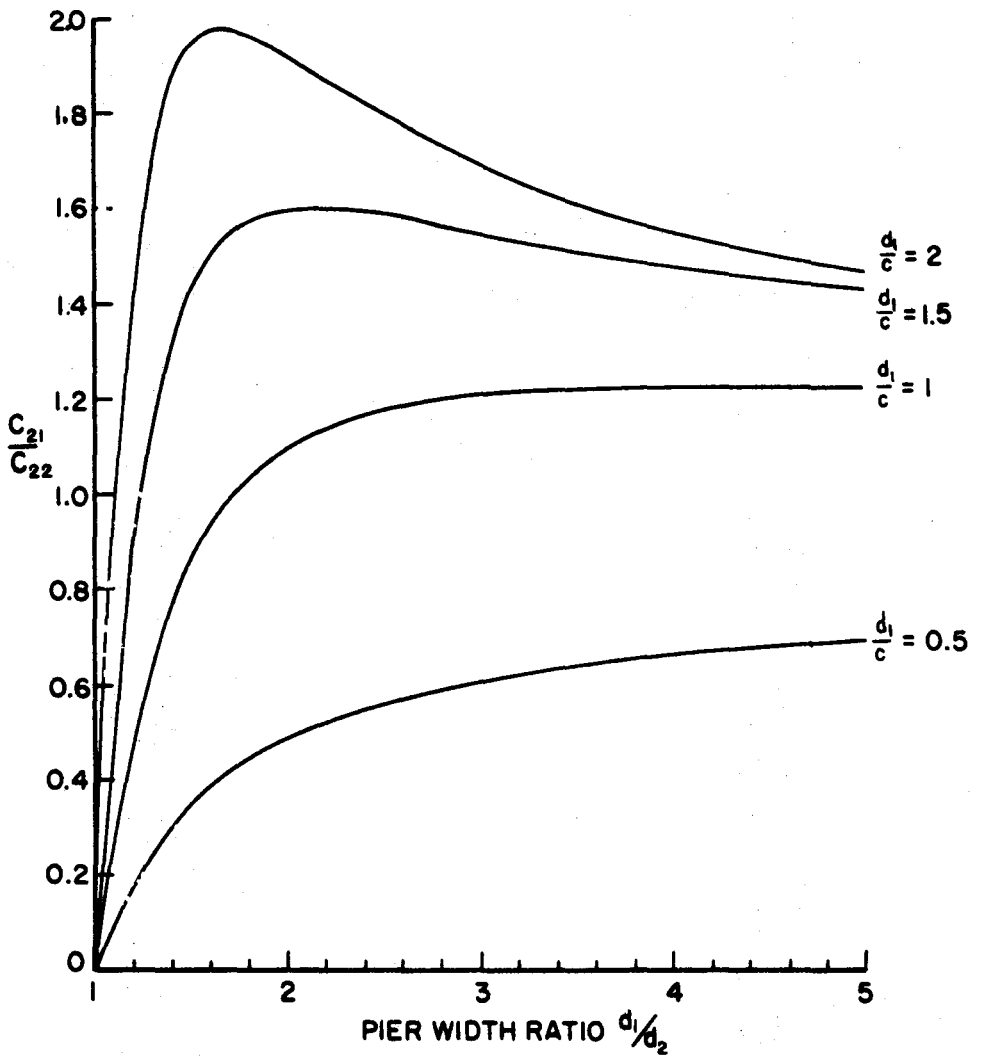

FIGURE 7c. VARIATION OF OFF-DIAGONAL TO DIAGONAL ELEMENT C_{21}/C_{22} WITH PIER WIDTH RATIO, FOR $d_b/c = 1/12$

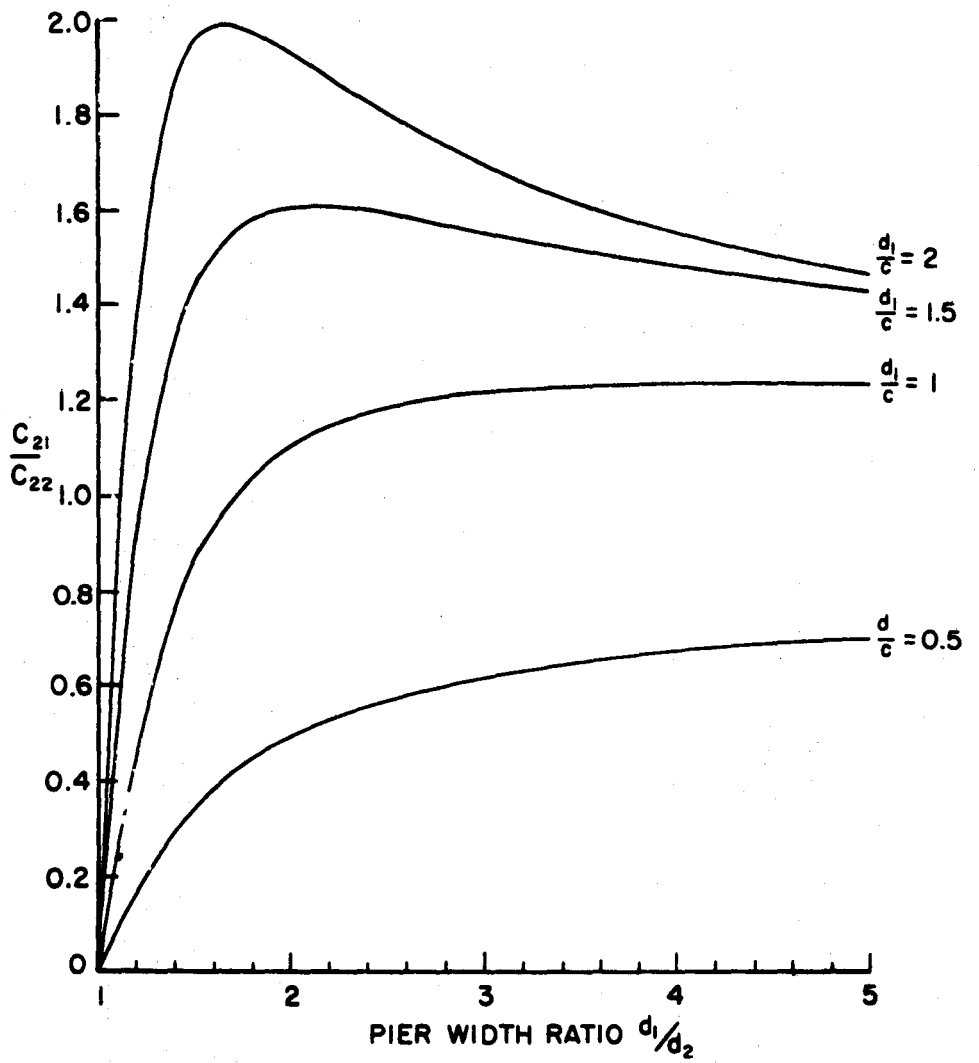

FIGURE 7d. VARIATION OF OFF-DIAGONAL TO DIAGONAL ELEMENT C_{21}/C_{22} WITH PIER WIDTH RATIO, FOR $d_b/c = 1/16$

2.6 Effect of Differential Foundation Settlement and Rotation on Symmetric Coupled Shear Walls

As an application of the above formulation of coupled shear walls under static loading, a problem of practical interest is examined. The problem of differential foundation settlement and rotation has been of concern, particularly in the case of apartment buildings situated above an escarpment. The instability of the slope induces differential settlement and rotation and the subsequent stresses in the structure may be disastrous.

For convenience, the case of a symmetric coupled shear wall where the foundation under the right pier has undergone a settlement Δ and a clockwise rotation θ is considered (Figure 8). The left foundation is assumed to remain fixed. It is convenient to divide the treatment of this topic into two subsections. The first subsection deals with the formulation of the problem. The second subsection contains an evaluation of the effect of foundation settlement and rotation on a shear wall model.

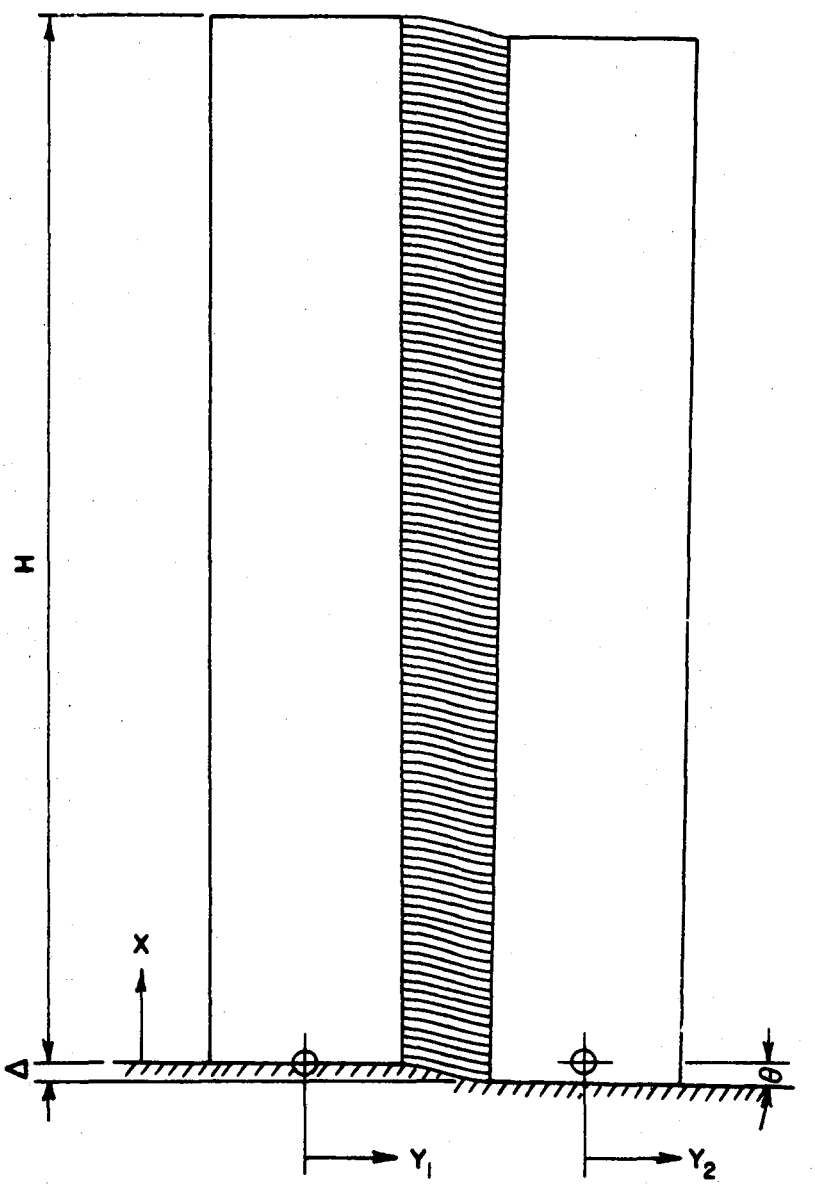

FIGURE 8

SHEAR WALL SUBJECTED TO DIFFERENTIAL FOUNDATION SETTLEMENT AND ROTATION

2.6.1 Derivation

Since the coefficients of the governing differential equations (2.67) and (2.68) depend only on the geometrical characteristics of the piers, the connecting beams and on the loading on the structure, the equations are valid for different foundation conditions. Defining non-dimensional constants $\bar{\alpha}^2$ and μ^2 as

$$\bar{\alpha}^2 = \frac{6H^2 I_b a_s^2 \gamma_s}{hc^3 \beta^2 I_s} \tag{2.96}$$

$$\mu^2 = \frac{2H^2 I_b}{hcI_s} \tag{2.97}$$

the differential equations can be written as

$$z_1^{iv} - \bar{\alpha}^2 z_1'' = \frac{H^2}{2EI_s} M'' - \frac{2\bar{\alpha}^2 H^2}{EA_s a_s^2 \gamma_s} M \tag{2.98}$$

$$z_2^{iv} - \mu^2 z_2'' + \frac{\mu^2 H^2 A_b}{I_b} z_2 = \frac{H^2}{2EI_s} \tilde{M}'' \tag{2.99}$$

The boundary conditions, which are not independent of foundation conditions, become

at $\xi = 0$

$$z_1 = \tfrac{1}{2}\theta\Delta \simeq 0 \tag{2.100}$$

$$z_2 = -\tfrac{1}{2}\theta\Delta \simeq 0 \tag{2.104}$$

$$z_1' = \tfrac{1}{2} H\theta \tag{2.101}$$

$$z_2' = -\tfrac{1}{2} H\theta \tag{2.105}$$

where it is noted that the exact zero displacement for the right pier occurs at $\xi = -\frac{\Delta}{H}$, but neglecting the second-order effect, $z_1(0)$ and $z_2(0)$ can be taken to be zero;

$$\text{at } \xi = 1 \qquad z_1'' = \frac{H^2}{2EI_s} M \tag{2.102}$$

$$z_2'' = \frac{H^2}{2EI_s} \tilde{M} \tag{2.106}$$

To obtain the other pair of boundary conditions at the top of the piers, it is necessary to express the unit shear in terms of the pier deflections. Integrating equation (2.18) (in the reduced form) with respect to x, it is obtained

$$\frac{hc^3\beta^2}{12EI_b} q\Big|_o^x = \frac{a_s\gamma_s}{2}\left(\frac{dy_1}{dx} + \frac{dy_2}{dx}\right)\Big|_o^x - \frac{2}{Ea_sA_s}\int_o^x M\, d\bar{x} \tag{2.108}$$

Unlike the case of a rigid foundation, the unit shear is not zero at the base. At the imaginary cut along the mid-points of the connecting laminas, the compatibility condition of zero relative vertical displacement is given by

$$\frac{a_s}{2}\left(\frac{dy_1}{dx} + \frac{dy_2}{dx}\right) - \frac{hc^3\beta^2}{12EI_b} q - \frac{2}{EA_s}\int_o^x \int_\eta^H q(\lambda)\,dx\,d\eta - \Delta = 0 \tag{2.109}$$

From equation (2.109), at x = 0, the unit shear q is given by

$$\frac{hc^3\beta^2}{12EI_b} q\,|_{x=0} = \frac{a_s}{2}\theta - \Delta \qquad (2.110)$$

Substituting equation (2.110) into equation (2.108) results in the required expression for the unit shear:

$$q(x) = \frac{12EI_b}{hc^3\beta^2}\left[\frac{a_s}{2}(1-\gamma_s)\theta-\Delta + \frac{a_s\gamma_s}{2}\left(\frac{dy_1}{dx}+\frac{dy_2}{dx}\right) - \frac{2}{Ea_sA_s}\int_o^x M d\bar{x}\right] \qquad (2.111)$$

Proceeding in parallel with Section 2.2 while keeping equation (2.111) in mind, one obtains the final set of boundary conditions, namely,

$$z_1''' - \bar{\alpha}^2 z_1' = \frac{H^2}{2EI_s}M' - \frac{2\bar{\alpha}^2H^2}{EA_sa_s^2\gamma_s}\int_o^1 M d\xi - \frac{2\bar{\alpha}^2HI_s}{A_sa_s^2\gamma_s}\theta - \frac{\bar{\alpha}^2H}{a_s\gamma_s}\Delta \qquad (2.103)$$

$$z_2''' - \mu^2 z_2' = \frac{H^2}{2EI_s}\tilde{M}' \qquad (2.107)$$

Thus, this analysis reduces to the solutions of equations (2.98) and (2.99) subjected to boundary conditions (2.100) through (2.103) and (2.104) through (2.107) respectively. The internal forces of the symmetric structure can then be obtained from equations (2.77) through (2.81).

Comparing the set of boundary conditions in this Section with that in Section 2.4, it can be seen that the differential foundation settlement and rotation affect only

the boundary conditions relating to the slope of the deflection at the bottom and to the shear force at the top of the piers. Furthermore, these effects are superimposed on the original formulation without differential settlement and rotation. Since the problem is strictly linear, it follows that solutions to the differential settlement and rotation problem can be obtained by superposition. From equation (2.105), it is seen that the symmetric mode of deflection is a function of the differential rotation. If there is no differential rotation and if it is assumed that the lateral loading is equally shared by the piers, i.e. $M_1 = M_2$, then a solution $z_2 \equiv 0$ will satisfy the governing differential equation (2.99) with boundary conditions (2.104) through (2.107). Since Rosman (5) is concerned with foundation settlement and with equal proportioning of the lateral loading for the case of a symmetric shear wall, his solution is valid and the assumption of contraflexure points at the mid-points of the laminas is again justified. It will be shown that when differential rotation does occur, the symmetric mode of deformation is significant at the lower floors of the structure.

2.6.2 Evaluation of Internal Forces

To study the effect of differential foundation settlement and rotation on the internal forces of the symmetric structure, the external load is set to zero; the governing differential equations become (from equations (2.98) and (2.99))

$$z_1^{iv} - \bar{\alpha}^2 z_1'' = 0 \tag{2.112}$$

$$z_2^{iv} - \mu^2 z_2'' + \frac{\mu^2 H^2 A_b}{I_b} z_2 = 0 \tag{2.113}$$

The boundary conditions (2.100) through (2.107) are obtained as

at $\xi = 0$,

$$z_1 = 0 \tag{2.114}$$

$$z_2 = 0 \tag{2.118}$$

$$z_1' = \tfrac{1}{2} H\theta \tag{2.115}$$

$$z_2' = -\tfrac{1}{2} H\theta \tag{2.119}$$

at $\xi = 1$,

$$z_1'' = 0 \tag{2.116}$$

$$z_2'' = 0 \tag{2.120}$$

$$z_1''' - \bar{\alpha}^2 z_1' = -\frac{2\bar{\alpha}^2 H I_s}{A_s a_s^2 \gamma_s}\theta - \frac{\bar{\alpha}^2 H}{a_s \gamma_s}\Delta \tag{2.117}$$

$$z_2''' - \mu^2 z_2' = 0 \tag{2.121}$$

The antisymmetric mode of deformation is governed by equation (2.112) subjected to boundary conditions (2.114) through (2.117). Since the equation is linear with constant coefficients, the solution can be readily obtained as

$$z_1(\xi) = \frac{H}{\bar{\alpha}\gamma_s}\left(\frac{\Delta}{a_s} - \frac{\theta}{2}\right)\left[\tanh\bar{\alpha}\,(\cosh\bar{\alpha}\xi - 1) - \sinh\bar{\alpha}\xi\right] + \left[\frac{H}{a_s\gamma_s}\,\Delta + \frac{H}{2}\left(1 - \frac{1}{\gamma_s}\right)\theta\right]\xi \tag{2.122}$$

The symmetric mode of deformation is governed by equation (2.113) subjected to boundary conditions (2.118) through (2.121). Seeking a solution to equation (2.113) of the form

$$z_2(\xi) = e^{s\xi} \tag{2.123}$$

the following characteristic equation is obtained

$$s^4 - \mu^2 s^2 + \frac{\mu^2 H^2 A_b}{I_b} = 0 \tag{2.124}$$

The roots of equation (2.124) can be written as

$$s = \pm\,\emptyset \pm i\chi \tag{2.125}$$

where $$\emptyset = \frac{\mu}{2}\sqrt{\frac{2H}{\mu r_b} + 1} \tag{2.126}$$

$$\chi = \frac{\mu}{2}\sqrt{\frac{2H}{\mu r_b} - 1} \tag{2.127}$$

$$r_b^2 = \frac{I_b}{A_b} \tag{2.128}$$

and $$i^2 = -1 \tag{2.129}$$

For practical consideration, the non-dimensional quantity H^2A_b/I_b is considerably larger than unity. Since $\frac{H}{\mu r_b} >> 1$, it is possible to make the simplification that

$$\phi \simeq \chi \simeq \sqrt{\frac{\mu H}{2r_b}} \tag{2.130}$$

The general solution of equation (2.124) can then be expressed as

$$z_2(\xi) = e^{\phi\xi}(B_1\sin\phi\xi + B_2\cos\phi\xi) + e^{-\phi\xi}(B_3\sin\phi\xi + B_4\cos\phi\xi) \tag{2.131}$$

where ϕ is given in equation (2.130) and B_1, B_2, B_3, B_4 are arbitrary constants to be determined by boundary conditions (2.118) through (2.121). To be consistent with the approximation made in equation (2.130), the boundary condition (2.121) becomes

$$\text{at } \xi = 1, \qquad z_2''' = 0 \tag{2.132}$$

Solving for the arbitrary constants and back substituting into equation (2.131) yields the complete solution for $z_2(\xi)$ as

$$z_2(\xi) = -\frac{H\theta}{2\phi}\frac{1}{(\cos^2\phi+\cosh^2\phi)}[\cosh\phi\sin\phi\xi\cosh\phi(1-\xi) + (\sin\phi\sin\phi\xi + \cos\phi\cos\phi\xi)\cos\phi\sinh\phi\xi] \tag{2.133}$$

It is noted that $z_2(\xi)$ is independent of Δ; that is,

the foundation settlement does not affect the symmetric mode of deformation.

The internal forces of a symmetric coupled shear wall as a result of differential foundation settlement Δ and rotation θ can be obtained utilizing equations (2.122) and (2.133) as

moment (from equation (2.77))

$$m(\xi) = -\frac{EI_b}{hc}\frac{\theta}{(\cos^2\phi+\cosh^2\phi)}\,[\cosh\phi\cos\phi\xi\cosh\phi(1-\xi) - \cosh\phi\sin\phi\xi\sinh\phi(1-\xi) + \sin\phi\cos\phi\xi\cos\phi\sinh\phi\xi + \sin\phi\sin\phi\xi\cos\phi\cosh\phi\xi - \cos\phi\sin\phi\xi\cos\phi\sinh\phi\xi + \cos\phi\cos\phi\xi\cos\phi\cosh\phi\xi] \quad (2.134)$$

axial force (from equation (2.78))

$$n(\xi) = -\frac{EA_bH}{hc\phi}\frac{\theta}{(\cos^2\phi+\cosh^2\phi)}\,[\cosh\phi\sin\phi\xi\cosh\phi(1-\xi) + (\sin\phi\sin\phi\xi + \cos\phi\cos\phi\xi)\cos\phi\sinh\phi\xi] \quad (2.135)$$

shear force (from equation (2.79))

$$q(\xi) = \frac{2EI_s\bar{\alpha}^2}{a_sH^2\gamma_s}\left(\frac{\Delta}{a_s} - \frac{\theta}{2}\right)(\tanh\bar{\alpha}\sinh\bar{\alpha}\xi - \cosh\bar{\alpha}\xi) \quad (2.136)$$

Moment on pier 1 (from equation (2.80)

$$M_{E1}(\xi) = \frac{EI_s}{H^2}\left\{\frac{H\bar{\alpha}}{\gamma_s}\left(\frac{\Delta}{a_s} - \frac{\theta}{2}\right)(\tanh\bar{\alpha}\cosh\bar{\alpha}\xi - \sinh\bar{\alpha}\xi) + \frac{H\phi\theta}{(\cos^2\phi+\cosh^2\phi)}[\cosh\phi\cos\phi\xi\sinh\phi(1-\xi) - \sin\phi\cos\phi\xi\cos\phi\cosh\phi\xi + \cos\phi\sin\phi\xi\cos\phi\cosh\phi\xi]\right\} \quad (2.137)$$

moment on pier 2 (from equation (2.81))

$$M_{E2}(\xi) = \frac{EI_s}{H^2}\left\{\frac{H\bar{\alpha}}{\gamma_s}\left(\frac{\Delta}{a_s} - \frac{\theta}{2}\right)(\tanh\bar{\alpha}\cosh\bar{\alpha}\xi - \sinh\bar{\alpha}\xi)\right.$$

$$\left. - \frac{H\phi\theta}{(\cos^2\phi+\cosh^2\phi)}[\cosh\phi\cos\phi\xi\sinh\phi(1-\xi) - \sin\phi\cos\phi\xi\cos\phi\cosh\phi\xi + \cos\phi\sin\phi\xi\cos\phi\cosh\phi\xi]\right\} \quad (2.138)$$

From the above expressions, it is noted that because the symmetric mode is independent of settlement Δ, so are the unit moment $m(\xi)$ and axial force $n(\xi)$. They are directly proportional to the differential rotation θ.

Evaluation of the unit moment, unit axial force, and unit shear force along the centerline of the structure and the total moments on the piers were performed on a shear wall system with the following geometrical characteristics and material properties

number of storeys	$N = 22$
storey height	$h = 9'$
total height	$H = 198'$
pier width	$d_s = 22'$
wall thickness	$t_w = 1'$
connecting beam span	$c = 5'$
connecting beam depth	$d_b = 1/2'$
elastic modulus	$E = 3 \times 10^6$ psi

In order to offer a meaningful presentation, the

internal forces of the shear wall system are normalized with respect to comparable quantities of the same system under the influence of a uniform lateral load w only. To be realistic, w is taken to be 1000 lb. per linear foot. The unit shear force q is normalized with respect to q_o where q_o is the maximum unit shear induced when the same shear wall is subjected to uniform load w. From Coull and Choudhury (9), q_o is given by

$$q_o = \frac{wH}{a_s} \frac{1}{\gamma_s} K_3' \tag{2.139}$$

where K_3' is the shear stress factor and can be obtained from Figure 4 of the same reference. The unit moment m is normalized with respect to m_o where m_o can be considered as a design quantity at the pier to beam connection. It is given by

$$m_o = q_o \frac{c}{2} \tag{2.140}$$

The unit axial force n is normalized with respect to n_o where n_o can be considered as the lateral load transmitted to the connecting beam; specifically,

$$n_o = \frac{1}{2} w \tag{2.141}$$

The total moments on the piers M_{E1} and M_{E2} are normalized with respect to M_o where M_o is the root moment of a cantilever pier subjected to $\frac{1}{2}$ w; namely

$$M_o = \frac{1}{4} wH^2 \qquad (2.142)$$

Thus, it can be seen that the normalized internal forces q/q_o, m/m_o, n/n_o, M_{E1}/M_o, and M_{E2}/M_o can be expressed in terms of a non-dimensional lateral load factor EH/w which, in this case, works out to be 9.9×10^7. Computations were done using the CDC 6400 electronic computer and the results are shown in Figures 9 through 15.

Figures 9 and 10 show the variation of the unit shear ratio q/q_o along the height of the structure for $\Delta = 0.5"$ at zero differential rotation and for $\theta = 0.2^o$ at zero differential settlement respectively. The variation is maximum at the base and decreases steadily tending to the ratio of 1 at the top in both cases. This implies that, the unit shear produced by a differential settlement of 0.5" or a differential rotation of 0.2^o can be as much as one (at the top) to more than two times (at the base) the maximum unit shear when the same shear wall structure is subjected to a lateral load w of 1000 plf or a lateral load factor EH/w of 9.9×10^7. Since the unit shear is a linear combination of rotation and settlement, combining Figures 9 and 10 will yield the unit shear ratio at any other values of differential settlement and rotation.

Figure 11 shows the variation of the unit moment ratio m/m_o along the height of the structure for a differential rotation of 0.2^o. The variation is primarily noticeable at

the bottom third of the structure with a positive maximum of about 0.03 at $\xi = 0.2$ and a negative maximum of about 0.16 at the base. This implies that a differential rotation of 0.2° induces a maximum unit moment of about 16% of the cantilever moment produced by the maximum unit shear when the same structure is subjected to a lateral load factor of 9.9×10^{7}. Since it is established that, at the base for $\theta = 0.2^{\circ}$, q is about twice q_o, the unit moment is thus insignificant in the design of the pier to beam connection.

Figure 12 shows the variation of the unit axial force ratio n/n_o along the height of the structure for a differential rotation of 0.2°. It can be seen from the exceedingly large ratios at the bottom third of the structure that the unit axial force as a result of a differential rotation of 0.2° cannot be reasonably estimated, because of the interaction of the piers, by the transmission of the lateral load when the same structure is subjected to a load factor of 9.9×10^{7}. It should be noted that since the unit moment and the unit axial force are independent of Δ and directly proportional to θ, their respective ratios can be readily obtained for other values of differential rotation.

Figure 13 shows the variation of the total moment ratios M_{E1}/M_o and M_{E2}/M_o along the height of the structure for a differential settlement of 0.5" at zero differential

rotation. It can be seen from equations (2.137) and (2.138) that $M_{E1} = M_{E2}$ when $\theta = 0$. The ratio decreases steadily from a maximum of about 0.4 at the base to zero at the top. Figures 14 and 15 show the variation of the total moment ratios M_{E1}/M_o and M_{E2}/M_o respectively along the height of the structure for a differential rotation of 0.2^o at zero differential settlement. The variation is significant at the bottom fifth of the structure where the total moment produced by a differential rotation of 0.2^o is as much as eight times (at the base) the root moment of a cantilever pier when the same structure is subjected to a load factor of 9.9×10^7. Although it is necessary to combine Figures 13 and 14 or Figures 13 and 15 to arrive at the total moment ratio (linear relationship as in unit shear) for other values of differential settlement and rotation, Figures 14 and 15 nevertheless reflects the significance of the symmetric mode of deformation at the bottom floors of the structure.

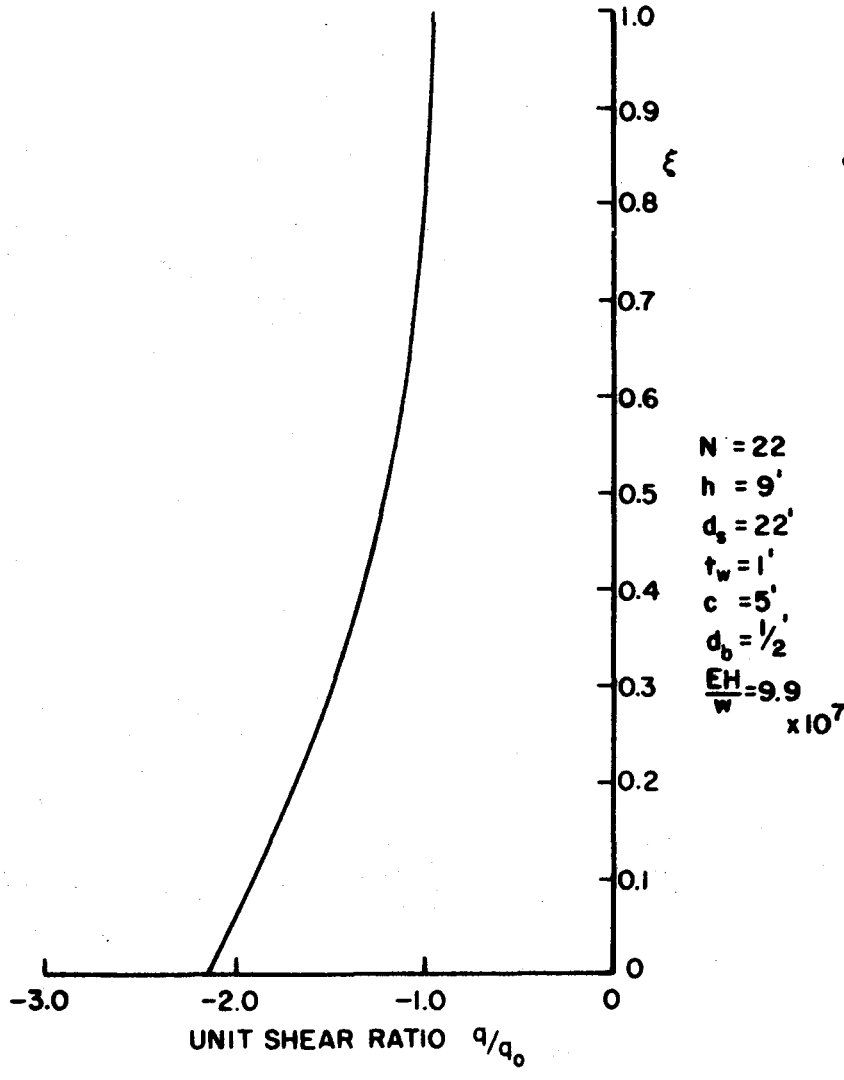

FIGURE 9. VARIATION OF UNIT SHEAR RATIO ALONG THE HEIGHT FOR $\theta = 0°$ $\Delta = 0.5"$

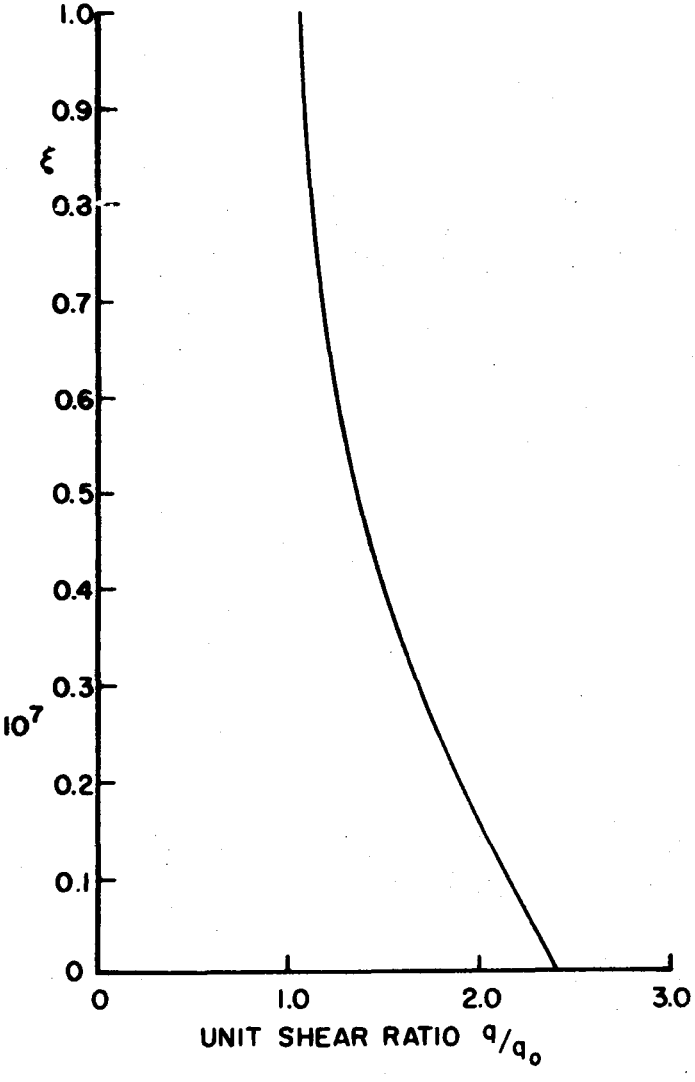

FIGURE 10. VARIATION OF UNIT SHEAR RATIO ALONG THE HEIGHT FOR $\theta = 0.2°$ $\Delta = 0"$

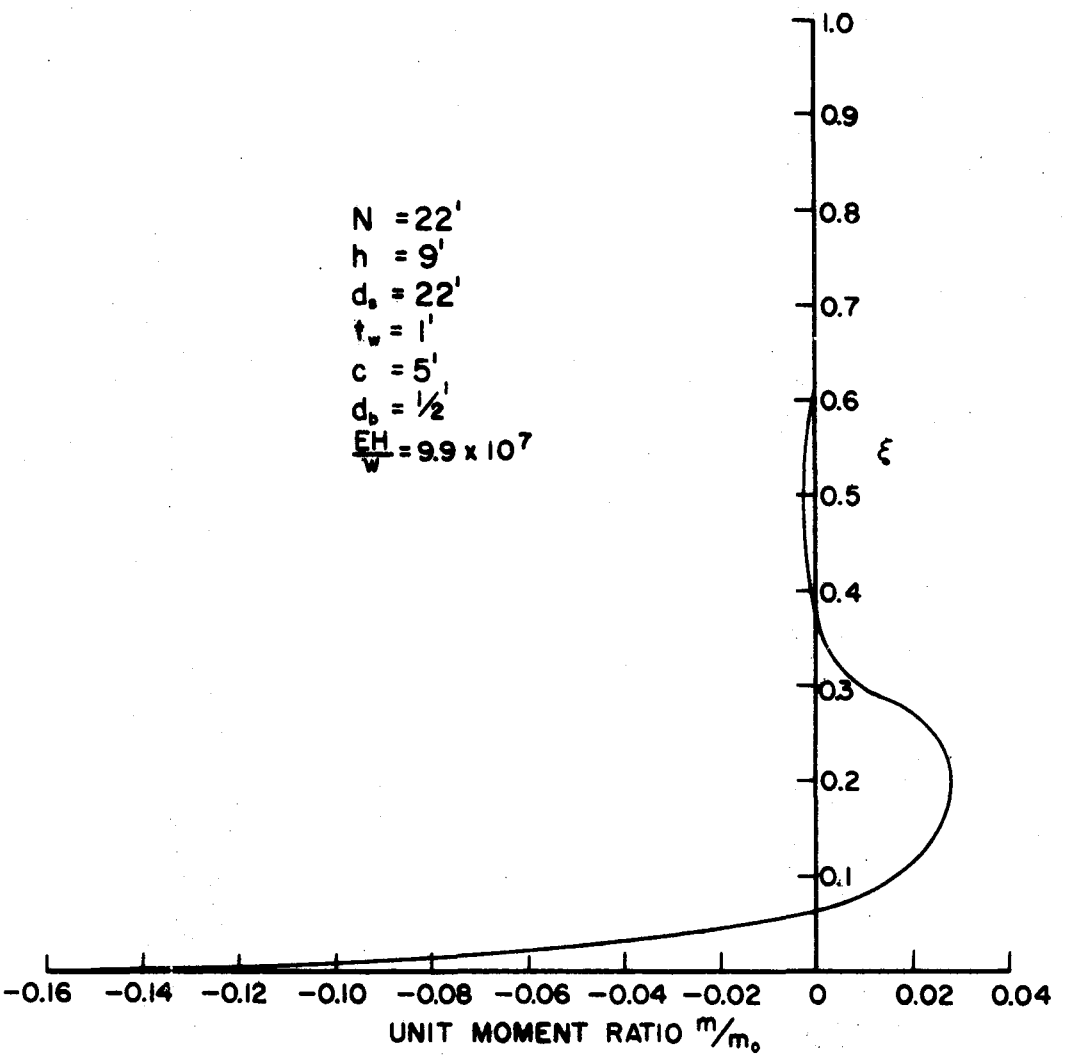

FIGURE 11. VARIATION OF UNIT MOMENT RATIO ALONG THE HEIGHT FOR DIFFERENTIAL FOUNDATION ROTATION $\theta = 0.2°$

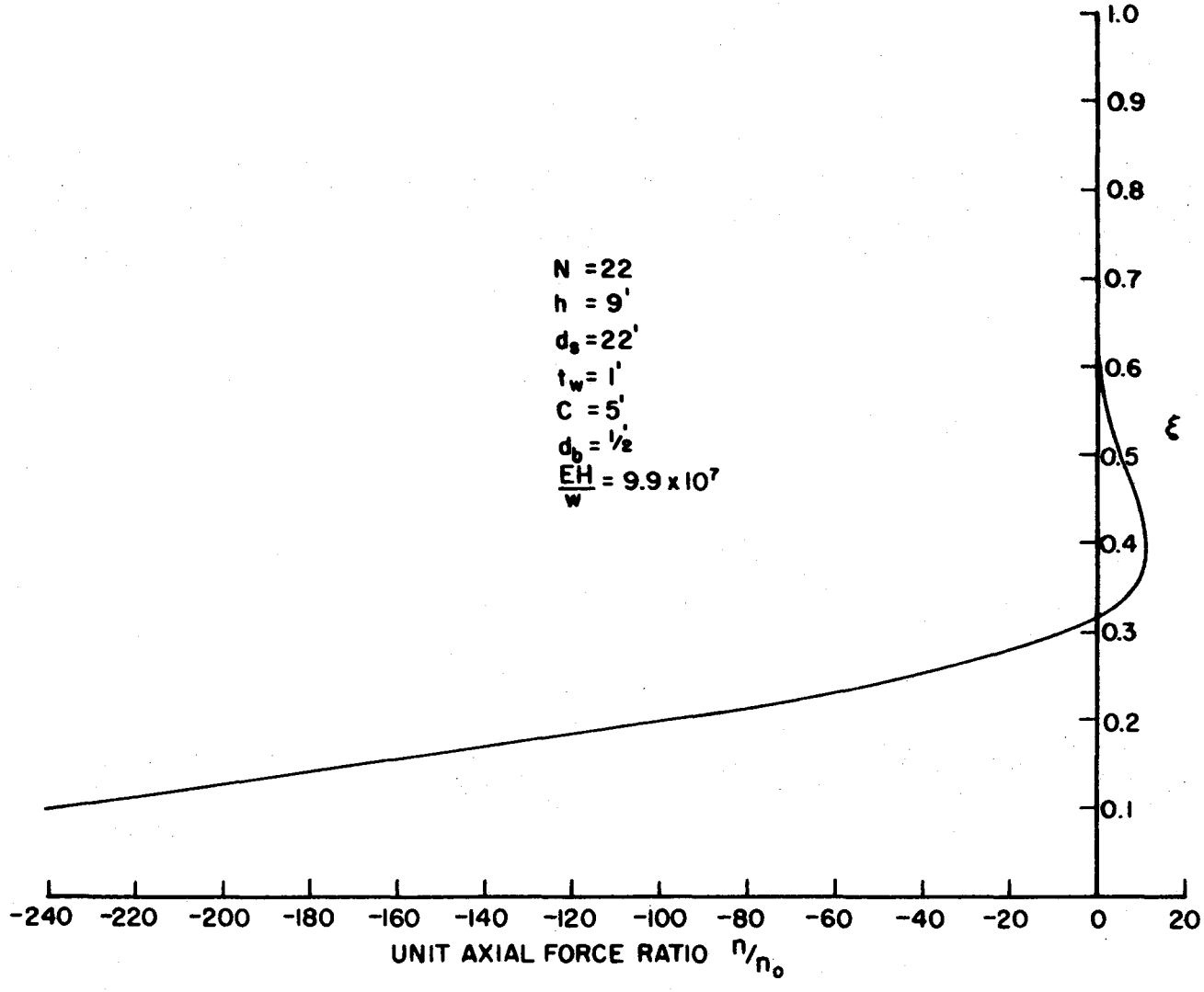

FIGURE 12. VARIATION OF UNIT AXIAL FORCE RATIO ALONG THE HEIGHT FOR DIFFERENTIAL FOUNDATION ROTATION θ =0.2°

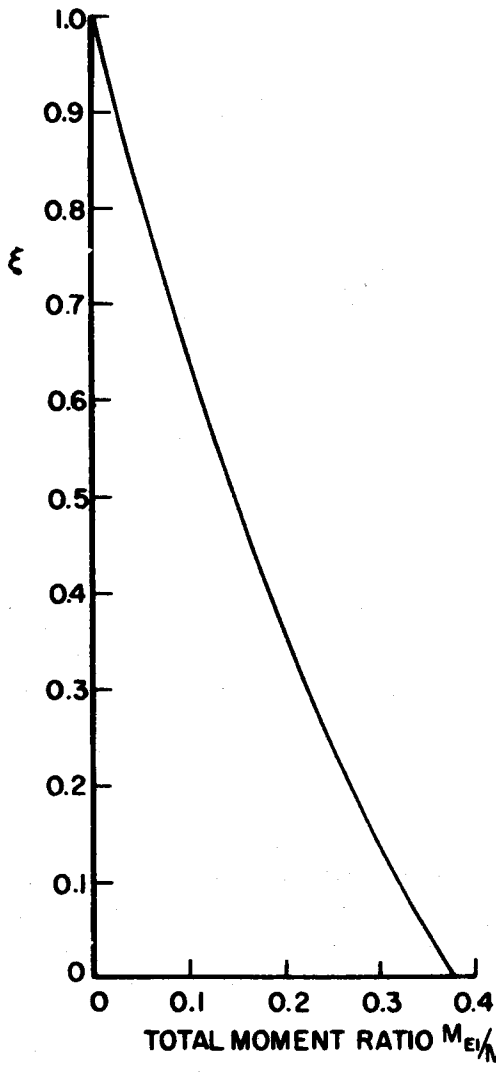

FIGURE 13. VARIATION OF THE TOTAL MOMENT RATIO ALONG THE HEIGHT FOR $\theta=0°$ $\Delta=0.5"$

$N = 22$
$h = 9'$
$d_s = 22'$
$t_w = 1'$
$c = 5'$
$d_b = 1/2'$
$\frac{EH}{w} = 9.9 \times 10^7$

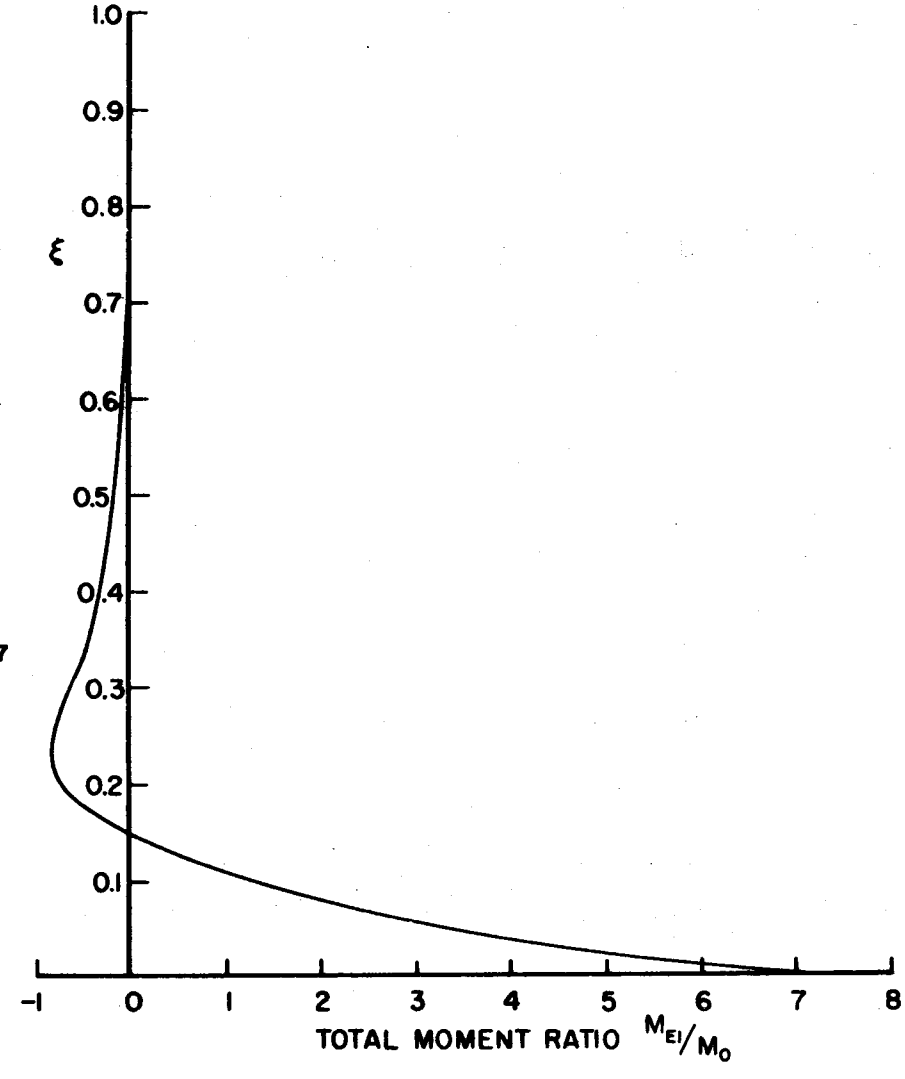

FIGURE 14. VARIATION OF THE TOTAL MOMENT RATIO OF PIER 1 ALONG THE HEIGHT FOR $\theta=0.2°$ $\Delta=0"$

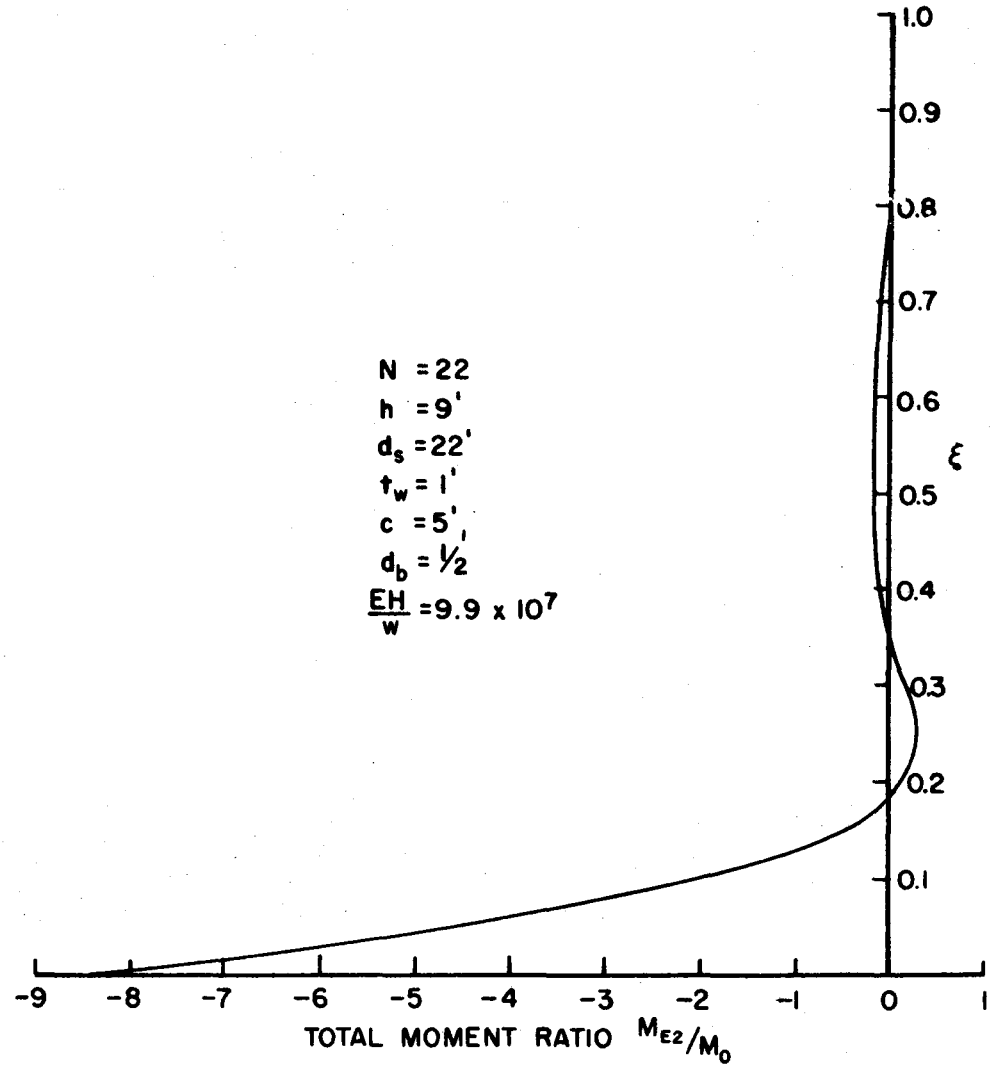

FIGURE 15. VARIATION OF THE TOTAL MOMENT RATIO OF PIER 2 ALONG THE HEIGHT FOR θ = 0.2° Δ = 0"

CHAPTER 3

ANALYSIS OF PLANE COUPLED SHEAR WALLS UNDER DYNAMIC LOADING

3.1 Introduction

In this chapter, the analysis of coupled shear walls under dynamic external loading is presented. The 'continuous' method of coupled shear wall analysis is extended into the regime of dynamics. Since the formulation given in Chapter 2 is in terms of the deflection variables of the piers, it is readily adaptable for dynamic analysis by taking into account the inertia effect of the piers. The derivation of the governing equation of motion and boundary conditions is given in Section 3.2. The governing equation takes the form of a pair of linear partial fourth-order coupled differential equations. In Section 3.3, the study is restricted to the aspect of free vibration of the structural system. Since the knowledge of the fundamental natural frequency is essential in seismic design by the spectrum technique, effort has been directed through normalizing and non-dimensionalizing procedures to arrive at a formulation for the normalized natural frequency which is readily soluble with the aid of a computer. In Section 3.4, this treatment is repeated for the case of a symmetric wall. Computerized results for the normalized natural frequency are presented in Section 3.5 in the form of design curves, followed by a discussion of the curves and of the non-dimensional

variables involved. The effect on the fundamental frequency by averaging the pier widths and the pier stiffnesses respectively to arrive at a substitutive symmetric system is examined in Section 3.6. It is shown that in the particular case considered, averaging the pier stiffnesses gives a better estimate of the fundamental frequency than averaging the widths of the piers. Finally, dynamic tests on a symmetric and an asymmetric model are described in Section 3.7. The experimentally determined frequencies are compared with the theoretical prediction; the agreement is found to be within 5%.

3.2 Derivation of Equation of Motion

In this derivation, the assumptions as given in Section 2.2 remain valid. If the external loading is time dependent: $w_1(x,t)$, $w_2(x,t)$, the deflections of the piers and the internal force distributions are also functions of time. Taking into account the inertial effect of the piers, the external moment expressions are

$$M_j(x,t) = \int_x^H (w_j - \rho_j \ddot{y}_j)(\bar{x}-x)\,d\bar{x} \quad (j = 1,2) \qquad (3.1)$$

where dots denote differentiation with respect to time t and ρ_j is taken as the mass of pier j plus half the mass of the connecting beams, per unit height of the shear wall. Substituting equation (3.1) into equation (2.45) and expressing the deflections in terms of $z_1(\xi,t)$ and $z_2(\xi,t)$ as in Section 2.3, the equation of motion can be written as

$$[L]\{Z\}' + \frac{H^4 A_b}{hc}\begin{bmatrix} 0 & 0 \\ 0 & 4 \end{bmatrix}\{Z\} + \frac{H^4}{E}\begin{bmatrix} \rho & \tilde{\rho} \\ \tilde{\rho} & \rho \end{bmatrix}\ddot{\{Z\}}$$

$$- \frac{\alpha^2 H^4}{EA}\int_\xi^1 \begin{bmatrix} \rho & \tilde{\rho} \\ \frac{\tilde{a}}{a}\rho & \frac{\tilde{a}}{a}\tilde{\rho} \end{bmatrix}\ddot{\{Z\}}\,(\bar{x}-\xi)\,d\bar{x} = \frac{H^4}{E}\begin{Bmatrix} w - \frac{\alpha^2}{A}\int_\xi^1 w(\bar{x}-\xi)\,d\bar{x} \\ \tilde{w} - \frac{\alpha^2 \tilde{a}}{aA}\int_\xi^1 w(\bar{x}-\xi)\,d\bar{x} \end{Bmatrix} \qquad (3.2)$$

where $\rho = \rho_1 + \rho_2$ (3.3)

$$\tilde{\rho} = \rho_1 - \rho_2 \tag{3.4}$$

$$w = w_1 + w_2 \tag{3.5}$$

$$\tilde{w} = w_1 - w_2 \tag{3.6}$$

The corresponding boundary conditions can be obtained in a similar manner from equations (2.52) through (2.55) as

$$\text{at } \xi = 0 \qquad \{\mathbf{Z}\} = \{0\} \tag{3.7}$$

$$\{Z\}' = \{0\} \tag{3.8}$$

$$\text{at } \xi = 1 \qquad \{Z\}'' = \{0\} \tag{3.9}$$

$$[L]\ \{Z\} - \frac{\alpha^2 H^4}{EA} \int_0^1 \int_\xi^1 \begin{bmatrix} \rho & \tilde{\rho} \\ \frac{\tilde{a}}{a}\rho & \frac{\tilde{a}}{a}\tilde{\rho} \end{bmatrix} \ddot{\{\mathbf{Z}\}}\ (\bar{x} - \xi)\ d\bar{x}d\xi$$

$$= \frac{-\alpha^2 H^4}{EA} \begin{Bmatrix} 1 \\ \frac{\tilde{a}}{a} \end{Bmatrix} \int_0^1 \int_\xi^1 w(\bar{x}-\xi)\ d\bar{x}d\xi \tag{3.10}$$

Thus, the study of dynamics of coupled shear walls subjected to time dependent lateral loading reduces to the solution of equation (3.2) subjected to boundary conditions (3.7) through (3.10).

3.3 Free Vibration

One of the parameters that is essential to the response analysis of any elastic structure is the natural frequency of that system. In particular, the fundamental natural frequency is of importance because of its role in seismic design by the spectrum technique. In the following, the fundamental frequency of coupled shear walls is studied in detail.

For free vibration, there are no external loadings, i.e.

$$w_1 = w_2 = 0 \tag{3.11}$$

Seeking a solution of the form

$$\{Z(\xi,t)\} = \{\eta(\xi)\}e^{i\omega t} \tag{3.12}$$

where ω is the natural frequency of the coupled shear wall and substituting equation (3.12) into equation (3.2), the equation for free vibration takes the form

$$[L]\{\eta\}' + \frac{H^4 A_b}{hc}\begin{bmatrix} 0 & 0 \\ 0 & 4 \end{bmatrix}\{\eta\} - \frac{\omega^2 H^4}{E}\begin{bmatrix} \rho & \tilde{\rho} \\ \tilde{\rho} & \rho \end{bmatrix}\{\eta\} + \frac{\omega^2\alpha^2 H^4}{EA}\int_\xi^1 \begin{bmatrix} \rho & \tilde{\rho} \\ \frac{\tilde{a}}{a}\rho & \frac{\tilde{a}}{a}\tilde{\rho} \end{bmatrix}\{\eta\}(\bar{x}-\xi)\,d\bar{x} = \{0\} \tag{3.13}$$

Equation (3.13) is a pair of linear coupled homogeneous integro-differential equations. For case of solution, it is convenient to reduce equation (3.13) into a pair of sixth-order differential equations. Differentiating equation (3.13) twice with respect to ξ, it is obtained

$$[L]\{\eta\}''' + \frac{H^4A_b}{hc}\begin{bmatrix}0 & 0\\ 0 & 4\end{bmatrix}\{\eta\}'' - \frac{\omega^2H^4}{E}\begin{bmatrix}\rho & \tilde{\rho}\\ \tilde{\rho} & \rho\end{bmatrix}\{\eta\}'' + \frac{\omega^2\alpha^2H^4}{EA}\begin{bmatrix}\rho & \tilde{\rho}\\ \frac{\tilde{a}}{a}\rho & \frac{\tilde{a}}{a}\tilde{\rho}\end{bmatrix}\{\eta\} = \{0\} \tag{3.14}$$

The boundary conditions to be satisfied can be obtained from equations (3.7) through (3.10):

$$\text{at } \xi = 0 \qquad \{\eta\} = \{0\} \tag{3.15}$$

$$\{\eta\}' = \{0\} \tag{3.16}$$

$$\text{at } \xi = 1 \qquad \{\eta\}'' \ \{0\} \tag{3.17}$$

$$[L]\{\eta\} + \frac{\omega^2\alpha^2H^4}{EA}\int_0^1\int_\xi^1 \begin{bmatrix}\rho & \tilde{\rho}\\ \frac{\tilde{a}}{a}\rho & \frac{\tilde{a}}{a}\tilde{\rho}\end{bmatrix}\{\eta\}\,(\bar{x}-\xi)\,d\bar{x}\,d\xi = \{0\} \tag{3.18}$$

Since equation (3.14) is of the sixth order, two additional pairs of boundary conditions are required to determine its solution. The additional boundary conditions can be obtained from equation (3.13) and its derivative, evaluating at $\xi = 1$, namely,

$$\text{at } \xi = 1 \quad [L]\{\eta\}' + \frac{H^4A_b}{hc}\begin{bmatrix}0 & 0\\ 0 & 4\end{bmatrix}\{\eta\} - \frac{\omega^2H^4}{E}\begin{bmatrix}\rho & \tilde{\rho}\\ \tilde{\rho} & \rho\end{bmatrix}\{\eta\} = \{0\} \tag{3.19}$$

$$[L]\{\eta\}'' + \frac{H^4A_b}{hc}\begin{bmatrix}0 & 0\\ 0 & 4\end{bmatrix}\{\eta\}' - \frac{\omega^2H^4}{E}\begin{bmatrix}\rho & \tilde{\rho}\\ \tilde{\rho} & \rho\end{bmatrix}\{\eta\}' = \{0\} \tag{3.20}$$

Thus, the determination of the natural frequency ω reduces to the solution of equation (3.14) subjected to boundary conditions (3.15) through (3.20).

To reduce the equations to non-dimensional form, the geometry of the coupled shear wall is normalized with respect to the length of the connecting beam c as follows

$$d_j = D_j c \quad (j = 1,2) \tag{3.21}$$

$$d_b = D_b c \tag{3.22}$$

$$h = \bar{H} c \tag{3.23}$$

where D_j, D_b and $\bar{H}$ are the normalized width of pier j, depth of connecting beam and floor height respectively. The natural frequency of the coupled shear wall is normalized with respect to the first frequency of lateral vibration of a cantilever beam having the stiffness of a pier and the mass equal to the mass of the pier plus half of the mass of attached connecting beams. Mathematically, this can be written as

$$\omega = \Omega_j \, \omega_{oj} \quad (j = 1,2) \tag{3.24}$$

where Ω_j is the normalized frequency, and

$$\omega_{oj} = \frac{3.52}{H^2} \sqrt{\frac{EI_j}{\rho_j}} \tag{3.25}$$

The relationship between Ω_1 and Ω_2 can be expressed in terms of the previously defined non-dimensional parameters as

$$\Omega_2^2 = \frac{D_1^3}{D_2^3} \left(\frac{D_b + 2\bar{H}D_2}{D_b + 2\bar{H}D_1} \right) \Omega_1^2 \tag{3.26}$$

From the seven basic non-dimensional parameters: N, D_1, D_2, D_b, $\bar{H}$, Ω_1 and Ω_2, the following parameters are defined as

$$n_1 = D_1^3 + D_2^3 \tag{3.27}$$

$$n_2 = D_1^3 - D_2^3 \tag{3.28}$$

$$n_3 = N^2 \bar{H} D_b^3 \tag{3.29}$$

$$n_4 = 1 + 1.2\, D_b^2 \left(\frac{E}{G}\right) \tag{3.30}$$

$$n_5 = N^4 \bar{H}^3 D_b \tag{3.31}$$

$$n_6 = (D_1 + D_2 + 2) \tag{3.32}$$

$$n_7 = D_1 - D_2 \tag{3.33}$$

$$n_8 = \frac{1}{D_1} + \frac{1}{D_2} \tag{3.34}$$

$$n_9 = \Omega_1^2 D_1^3 + \Omega_2^2 D_2^3 \tag{3.35}$$

$$n_{10} = \Omega_1^2 D_1^3 - \Omega_2^2 D_2^3 \tag{3.36}$$

The differential equation (3.14) and boundary conditions (3.15) through (3.20) can then be written in terms of n_j ($j = 1,2,\ldots,10$) as

$$[P]\,\{\eta\}^{vi} + [Q]\,\{\eta\}^{iv} + [R]\,\{\eta\}'' + [S]\,\{\eta\} = \{0\} \tag{3.37}$$

$$\text{at } \xi = 0 \qquad \{\eta\} = \{0\} \tag{3.38}$$

$$\{\eta\}' = \{0\} \tag{3.39}$$

$$\text{at } \xi = 1 \qquad \{\eta\}'' = \{0\} \tag{3.40}$$

$$[P]\{\eta\}''' + [Q]\{\eta\}' + [S]\int_0^1\int_\xi^1 \{\eta\}(\bar{x} - \xi)d\bar{x}\, d\xi = \{0\} \qquad (3.41)$$

$$[P]\{\eta\}^{iv} + [Q]\{\eta\}'' + [R]\{\eta\} = \{0\} \qquad (3.42)$$

$$[p]\{\eta\}^{v} + [Q]\{\eta\}''' + [R]\{\eta\}' = \{0\} \qquad (3.43)$$

where
$$[P] = \begin{bmatrix} n_1 & n_2 \\ n_2 & n_1 \end{bmatrix} \qquad (3.44)$$

$$[Q] = \frac{-n_3}{n_4}\begin{bmatrix} 3n_6^2 + n_1n_8 & 3n_6n_7 + n_2n_8 \\ 3n_6n_7 + n_1n_8\,\frac{n_7}{n_6} & 3n_7^2 + n_2n_8\,\frac{n_7}{n_6} + 4n_4 \end{bmatrix} \qquad (3.45)$$

$$[R] = -\begin{bmatrix} 12.4\ n_9 & 12.4\ n_{10} \\ 12.4\ n_{10} & 12.4\ n_9 - 48n_5 \end{bmatrix} \qquad (3.46)$$

$$[S] = \frac{12.4\ n_3n_8}{n_4}\begin{bmatrix} n_9 & n_{10} \\ \frac{n_7}{n_6}\,n_9 & \frac{n_7}{n_6}\,n_{10} \end{bmatrix} \qquad (3.47)$$

Thus, in non-dimensional form, the problem reduces to the solution of equation (3.37) subjected to boundary conditions (3.38) through (3.43). The solution to equation (3.37) can be obtained by seeking a solution of the form

$$\{\eta\} = \{\Phi\}e^{\lambda\xi} \qquad (3.48)$$

Substituting equation (3.48) into equation (3.37) leads to

$$[\lambda^6[P] + \lambda^4[Q] + \lambda^2[R] + [S]]\{\Phi\} = \{0\} \qquad (3.49)$$

where, for non-trivial solutions, the determinant of the matrix $[\lambda^6[P] + \lambda^4[Q] + \lambda^2[R] + [S]]$ must be zero yielding a twelve degree characteristic equation in λ as

$$\lambda^{12}(P_{11}P_{22}-P_{12}P_{21})+ \lambda^{10}(P_{11}Q_{22}+Q_{11}P_{22}-P_{21}Q_{12}-Q_{21}P_{12})+\lambda^8(P_{11}R_{22}$$
$$+Q_{11}Q_{22}+R_{11}P_{22}-P_{21}R_{12}-Q_{21}Q_{12}-R_{21}P_{12})+ \lambda^6(P_{11}S_{22}+Q_{11}R_{22}$$
$$+R_{11}Q_{22}+S_{11}P_{22}-P_{21}S_{12}-Q_{21}R_{12}-R_{21}Q_{12}-S_{21}P_{12})+ \lambda^4(Q_{11}S_{22}$$
$$+R_{11}R_{22}+S_{11}Q_{22}-Q_{21}S_{12}-R_{21}R_{12}-S_{21}Q_{12})+ \lambda^2(R_{11}S_{22}+S_{11}R_{22}$$
$$-R_{21}S_{12}-S_{21}R_{12})+ \lambda^0(S_{11}S_{22}-S_{12}S_{21}) = 0 \qquad (3.50)$$

where P_{ij} $(i,j = 1,2)$ represents element ij in matrix [P]

Let the roots of the characteristic equation be $\lambda_i (i = 1,2,\ldots,12)$ and the associated vector corresponding to λ_i be denoted by $\{\Phi\}_i$. From equation (3.49), $\{\Phi\}_i$ can be determined up to an arbitrary constant K_i. It should be noted from equations (3.47) and (3.50) that since the determinant of matrix [S] is always zero, a double root of $\lambda = 0$ results. Let λ_{11} and $\lambda_{12} = 0$, then

$$\{\Phi\}_{11} = \{\Phi\}_{12} = \begin{Bmatrix} 1 \\ n_9 \\ \hline n_{10} \end{Bmatrix} \qquad (3.51)$$

Hence, the general solution of equation (3.37) can be written as

$$\{\eta\} = \sum_{i=1}^{10} K_i \{\Phi\}_i e^{\lambda_i \xi} + (K_{11} + K_{12}\xi) \{\Phi\}_{11} \tag{3.52}$$

Substituting equation (3.52) into the boundary conditions (3.38) through (3.43) gives twelve homogeneous linear algebraic equations for the constants K_i (i = 1,2,...,12) as follows

$$\sum_{i=1}^{11} K_i \{\Phi\}_i = \{0\} \tag{3.53}$$

$$\sum_{i=1}^{10} K_i \lambda_i \{\Phi\}_i + K_{12}\{\Phi\}_{11} = \{0\} \tag{3.54}$$

$$\sum_{i=1}^{10} K_i \lambda_i^2 \{\Phi\}_i e^{\lambda_i} = \{0\} \tag{3.55}$$

$$\sum_{i=1}^{10} K_i \left[\lambda_i^3 [P] + \lambda_i [Q] + [S] \left(\frac{1}{2\lambda_i} - \frac{1}{\lambda_i^2} + \frac{1}{\lambda_i^3} - \frac{1}{\lambda_i^3 e^{\lambda_i}}\right)\right]$$

$$\{\Phi\}_i e^{\lambda_i} + \frac{1}{6} K_{11}[S]\{\Phi\}_{11} + K_{12}\left[[Q] + \frac{1}{8}[S]\right] \{\Phi\}_{11} = \{0\} \tag{3.56}$$

$$\sum_{i=1}^{10} K_i \left[\lambda_i^4 [P] + \lambda_i^2 [Q] + [R]\right]\{\Phi\}_i e^{\lambda_i} + (K_{11} + K_{12})[R]\{\Phi\}_{11} = \{0\} \tag{3.57}$$

$$\sum_{i=1}^{10} K_i \left[\lambda_i^5 [P] + \lambda_i^3 [Q] + \lambda_i [R]\right] \{\Phi\}_i e^{\lambda_i} + K_{12}[R]\{\Phi\}_{11} = \{0\} \tag{3.58}$$

The condition for determining the natural frequency is to require the determinant of the coefficients of K_i (i = 1,2,...,12) to be zero. The actual numerical evaluation of the natural frequency makes use of the trial and error technique. A value of Ω_i (i = 1 or 2) is assumed in equation (3.50) and the roots λ_i (i = 1,2,...,10) are determined.

The determinant of the coefficients of K_i ($i = 1,2,\ldots,12$) is then evaluated. In general, the determinant is not zero. The procedure is then repeated by assuming another value of Ω_i, until the determinant vanishes. An indication for this condition is when the value of the determinant changes sign between two successive trial frequencies. Knowing Ω_i ($i = 1$ or 2), the actual natural frequency can be obtained from equation (3.24).

3.4 Reduction to Wall of Equal Piers

In this section, the general formulation is reduced to the particular case of a coupled symmetric shear wall.

In addition to equations (2.62) through (2.66), symmetry also implies that

$$\rho_1 = \rho_2 = \rho_s \tag{3.59}$$

Substituting equations (2.62) through (2.66) and (3.59) in equation (3.2), the equation of motion takes the form of a pair of uncoupled equations, namely,

$$z_1^{iv} - \frac{6H^2 I_b a_s^2 \gamma_s}{hc^3\beta^2 I_s} z_1'' + \frac{H^4\rho_s}{EI_s}\ddot{z}_1 - \frac{24H^6 I_b \rho_s}{EA_s hc^3\beta^2 I_s}\int_\xi^1 \ddot{z}_1(\bar{x}-\xi)\, d\bar{x}$$
$$= \frac{H^4}{2EI_s} w - \frac{12H^6 I_b}{EA_s hc^3\beta^2 I_s}\int_\xi^1 w(\bar{x}-\xi)\, d\bar{x} \tag{3.60}$$

$$z_2^{iv} - \frac{2H^2 I_b}{hcI_s} z_2'' + \frac{2H^4 A_b}{hcI_s} z_2 + \frac{H^4\rho_s}{EI_s}\ddot{z}_2 = \frac{H^4}{2EI_s}\tilde{w} \tag{3.61}$$

By a similar substitution, the boundary conditions (from equations (3.7) through (3.10)) become

$$\text{at } \xi = 0 \qquad z_1 = 0 \tag{3.62}$$

$$z_2 = 0 \tag{3.66}$$

$$z_1' = 0 \tag{3.63}$$

$$z_2' = 0 \tag{3.67}$$

$$\text{at } \xi = 1 \qquad z_1'' = 0 \tag{3.64}$$

$$z_2'' = 0 \tag{3.68}$$

$$z_1''' - \frac{6H^2 I_b a_s^2 \gamma_s}{hc^3\beta^2 I_s} z_1' - \frac{24H^6 I_b \rho_s}{EA_s hc^3\beta^2 I_s} \int_0^1 \int_\xi^1 \ddot{z}_1 \, (\bar{x}-\xi) d\bar{x} d\xi$$

$$= - \frac{12H^6 I_b}{EA_s hc^3\beta^2 I_s} \int_0^1 \int_\xi^1 w(\bar{x}-\xi) \, d\bar{x} d\xi \tag{3.65}$$

$$z_2''' - \frac{2H^2 I_b}{hcI_s} z_2' = 0 \tag{3.69}$$

Equation (3.60) with boundary conditions (3.62) through (3.65) defines the antisymmetric mode response problem of a coupled symmetric shear wall under dynamic lateral loading. Equation (3.61) with boundary conditions (3.66) through (3.69) defines the symmetric mode response. From the practical point of view, the symmetric mode is seldom excited. It is the antisymmetric mode response that is being excited when the coupled symmetric shear wall is subjected to loadings such as wind and earthquake excitation.

In a similar pattern as in Section 3.3, the fundamental natural frequency of a symmetric coupled shear wall in its antisymmetric mode of vibration is considered. Setting the external loadings w_1 and w_2 to zero and seeking a solution of the form,

$$z_1(\xi,t) = \eta_s(\xi)e^{i\omega t} \tag{3.70}$$

equations (3.60) and (3.62) through (3.65) become

$$\eta_s^{iv} - \bar{\alpha}^2 \eta_s'' - \frac{\omega^2 H^4 \rho_s}{EI_s}\eta_s + \frac{24\omega^2 H^6 I_b \rho_s}{EA_s hc^3\beta^2 I_s}\int_\xi^1 \eta_s(\bar{x}-\xi)d\bar{x} = 0 \tag{3.71}$$

$$\text{at } \xi = 0 \qquad \eta_s = 0 \tag{3.72}$$

$$\eta_s' = 0 \tag{3.73}$$

$$\text{at } \xi = 1 \qquad \eta_s'' = 0 \tag{3.74}$$

$$\eta_s''' - \bar{\alpha}^2 \eta_s' + \frac{24\omega^2 H^6 I_b \rho_s}{EA_s hc^3\beta^2 I_s}\int_0^1\int_\xi^1 \eta_s(\bar{x}-\xi)d\bar{x}d\xi = 0 \tag{3.75}$$

Differentiating equation (3.71) twice with respect to ξ, it is obtained

$$\eta_s^{vi} - \bar{\alpha}^2 \eta_s^{iv} - \frac{\omega^2 H^4 \rho_s}{EI_s}\eta_s'' + \frac{24\omega^2 H^6 I_b \rho_s}{EA_s hc^3\beta^2 I_s}\eta_s = 0 \tag{3.76}$$

The additional boundary conditions can be obtained from equation (3.71) and its derivative, evaluating at $\xi = 1$, namely,

$$\text{at } \xi = 1 \qquad \eta_s^{iv} - \bar{\alpha}^2 \eta_s'' - \frac{\omega^2 H^4 \rho_s}{EI_s}\eta_s = 0 \tag{3.77}$$

$$\eta_s^{v} - \bar{\alpha}^2 \eta_s''' - \frac{\omega^2 H^4 \rho_s}{EI_s} \eta_s' = 0 \qquad (3.78)$$

Thus, the determination of the natural frequency ω reduces to the solution of equation (3.76) subjected to boundary conditions (3.72) through (3.75), (3.77) and (3.78)

To reduce the equations to non-dimensional form, the geometry of the coupled shear wall is normalized with respect to the length of the connecting beam c as

$$d_s = D_s c \qquad (3.79)$$

$$d_b = D_b c \qquad (3.22)$$

$$h = \bar{H} c \qquad (3.23)$$

where D_s is the normalized width of the pier. Normalizing the natural frequency as in Section 3.3, the expression becomes

$$\omega = \Omega_s \omega_o \qquad (3.80)$$

where Ω_s is the normalized frequency of the symmetric wall and

$$\omega_o = \frac{3.52}{H^2} \sqrt{\frac{EI_s}{\rho_s}} \qquad (3.81)$$

From the five basic non-dimensional parameters: N_1, D_s, D_b, $\bar{H}$ and Ω_s, γ_s and $\bar{\alpha}^2$ can be written as

$$\gamma_s = 1 + \frac{1}{3(1+\frac{1}{D_s})^2} \qquad (3.82)$$

$$\bar{\alpha}^2 = \frac{6N^2 \bar{H} D_b^3 [(1+\frac{1}{D_s})^2 + \frac{1}{3}]}{D_s [1+1.2 D_b^2 (\frac{E}{G})]} \qquad (3.83)$$

The differential equation (3.76) and boundary conditions (3.72) through (3.75), (3.77) and (3.78) can be expressed as

$$\eta_s^{vi} - \bar{\alpha}^2 \eta_s^{iv} - 12.4 \Omega_s^2 \eta_s'' + 12.4 \bar{\alpha}^2 (1-\frac{1}{\gamma_s}) \Omega_s^2 \eta_s = 0 \qquad (3.84)$$

$$\text{at } \xi = 0 \qquad \eta_s = 0 \tag{3.85}$$

$$\eta_s' = 0 \tag{3.86}$$

$$\text{at } \xi = 1 \qquad \eta_s'' = 0 \tag{3.87}$$

$$\eta_s''' - \bar{\alpha}^2\eta_s' + 12.4\bar{\alpha}^2\left(1-\frac{1}{\gamma_s}\right)\Omega_s^2\int_0^1\int_\xi^1 \eta_s(\bar{x}-\xi)\,d\bar{x}\,d\xi = 0 \tag{3.88}$$

$$\eta_s^{iv} - \bar{\alpha}^2\eta_s'' - 12.4\Omega_s^2\eta_s = 0 \tag{3.89}$$

$$\eta_s^{v} - \alpha^2\eta_s''' - 12.4\Omega_s^2\eta_s' = 0 \tag{3.90}$$

The solution to equation (3.84) can be obtained by seeking a solution of the form

$$\eta_s = e^{\lambda\xi} \tag{3.91}$$

Substituting equation (3.91) into equation (3.84) yields a sixth degree characteristic equation in λ given by

$$\lambda^6 - \bar{\alpha}^2\lambda^4 - 12.4\Omega_s^2\lambda^2 + 12.4\bar{\alpha}^2\left(1-\frac{1}{\gamma_s}\right)\Omega_s^2 = 0 \tag{3.92}$$

Let the roots of the characteristic equation be $\lambda_i (i = 1,2,\ldots,6)$. Then the general solution of equation (3.84) can be written as

$$\eta_s = \sum_{i=1}^{6} K_i e^{\lambda_i\xi} \tag{3.93}$$

where $K_i (i = 1,2,\ldots,6)$ are arbitrary constants. Substituting equation (3.93) into the boundary conditions (3.85) through (3.90) gives six homogeneous linear algebraic equations for the constants $K_i (i = 1,2,\ldots,6)$ as follows

$$\sum_{i=1}^{6} K_i = 0 \tag{3.94}$$

$$\sum_{i=1}^{6} K_i \lambda_i = 0 \tag{3.95}$$

$$\sum_{i=1}^{6} K_i \lambda_i^2 e^{\lambda_i} = 0 \tag{3.96}$$

$$\sum_{i=1}^{6} K_i \left[\lambda_i^3 - \bar{\alpha}^2 \lambda_i + 12.4\bar{\alpha}^2 \left(1-\frac{1}{\gamma_s}\right)\left(\frac{1}{2\lambda_i} - \frac{1}{\lambda_i^2} + \frac{1}{\lambda_i^3} - \frac{1}{\lambda_i^3 e^{\lambda_i}}\right) \Omega_s^2\right] e^{\lambda_i} = 0 \tag{3.97}$$

$$\sum_{i=1}^{6} K_i \left[\lambda_i^4 - \bar{\alpha}^2 \lambda_i^2 - 12.4\Omega_s^2\right] e^{\lambda_i} = 0 \tag{3.98}$$

$$\sum_{i=1}^{6} K_i \left[\lambda_i^5 - \bar{\alpha}^2 \lambda_i^3 - 12.4\Omega_s^2 \lambda_i\right] e^{\lambda_i} = 0 \tag{3.99}$$

The condition for determining the natural frequency is to require the determinant of the coefficients of $K_i (i=1,2,\ldots,6)$ to be zero. The procedure is the same as that in Section 3.3.

3.5 Design Curves

To obtain the fundamental natural frequency as described in Sections 3.3 and 3.4 is often laborious. In this Section, sets of design curves are presented so that the fundamental frequency of coupled shear walls of a wide variety of configurations can be obtained with relative ease.

To arrive at the fundamental frequency of coupled shear walls in the normalized form, six independent non-dimensional variables are invloved: the number of storeys N, the floor height to beam length ratio $\bar{H}$, the pier width to beam length ratio D_1 and D_2, the depth of beam to length of beam ratio D_b and the normalized frequency of one of the piers Ω_1 or Ω_2. For a symmetric wall, only five quantities are involved, namely, N, $\bar{H}$, D_s, D_b, and Ω_s. To cover the most practical configurations of coupled shear walls, N varies from 10 to 40 storeys; $\bar{H}$ ranges from 0.2 to 3.0; D_1 ranges from 0.50 to 2.0 while keeping D_2 at unity and D_b ranges from 1/16 to 1/4. Computer programs in Fortran IV language are written for the procedures described in Sections 3.3 and 3.4, and Appendix 1 gives the program for the asymmetric coupled shear wall. Computations were done on the CDC Model 6400 electronic computer and the results are presented in Figures 16 through 31, which represent sixteen sets of curves, four for each value of N where N = 10, 20, 30, and 40. For each N, sets of curves are

given for D_b = 1/4, 1/8, 1/12 and 1/16. Since D_2 is kept at unity, Ω_2 is plotted against $\bar{H}$ to show the effect on the fundamental frequency for various D_1's from 0.50 to 2.0. The bending to shear stiffness ratio $\frac{E}{G}$ is taken to be 2.60 corresponding to a Poisson ratio of 0.30. This choice is only for the sake of convenience, and it can be shown that the choice of Poisson ratio has little effect on the outcome of the normalized frequency.

For each set of curves, the general trend is logical. The normalized frequency is a monotonic increasing function with the floor height to length of beam ratio. This may be explained by the fact that as $\bar{H}$ decreases, the length of the connecting beam can be considered to increase (compared to the floor height), thereby resulting in a less stiff structure. On examining the frequency variation with D_1, a higher pier width to beam length ratio would imply a stiffer structure and therefore a higher frequency. The frequency variation with D_b can be explained in a similar manner.

Thus, knowing the normalized frequency, the actual fundamental frequency for a given coupled shear wall can be obtained from equations (3.24) or (3.80). It should be noted that a higher normalized frequency does not necessarily imply a higher actual frequency. This is especially true when comparing structures of different number of storeys, because of the normalizing procedure.

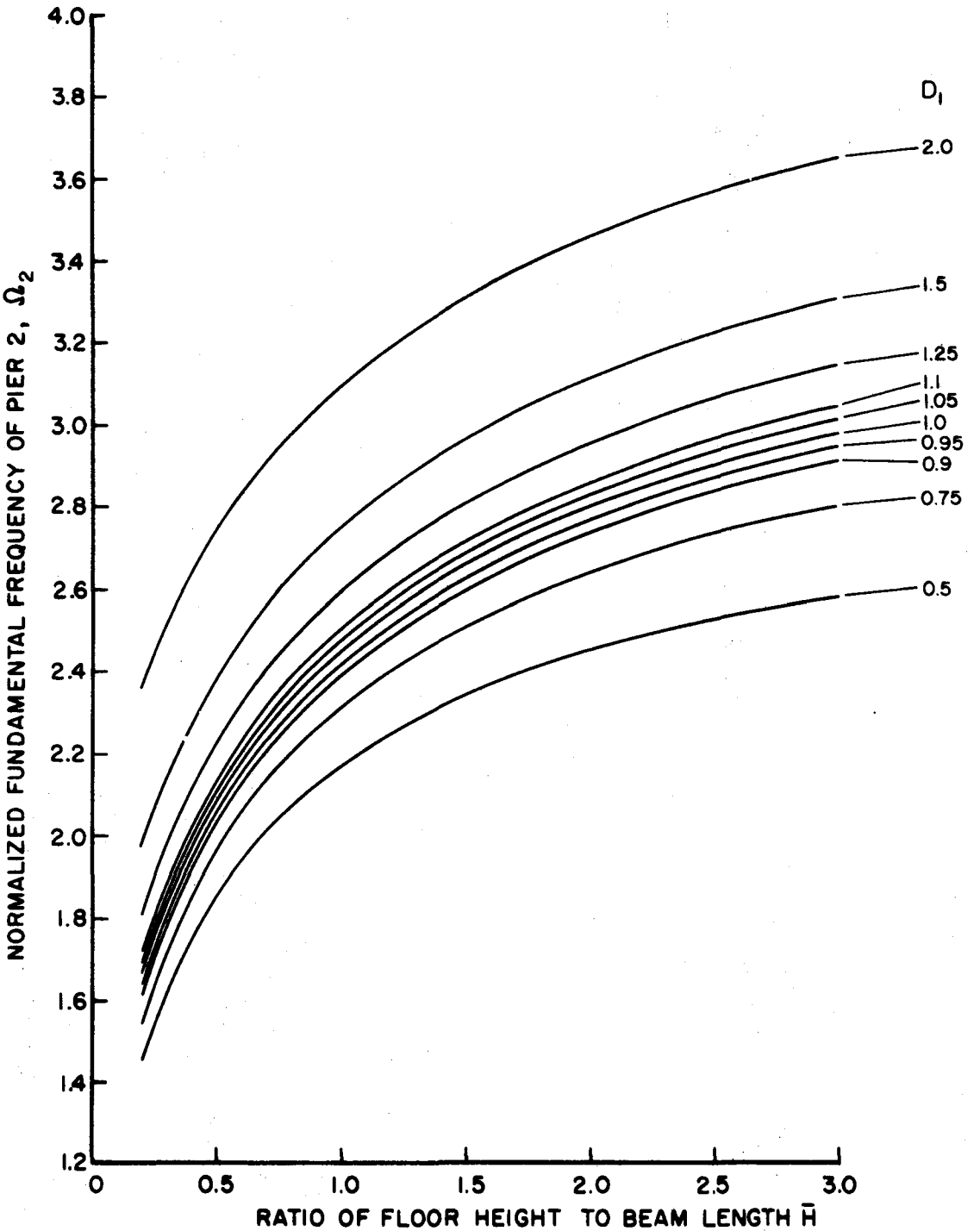

FIGURE 16. FUNDAMENTAL FREQUENCY DESIGN CURVES FOR COUPLED SHEAR WALLS WITH, N=10, D_2=1, D_b= 1/4

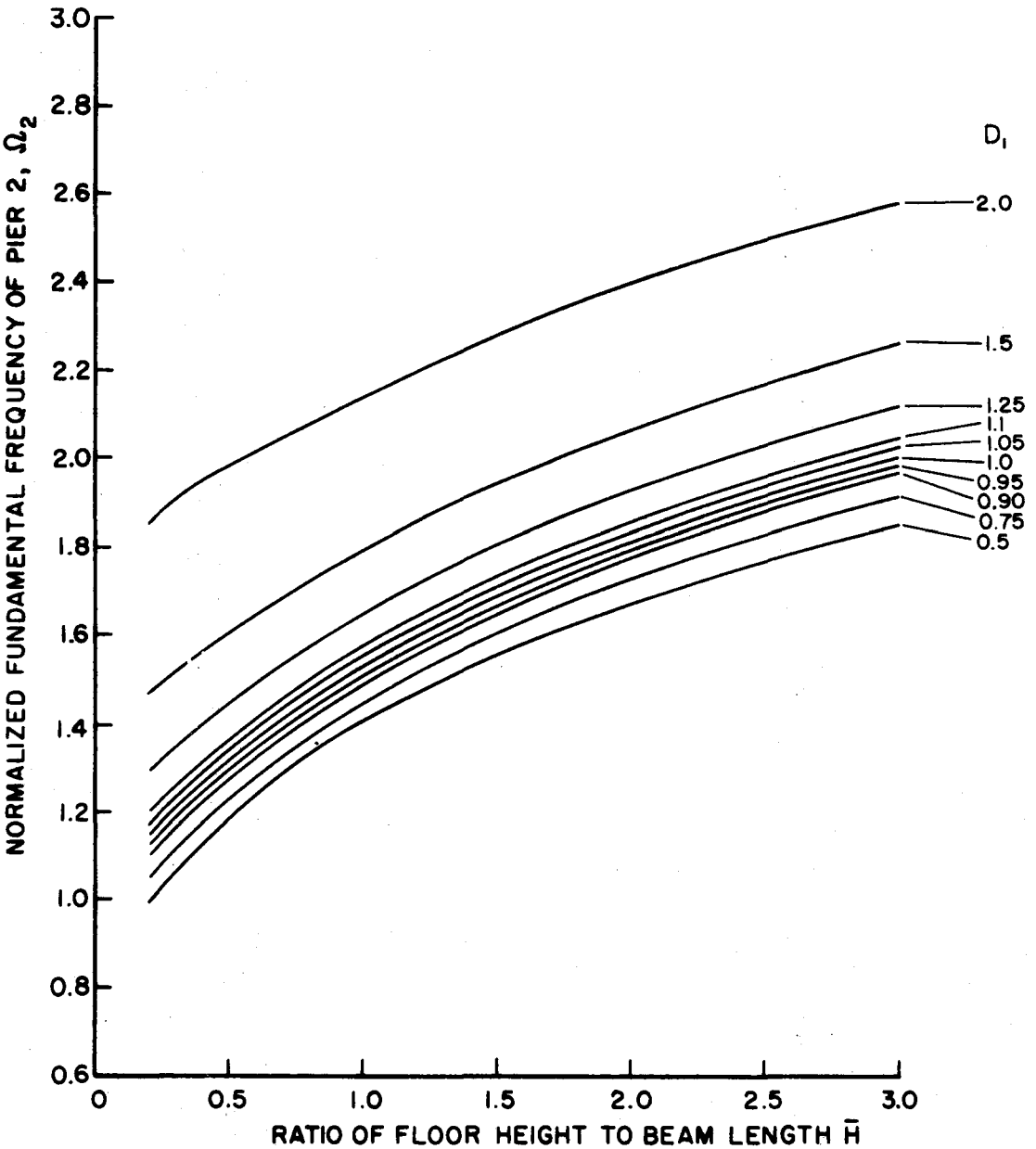

FIGURE 17. FUNDAMENTAL FREQUENCY DESIGN CURVES FOR COUPLED SHEAR WALLS WITH, $N=10$, $D_2=1$, $D_b=1/8$

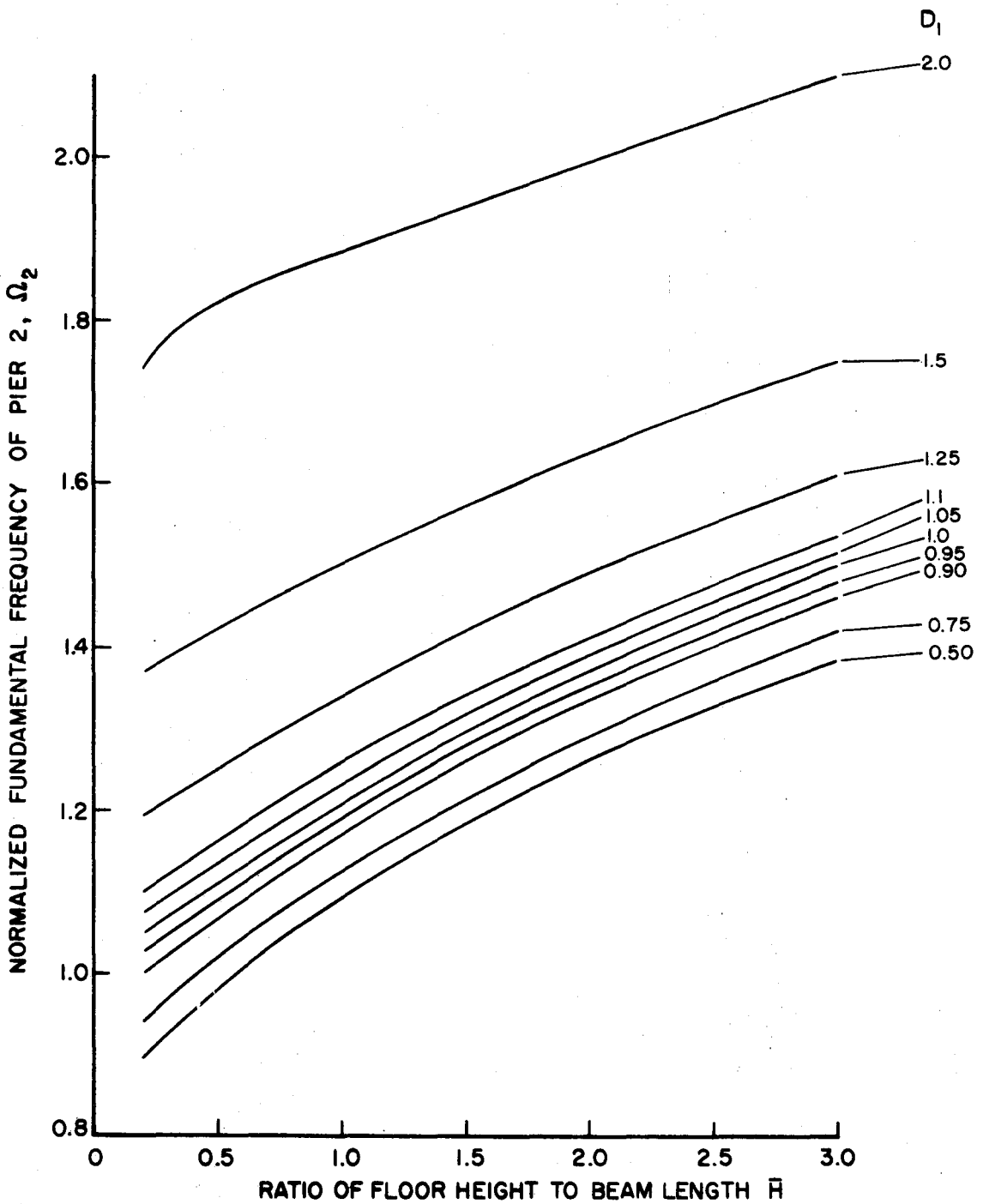

FIGURE 18. FUNDAMENTAL FREQUENCY DESIGN CURVES FOR COUPLED SHEAR WALLS WITH, N=10, $D_2=1$, $D_b = 1/12$

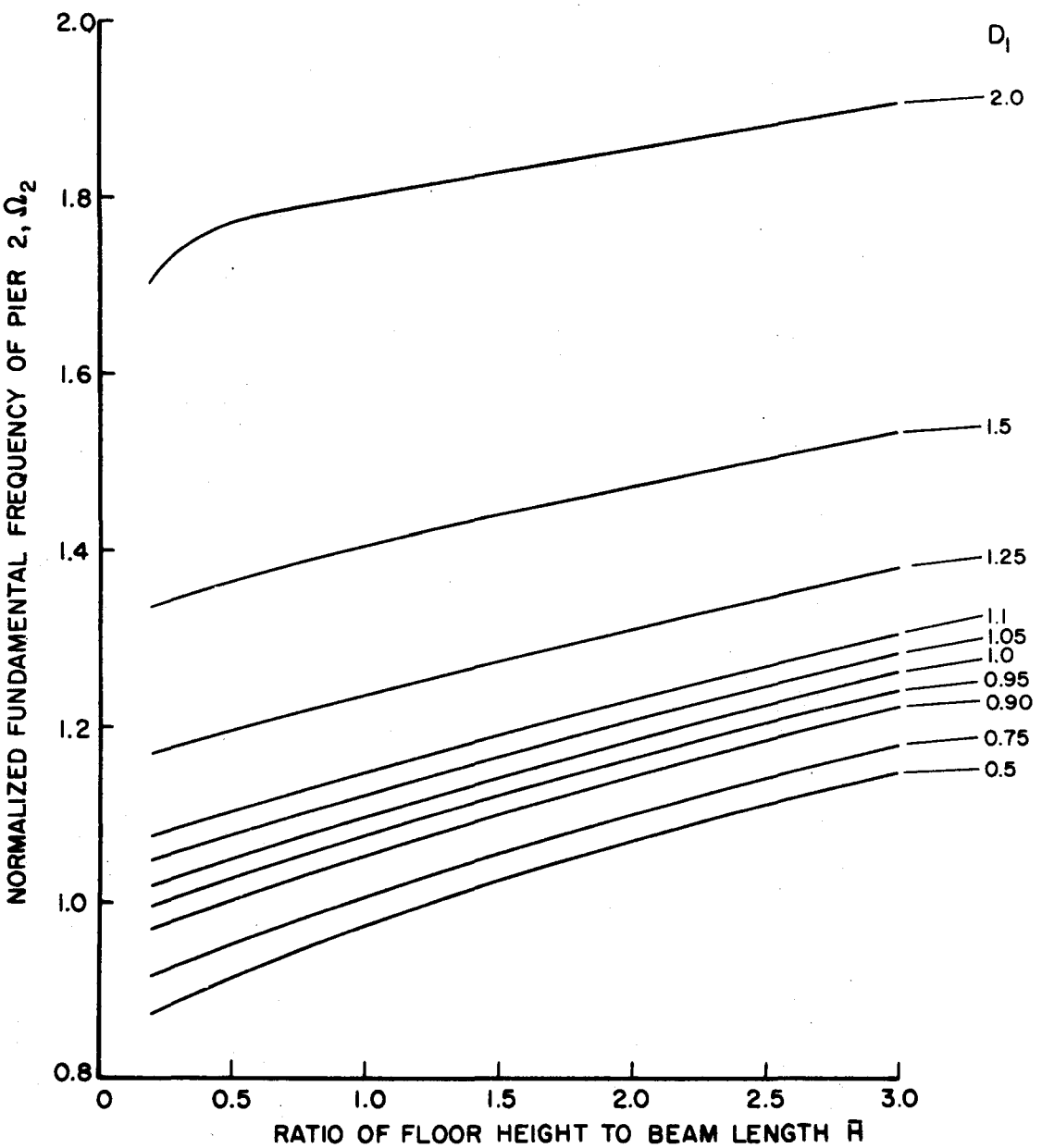

FIGURE 19. FUNDAMENTAL FREQUENCY DESIGN CURVES FOR COUPLED SHEAR WALLS WITH, N=10, $D_2 = 1$, $D_b = 1/16$

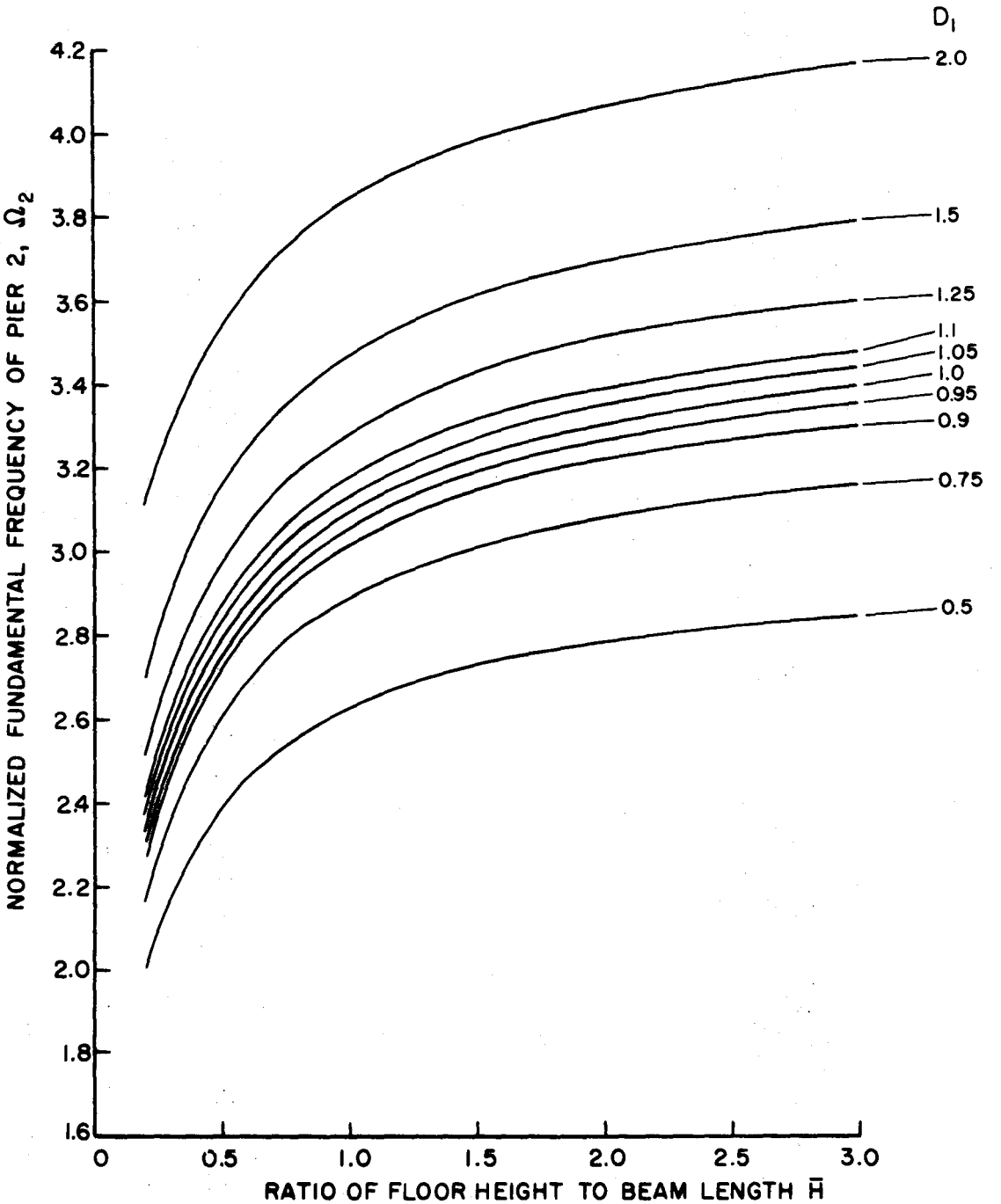

FIGURE 20. FUNDAMENTAL FREQUENCY DESIGN CURVES FOR COUPLED SHEAR WALLS WITH, N=20, $D_2 = 1$, $D_b = 1/4$

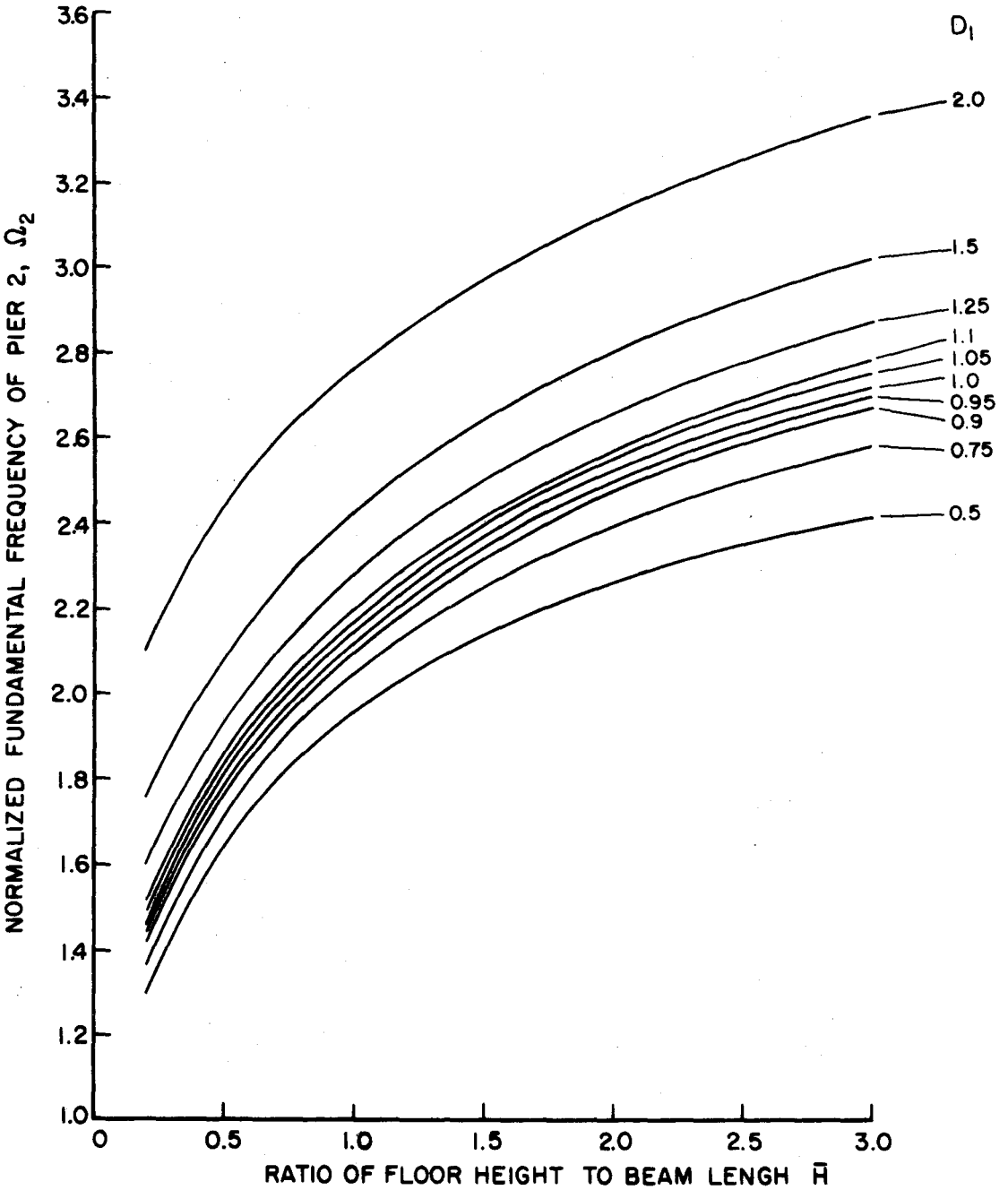

FIGURE 21. FUNDAMENTAL FREQUENCY DESIGN CURVES FOR COUPLED SHEAR WALLS WITH, $N=20$, $D_2=1$, $D_b=1/8$

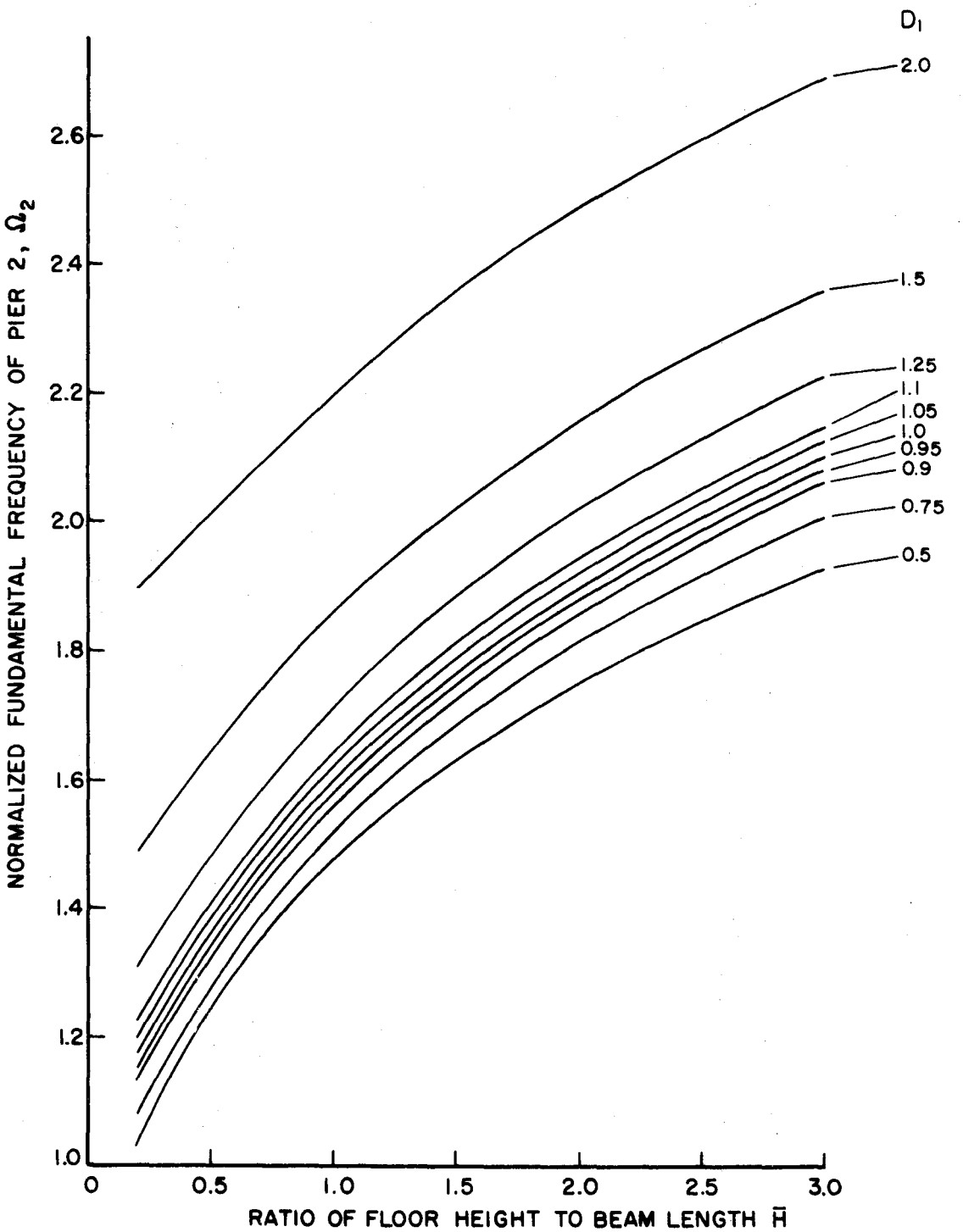

FIGURE 22. FUNDAMENTAL FREQUENCY DESIGN CURVES FOR COUPLED SHEAR WALLS WITH, $N=20$, $D_2=1$, $D_b=1/12$

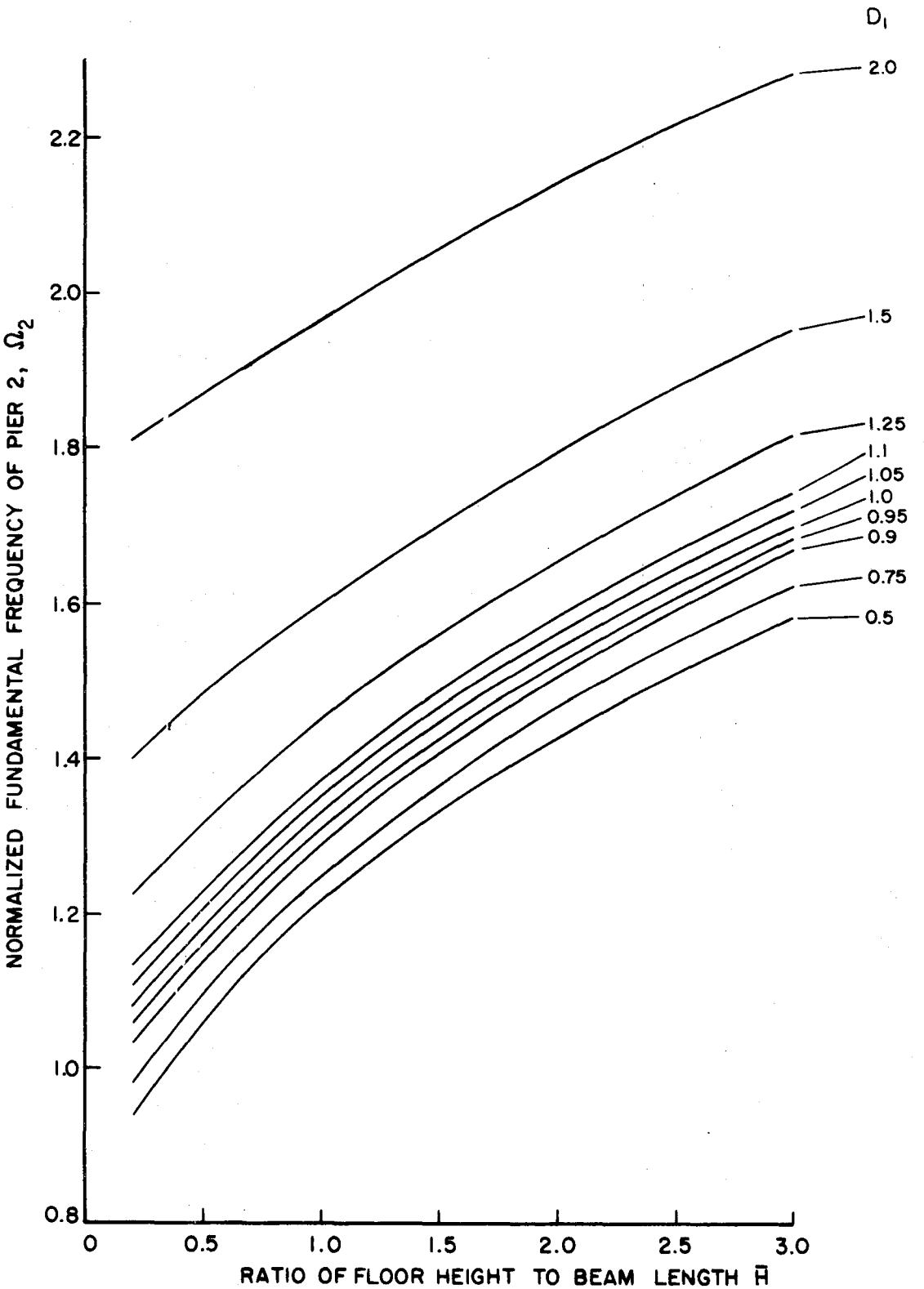

FIGURE 23. FUNDAMENTAL FREQUENCY DESIGN CURVES FOR COUPLED SHEAR WALLS WITH, $N=20$, $D_2=1$, $D_b=1/16$

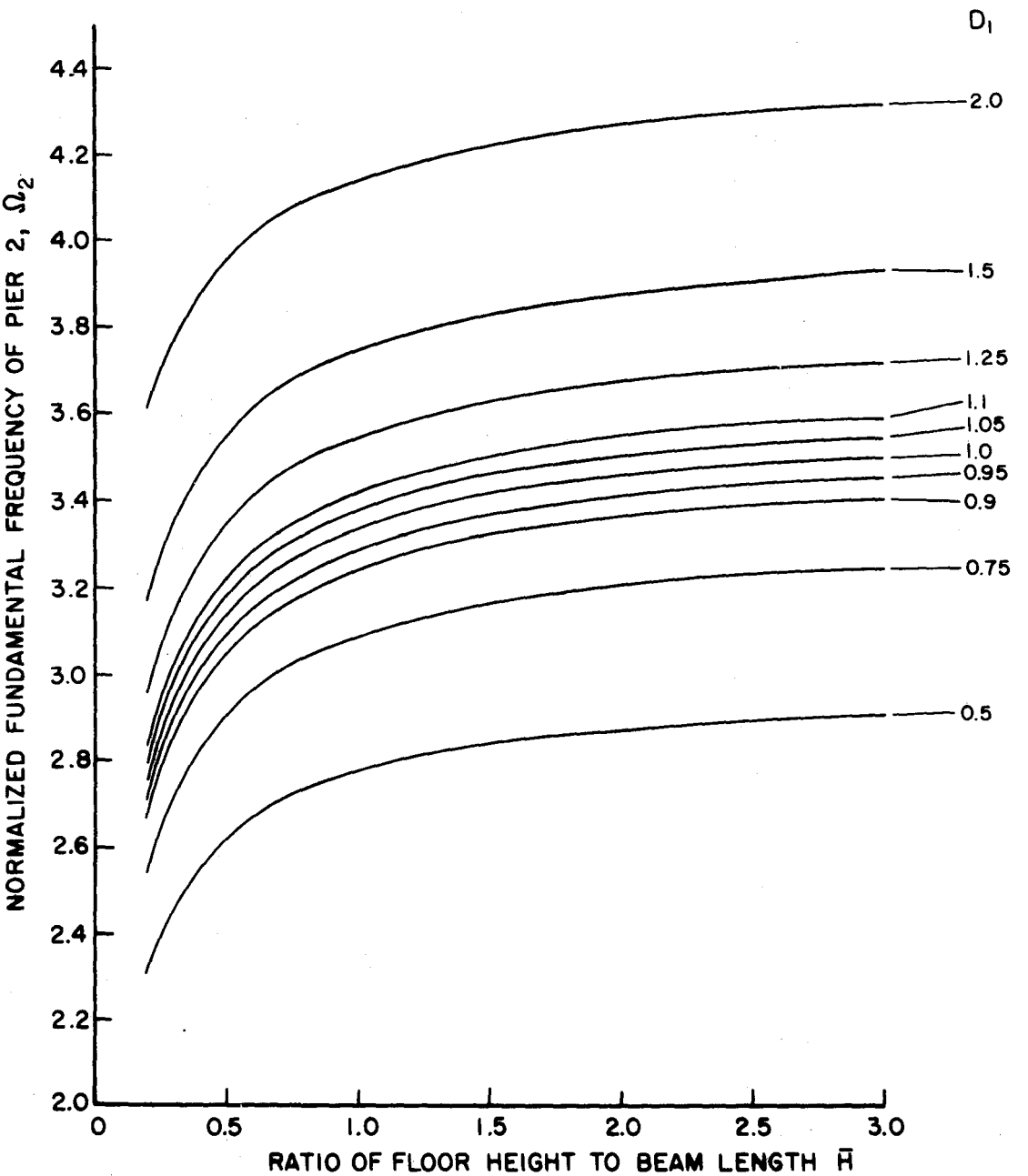

FIGURE 24. FUNDAMENTAL FREQUENCY DESIGN CURVES FOR COUPLED SHEAR WALLS WITH, N=30, D_2= 1, D_b= 1/4

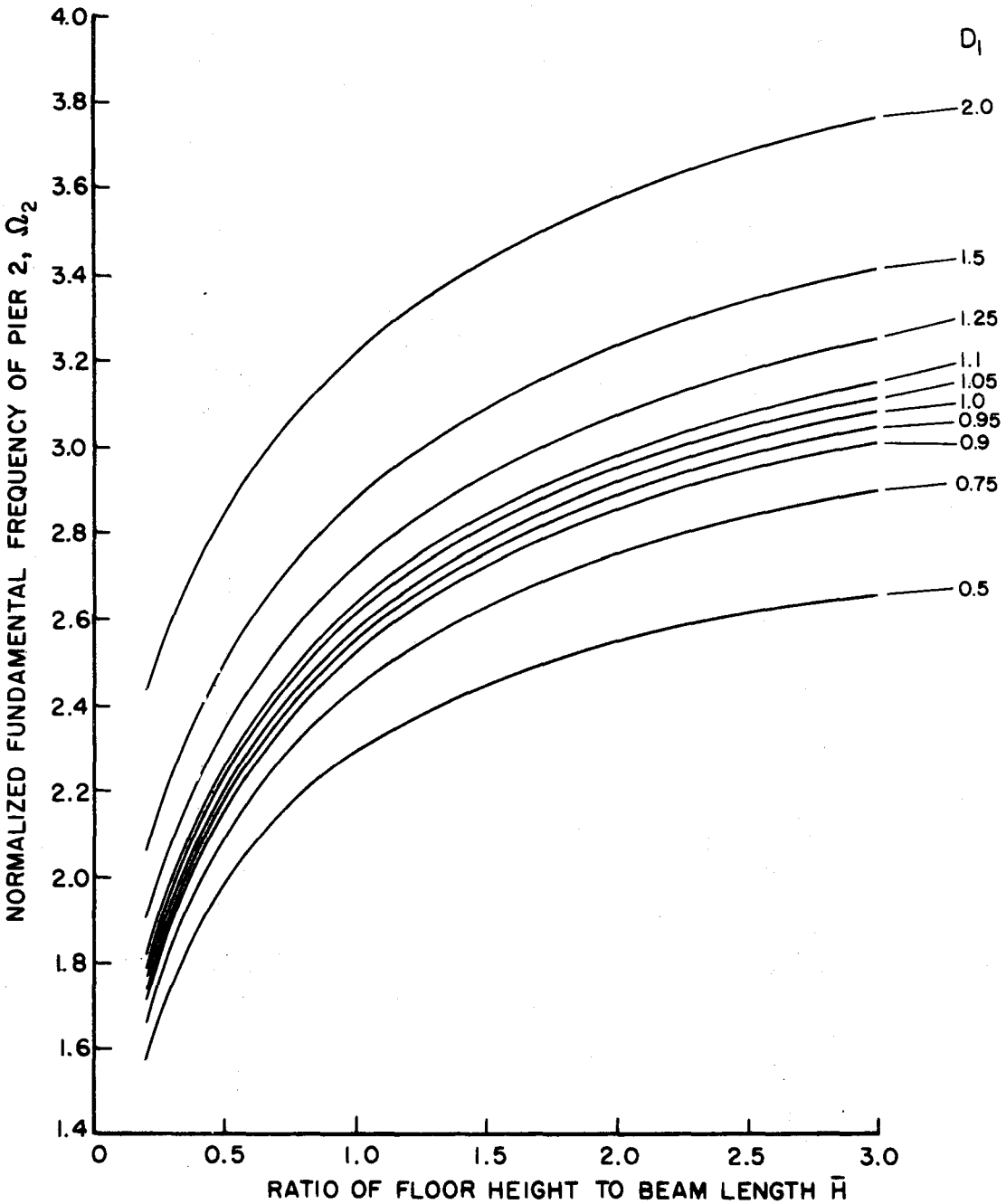

FIGURE 25. FUNDAMENTAL FREQUENCY DESIGN CURVES FOR COUPLED SHEAR WALLS WITH, $N=30$, $D_2=1$ $D_b=1/8$

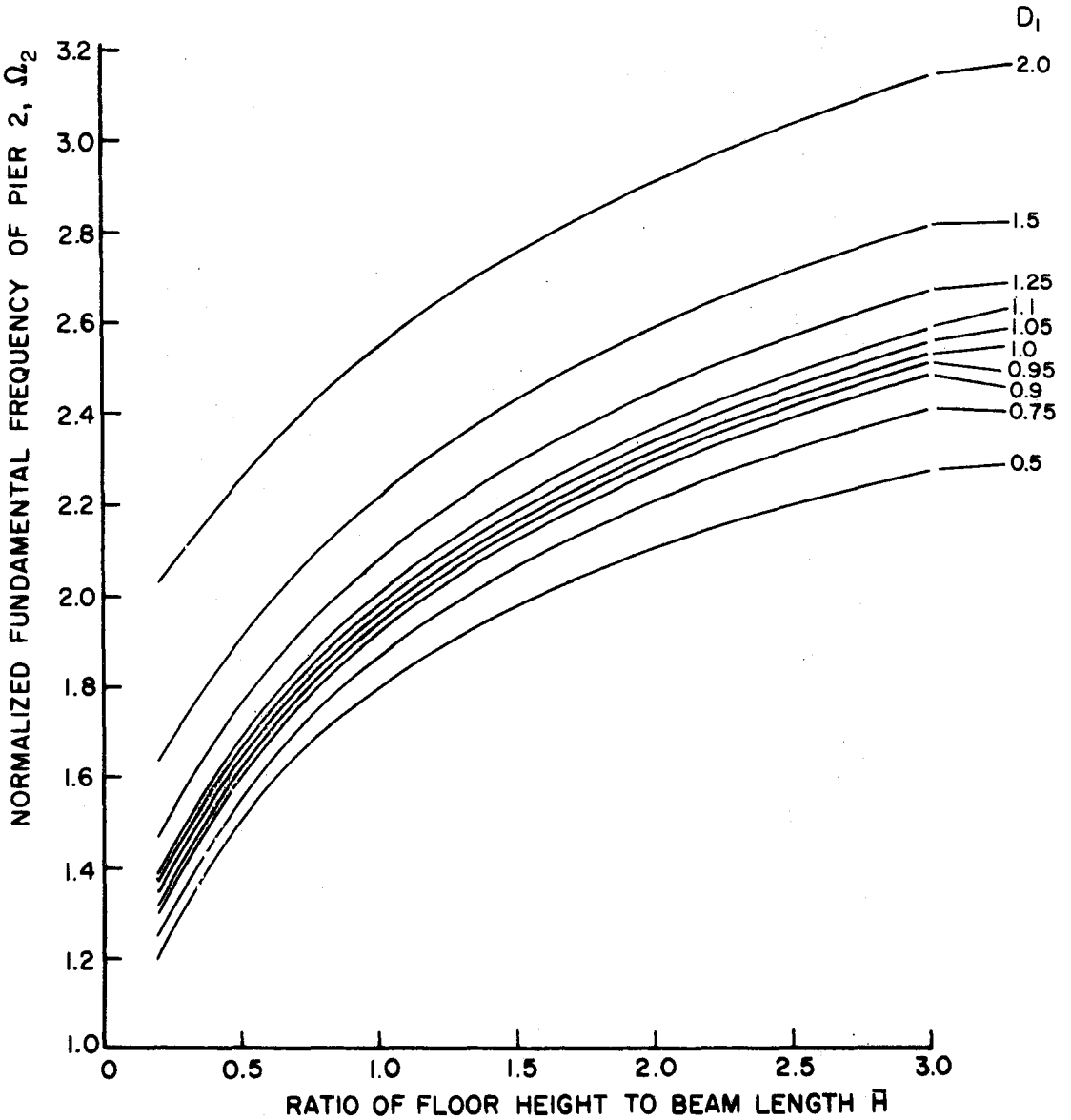

FIGURE 26. FUNDAMENTAL FREQUENCY DESIGN CURVES FOR COUPLED SHEAR WALLS WITH, N=30, D_2=1, D_b = 1/12

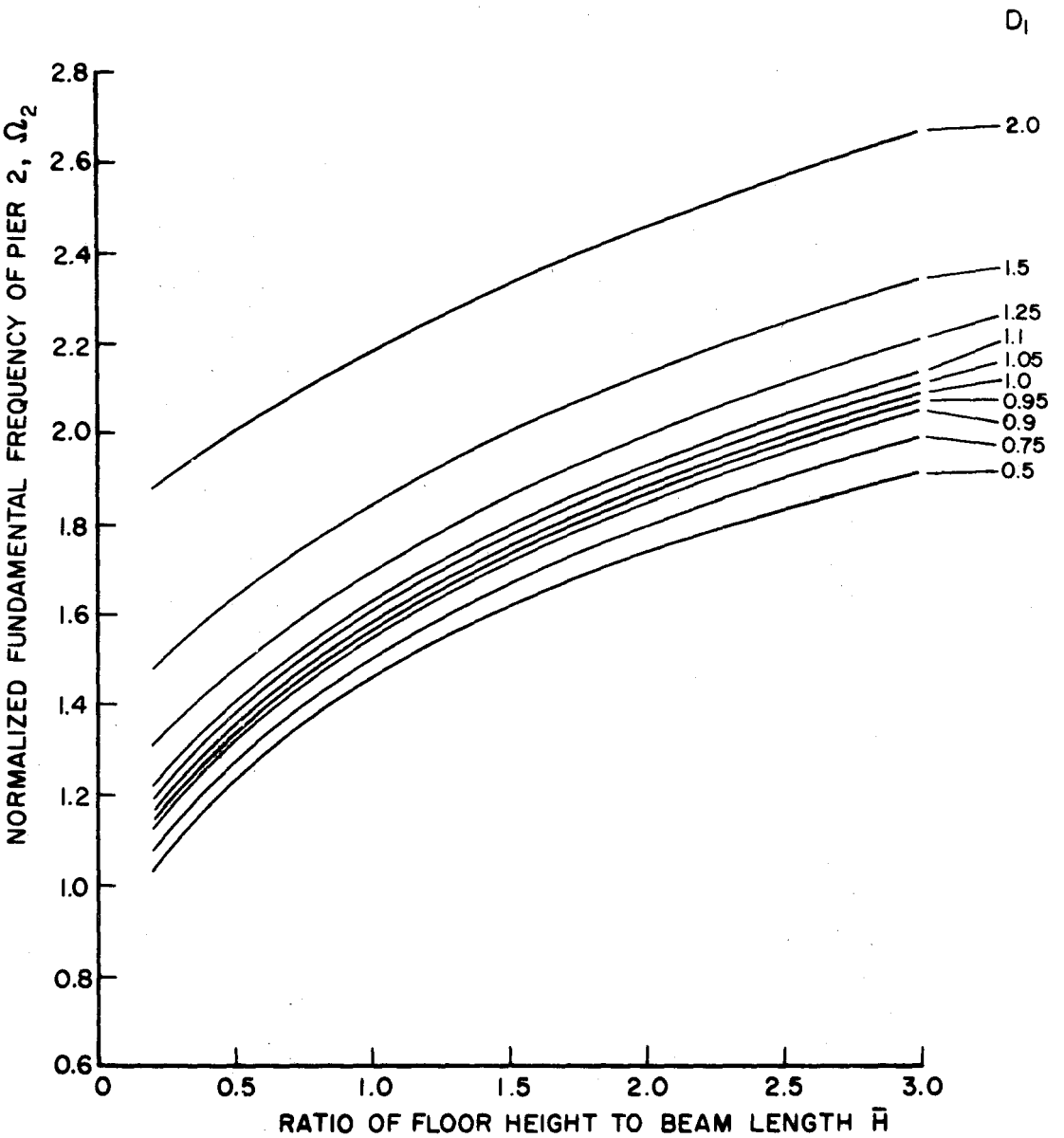

FIGURE 27. FUNDAMENTAL FREQUENCY DESIGN CURVES FOR COUPLED SHEAR WALLS WITH, $N=30$, $D_2=1$, $D_b=1/16$

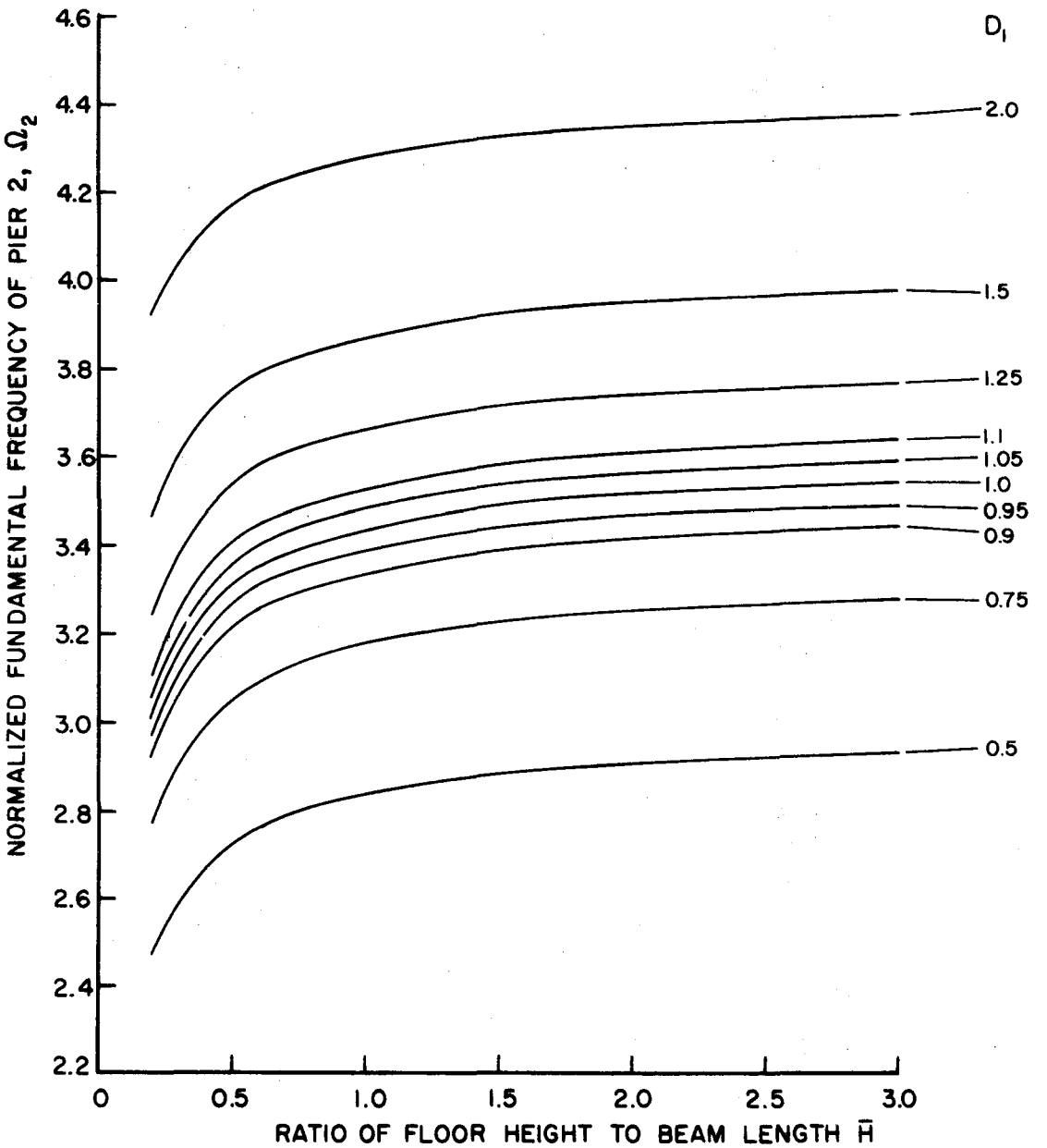

FIGURE 28. FUNDAMENTAL FREQUENCY DESIGN CURVES FOR COUPLED SHEAR WALLS WITH, $N=40$, $D_2=1$, $D_b=1/4$

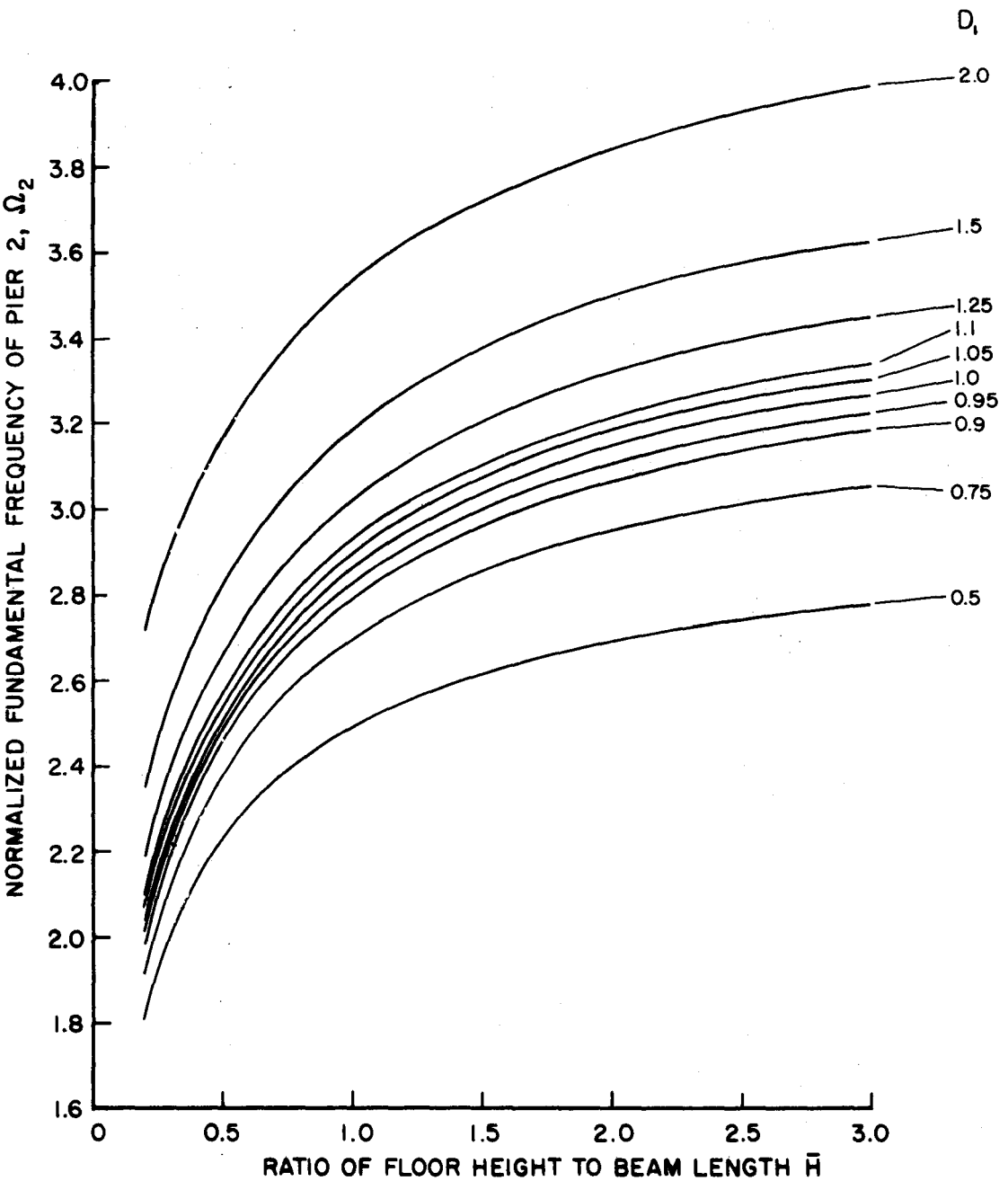

FIGURE 29. FUNDAMENTAL FREQUENCY DESIGN CURVES FOR COUPLED SHEAR WALLS WITH, $N=40$, $D_2=1$, $D_b=1/8$

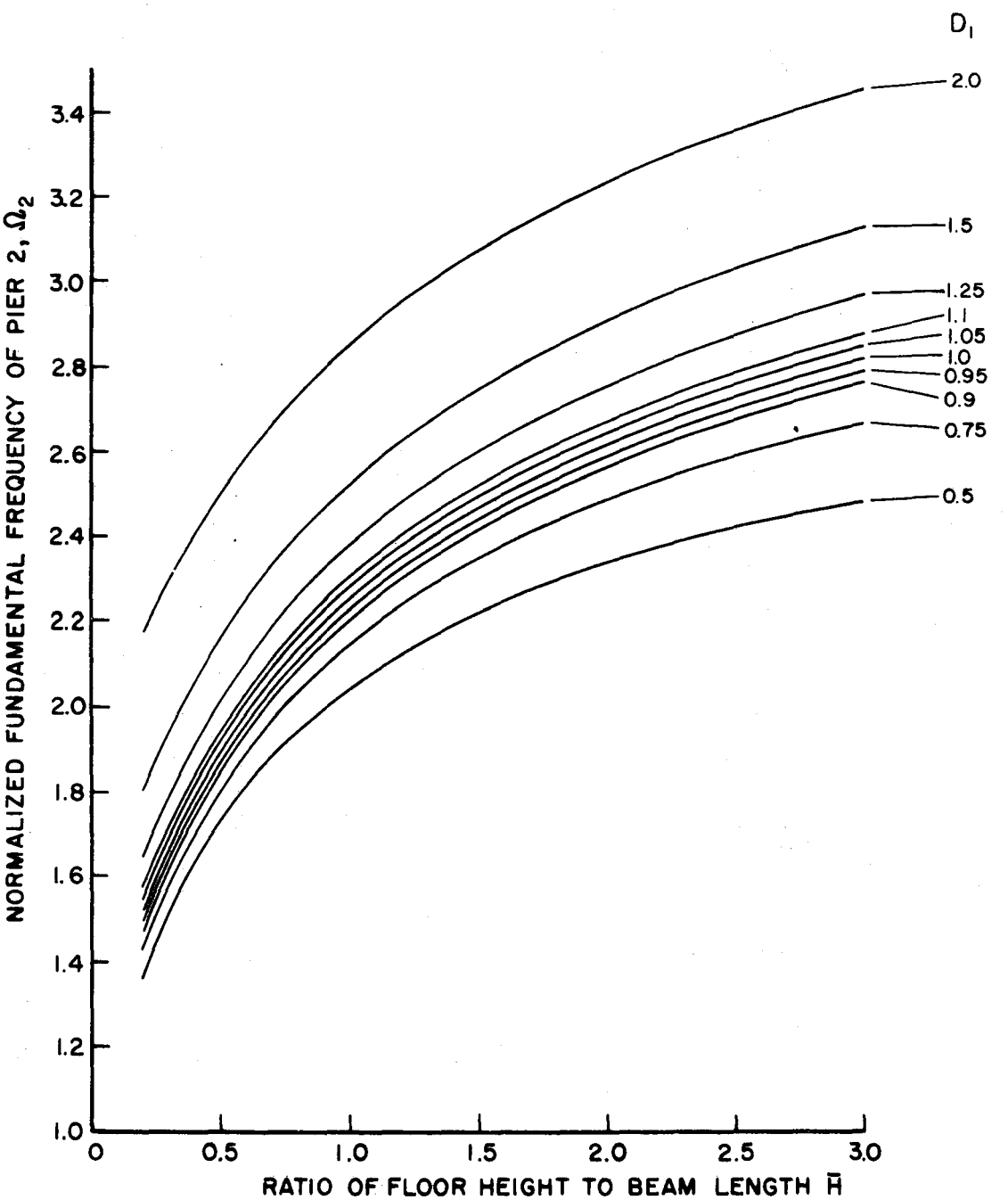

FIGURE 30. FUNDAMENTAL FREQUENCY DESIGN CURVES FOR COUPLED SHEAR WALLS WITH, $N=40$, $D_2=1$, $D_b=1/12$

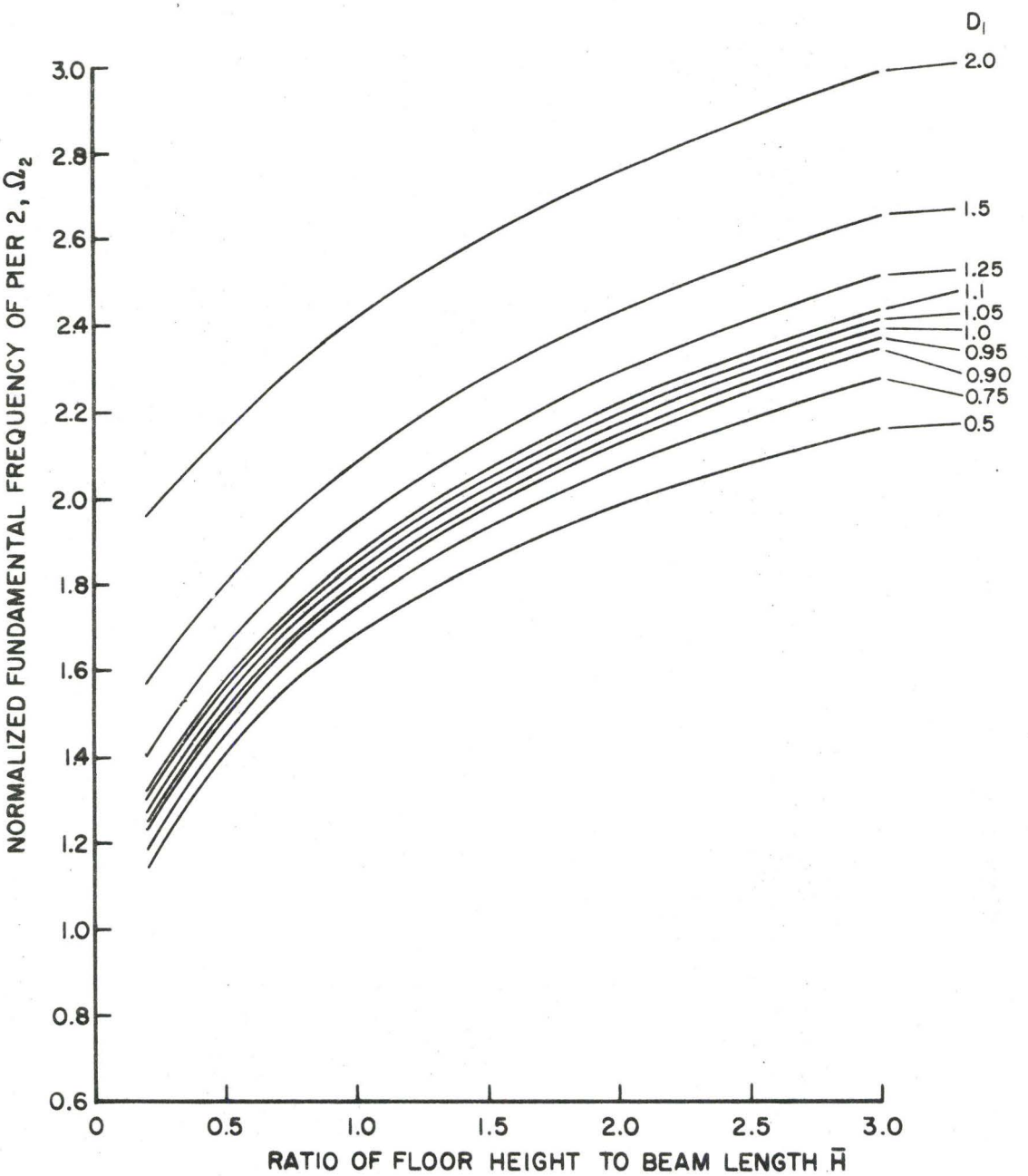

FIGURE 31. FUNDAMENTAL FREQUENCY DESIGN CURVES FOR COUPLED SHEAR WALLS WITH, $N=40$, $D_2=1$, $D_b=1/16$

3.6 Effect on Fundamental Frequency by Averaging

While frequency design curves can be established with the aid of the computer as in Section 3.5, it is meaningful to study the effect on the fundamental frequency of an asymmetric coupled shear wall by considering a substitutive symmetric model. A considerable amount of labour may be saved as the symmetric case is more easily soluble.

The most direct way to attain a substitutive symmetric model is by averaging the pier widths of the asymmetric system. This has the merit of keeping the total seismic loading constant and will be studied in detail in Subsection 3.6.1. Another way is by averaging the second moments of area of the piers of the asymmetric system. This has the merit of keeping the total bending stiffness constant and will be studied in detail in Subsection 3.6.2.

For convenience, a particular case is considered where the asymmetric shear wall is 20 storeys high and the floor height to beam length ratio is 1.6. To utilize some of the results obtained in Section 3.5, D_b ranges from 1/8 to 1/16; D_2 is taken to be unity and $\frac{E}{G}$ is kept at 2.60. With the above limitations, the ratio of the frequency of the substitutive symmetric model to that of the asymmetric system is expressed as a function of the pier width ratio and the results are represented graphically.

3.6.1 Averaging Pier Widths

Figure 32a represents the asymmetric shear wall system and the substitutive symmetric model by averaging the pier widths is shown in Figure 32b. The average pier width, designated by $d_{av.}$ is simply

$$d_{av.} = \tfrac{1}{2}(d_1+d_2) \tag{3.100}$$

The fundamental frequency of the asymmetric system ω_a is given by equations (3.24) and (3.25),

$$\omega_a = \Omega_2 \frac{3.52}{H^2} \sqrt{\frac{EI_2}{\rho_2}} \tag{3.101}$$

The corresponding expression for the symmetric model is given by equations (3.80) and (3.81),

$$\omega_s = \Omega_s \frac{3.52}{H^2} \sqrt{\frac{EI_s}{\rho_s}} \tag{3.102}$$

Dividing equation (3.102) by equation (3.101) results

$$\frac{\omega_s}{\omega_a} = \frac{\Omega_s}{\Omega_2} \sqrt{\frac{I_s}{I_2} \frac{\rho_2}{\rho_s}} \tag{3.103}$$

I_s/I_2 can be expressed in terms of $\frac{d_1}{d_2}$ as follows

$$\frac{I_s}{I_2} = \frac{d_{av.}^3}{d_2^3} = \frac{1}{8}(1 + \frac{d_1}{d_2})^3 \tag{3.104}$$

Assuming the attached mass of the connecting beams is small, it is obtained

$$\frac{\rho_2}{\rho_s} = \frac{d_2}{d_{av.}} = \frac{2}{1+\frac{d_1}{d_2}} \tag{3.105}$$

Substituting equations (3.104) and (3.105) into equation (3.103), the frequency ratio becomes

$$\frac{\omega_s}{\omega_a} = \frac{1}{2}\frac{\Omega_s}{\Omega_2}\left(1 + \frac{d_1}{d_2}\right) \tag{3.106}$$

For the particular case of $D_2 = 1$, the frequency ratio is also given by

$$\frac{\omega_s}{\omega_a} = \frac{\Omega_s}{\Omega_2} D_s \tag{3.107}$$

where $$D_s = \frac{d_{av.}}{c} \tag{3.108}$$

Figure 33 shows the variation of the frequency ratio $\frac{\omega_s}{\omega_a}$ as a monotonic decreasing function of the pier width ratio $\frac{d_1}{d_2}$ for $D_b = 1/8$, $1/12$, and $1/16$. It is observed that a better estimate of the actual frequency is obtained for a stiffer system (higher D_b) although the estimate in this case by averaging the pier widths is in general not very accurate. For example, for $D_b = 1/16$, when pier 1 is twice as wide as pier 2, the symmetric model yields a

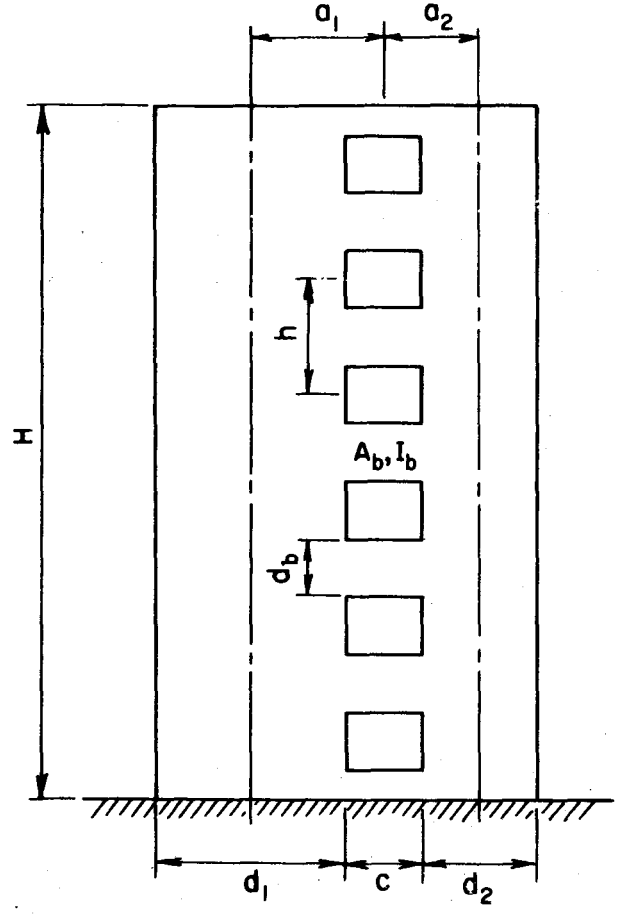

FIGURE 32 a
CONFIGURATION OF ASYMMETRIC
COUPLED SHEAR WALL

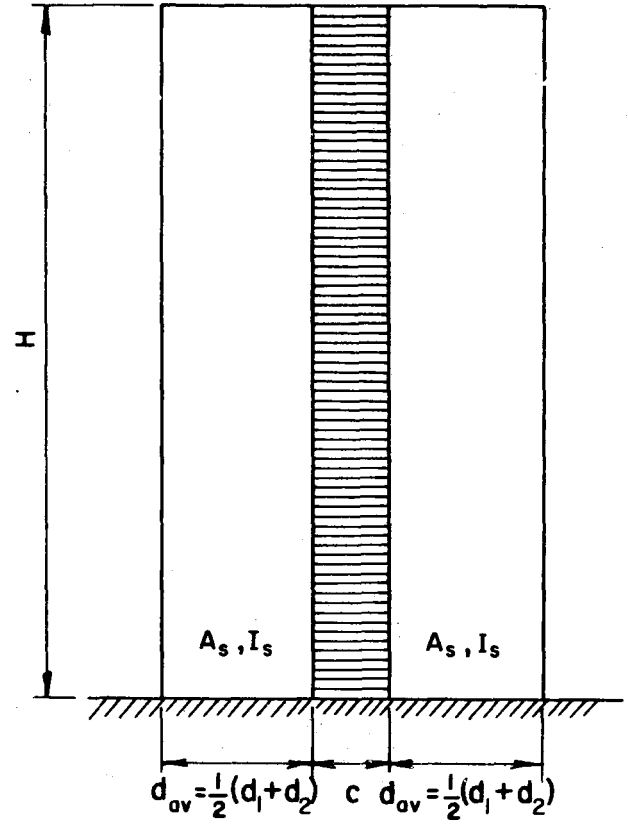

FIGURE 32 b
CONFIGURATION OF SUBSTITUTIVE
SYMMETRIC SYSTEM BY AVERAGING
PIER WIDTHS

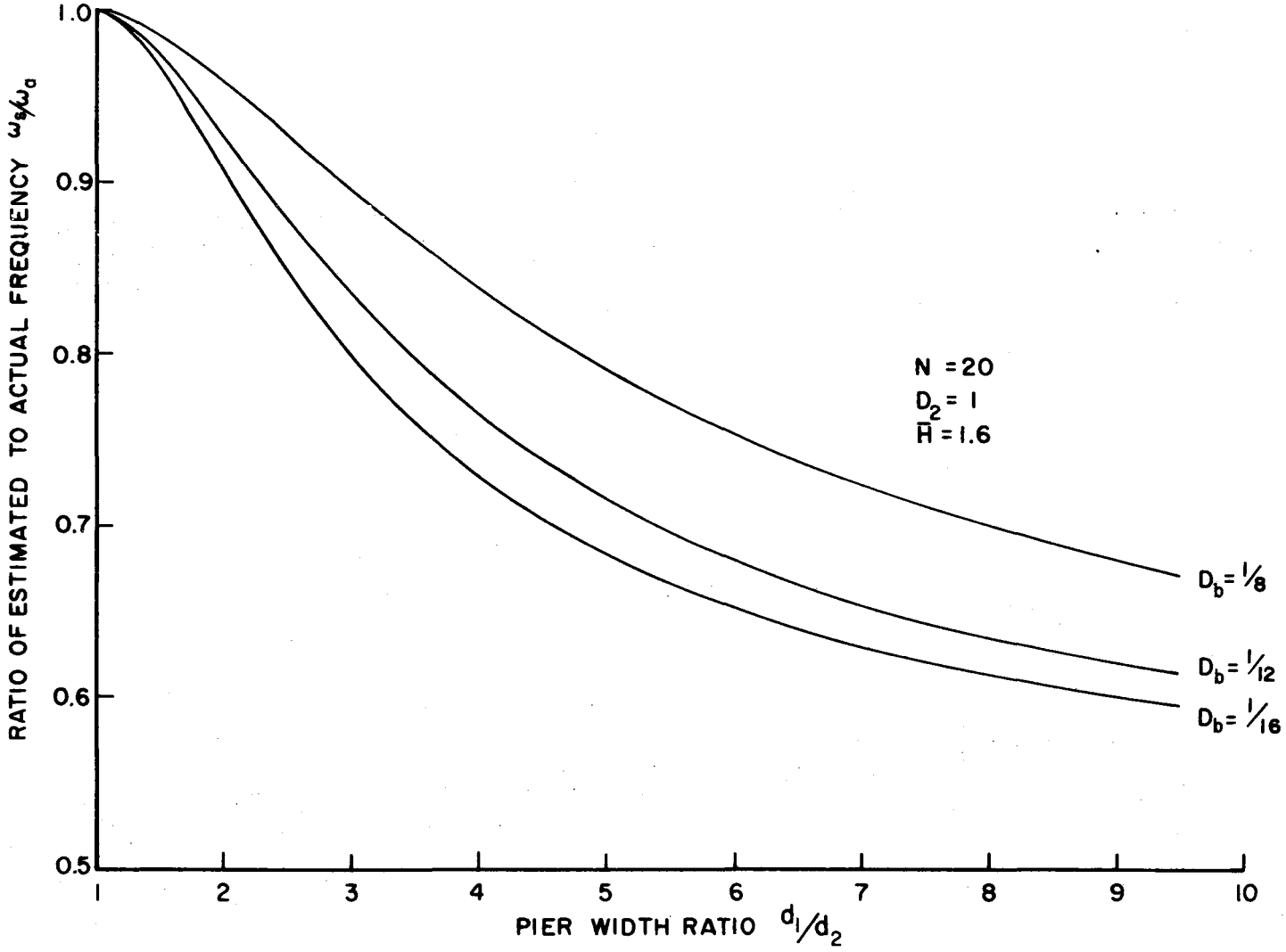

FIGURE 33. VARIATION OF ESTIMATED FREQUENCY WITH PIER WIDTH RATIO (BY AVERAGING PIER WIDTHS)

frequency 90% of the actual value; and when $\frac{d_1}{d_2} = 3$, the estimate drops to 80%.

3.6.2 Averaging Pier Stiffnesses

Figure 34a represents the asymmetric shear wall system and the substitutive symmetric model by averaging the pier stiffnesses is shown in Figure 34b. The average pier stiffness, designated by $I_{av.}$, is

$$I_{av.} = \frac{1}{2}(I_1 + I_2) \tag{3.109}$$

The corresponding pier width of the symmetric model is hence

$$d_s = \sqrt[3]{\tfrac{1}{2}(d_1^{\,3}+d_2^{\,3})} \tag{3.110}$$

The frequency ratio, in this case, from equation (3.103) is given by

$$\frac{\omega_s}{\omega_a} = \frac{\Omega_s}{\Omega_2}\sqrt{\frac{I_{av.}}{I_2}\frac{\rho_2}{\rho_s}} \tag{3.111}$$

In terms of $\frac{d_1}{d_2}$, $\frac{I_{av.}}{I_2}$ is expressed as

$$\frac{I_{av.}}{I_2} = \frac{d_s^{\,3}}{d_2^{\,3}} = \frac{1}{2}\left(1 + \frac{d_1^{\,3}}{d_2^{\,3}}\right) \tag{3.112}$$

Assuming the attached mass of the connecting beam is small, it is obtained

$$\frac{\rho_2}{\rho_s} = \frac{d_2}{d_s} = \frac{1}{\sqrt[3]{\frac{1}{2}\left(1 + \frac{d_1^{\,3}}{d_2^{\,3}}\right)}} \tag{3.113}$$

Substituting equations (3.112) and (3.113) into equation (3.111), the frequency ratio becomes

$$\frac{\omega_s}{\omega_a} = \frac{\Omega_s}{\Omega_2}\sqrt[3]{\frac{1}{2}\left(1 + \frac{d_1^{\,3}}{d_2^{\,3}}\right)} \tag{3.114}$$

For the particular case of $D_2 = 1$, the frequency ratio is also given by

$$\frac{\omega_s}{\omega_a} = \frac{\Omega_s}{\Omega_2}\, D_s \tag{3.115}$$

where $D_s = \frac{d_s}{c}$ (3.116)

Figure 35 shows the variation of the frequency ratio $\frac{\omega_s}{\omega_a}$ again as a monotonic decreasing function of the pier width ratio $\frac{d_1}{d_2}$ for $D_b = 1/8$, $1/12$, and $1/16$. It is observed that a much better estimate is obtained in general by averaging the pier stiffnesses than by averaging the pier widths. The estimate can be obtained to within 10% of the actual frequency for a pier width ratio up to 4 when $D_b = 1/16$.

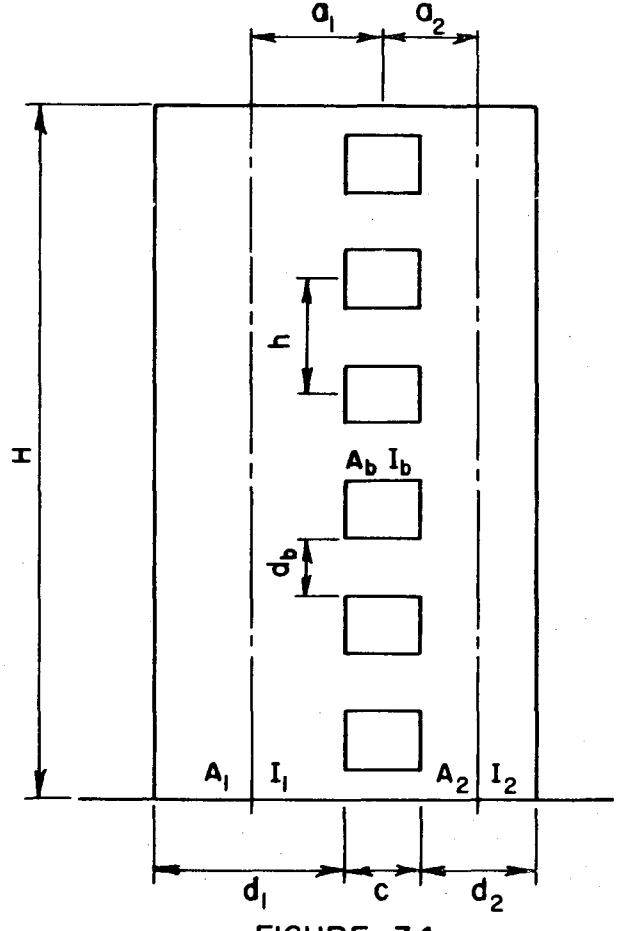

FIGURE 34 a

CONFIGURATION OF ASYMMETRIC COUPLED SHEAR WALL

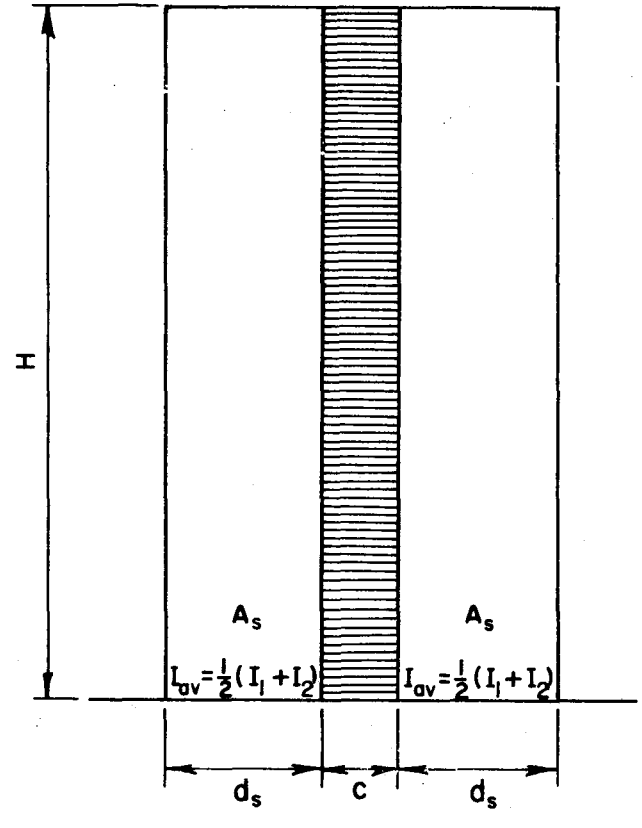

FIGURE 34 b

CONFIGURATION OF SUBSTITUTIVE SYMMETRIC SYSTEM BY AVERAGING PIER STIFFNESSES

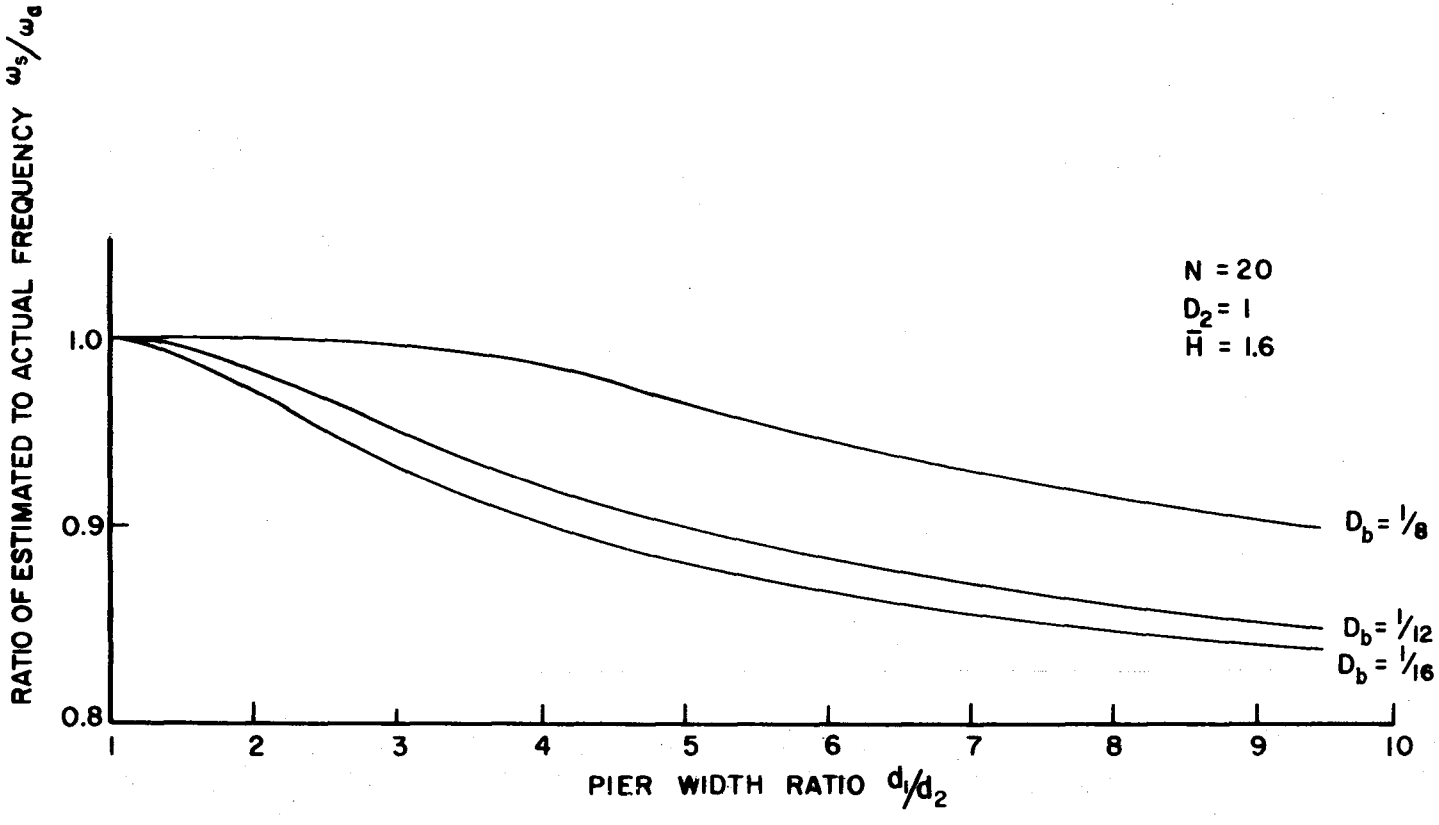

FIGURE 35. VARIATION OF ESTIMATED FREQUENCY WITH PIER WIDTH RATIO (BY AVERAGING PIER STIFFNESSES)

3.7 Experimental Work

Two model tests were carried out under dynamic conditions to verify the accuracy of the analysis. The symmetric model was designated as Model I and the asymmetric as Model II. The models were cut from cast acrylics sheets, Johnston Type 1010-0-32, of 0.50"± 0.044" thickness. Their overall dimensions were 36" high and 7" wide. Figures 36 and 37 show the actual Models I and II respectively. Model I was painted just for photographic purposes.

Model I was 20 storeys high with a floor height of 1.8". The 3" wide piers were separated by a series of 1" wide openings. Model II was 15 storeys high with a floor height of 2.4". Pier 1 was 4.2" wide while both pier 2 and the openings were 1.4". A step by step enlargement of the openings (height-wise) and the corresponding determination of the fundamental frequency of the model provided the necessary frequency variation for comparison with theoretical values.

The cast acrylics has a specific gravity of 1.19 with a Poisson ratio of 0.49. The more important physical property is the modulus of elasticity which was found to be 605,000 psi. A cantilever beam of the same material and overall dimensions as the test models was subjected to vibration under actual experimental conditions to determine its fundamental frequency, from which the elastic modulus of the material was readily calculated. The cantilever model

was then cut in half (longitudinally) and the test was repeated for the half-cantilever. This served as a check against any errors in the resulting elastic modulus that might arise from the "deep beam" effect of the full cantilever.

3.7.1 Experimental Set-Up

The dynamic loading was generated by means of a loading system designed by LTV Ling Altec Electronics Inc. which consists mainly of the CP-5/6 Power Amplifier, the SD 105A Amplitude Servo/Monitor, the SD 104A-5D Sweep Oscillator (the latter two being equipments of the Structural Dynamics Corporation of San Diego) and the ANA-101 Accelerometer Normalizing Amplifier, all grouped in the Control Console Assembly (Figure 38). The loading thus generated was transmitted to the model through the B290 Shaker with a rated force (sine vector) of 1500 lbs., a rated displacement of 1" and a frequency range of 5 to 4000 cps. Figure 39 shows the head of the shaker and the glide-table on which the model was mounted by means of steel angles to similate a fixed end condition. Budd C40-141B Type strain gauges with 2.05± 1/2% gauge factor and 120± 0.2 ohms resistance were used to detect the strain response of the model. The locations of the two strain gauges, one on each side of the model, were not critical so long as they were close to the ground floor level where maximum response

occurred. The strain response signals were amplified by the Ellis Bridge, Model BA-4 before going through the KH Filter Model 335 which screened off undesirable frequencies and noises. The relative magnitudes of the response could then be viewed on the Packard-Bell Oscilloscope. The frequency of applied excitation was read on a Hewlett Packard Frequency Counter #5223L which was connected to the Control Console Assembly. All these instruments can be observed in Figure 38.

3.7.2 Experimental Procedure

Once the model was mounted on the glide-table, the procedure to determine its fundamental frequency was quite straight forward. The model was subjected to excitation frequencies from 30 cps to 120 cps and the corresponding response as read on the oscilloscope was recorded. Figure 40 shows a typical experimental frequency-response plot. Where the highest peak occurred was the fundamental frequency. The second, much smaller peak indicated the second natural frequency which was approximately 20 cps higher. The model was then dismounted and milled to the next opening size before the test was repeated. In sequence, the heights of the openings of the symmetric model were 3/8", 3/4", 1 1/8", 1 1/4", 1 3/8", 1 1/2", and 1 5/8" while those for the asymmetric model were 3/8", 3/4", 1 1/8", 1 3/8", 1 5/8", 1 7/8", 2" and 2 1/8".

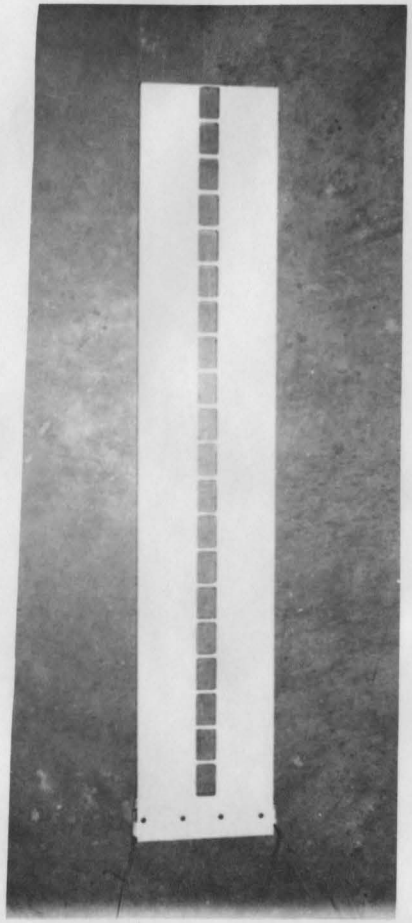

FIGURE 36. EXPERIMENTAL SYMMETRIC MODEL

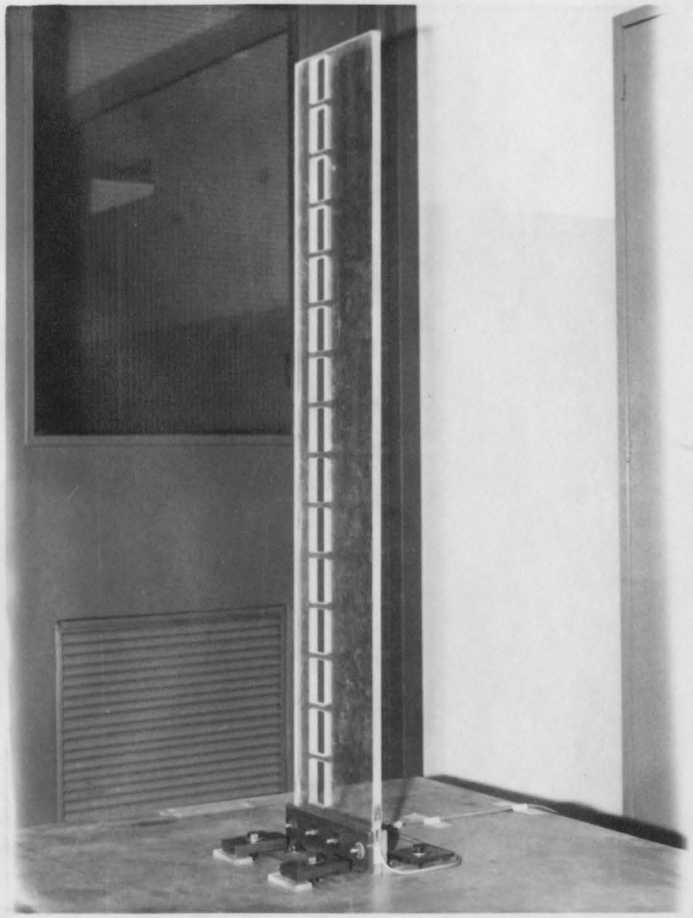

FIGURE 37. EXPERIMENTAL ASYMMETRIC MODEL

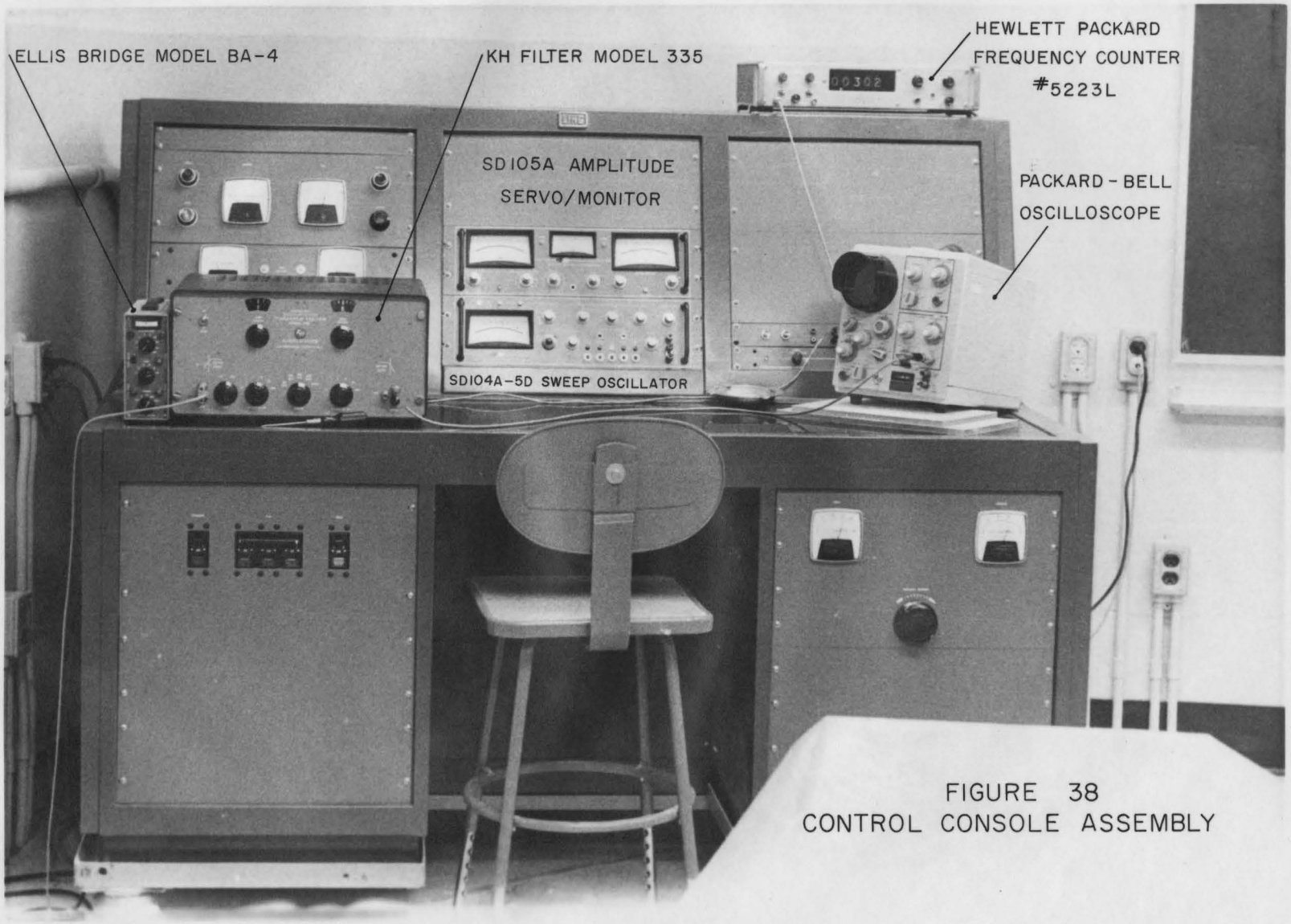

FIGURE 38
CONTROL CONSOLE ASSEMBLY

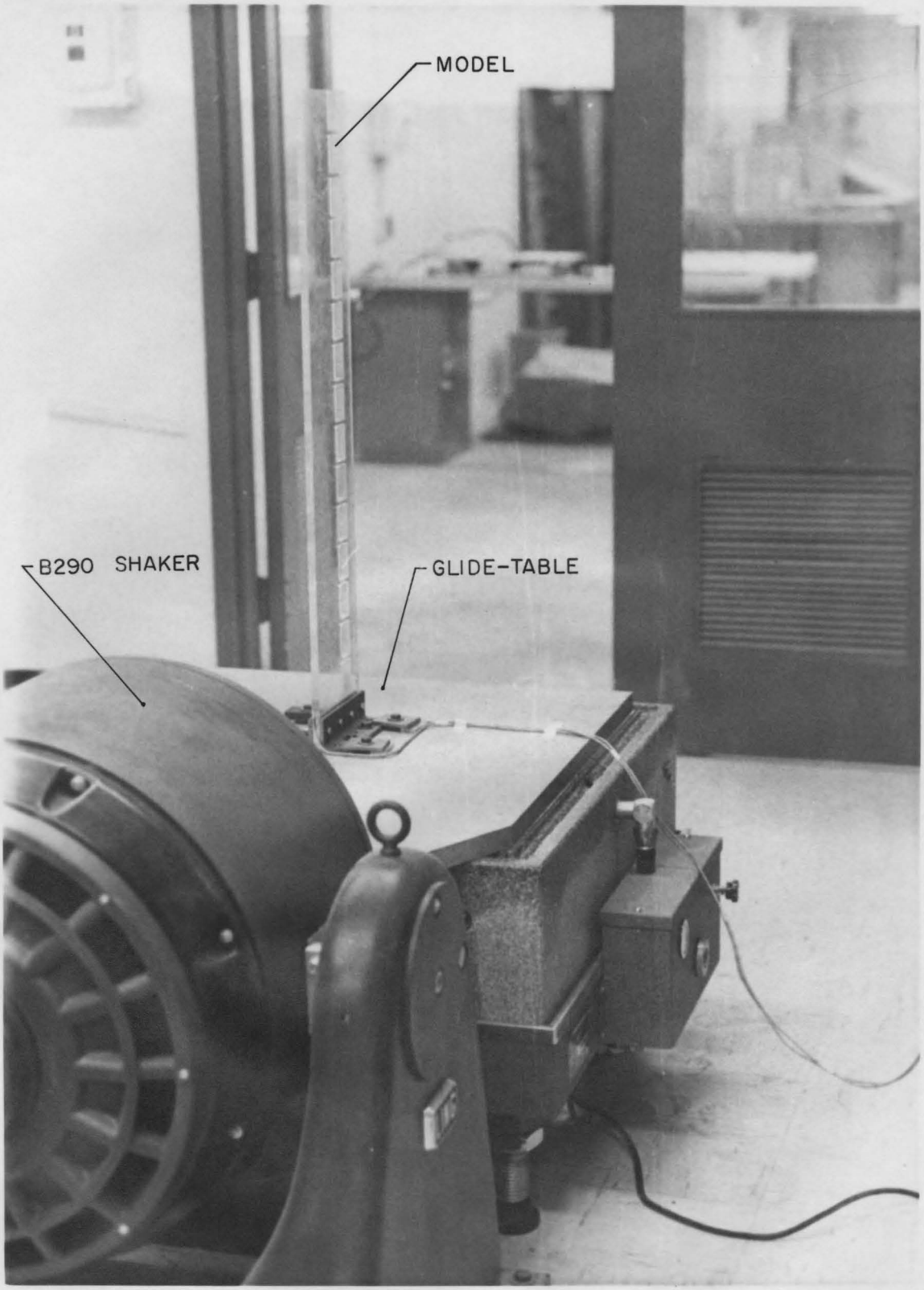

FIGURE 39. SHAKER AND GLIDE-TABLE

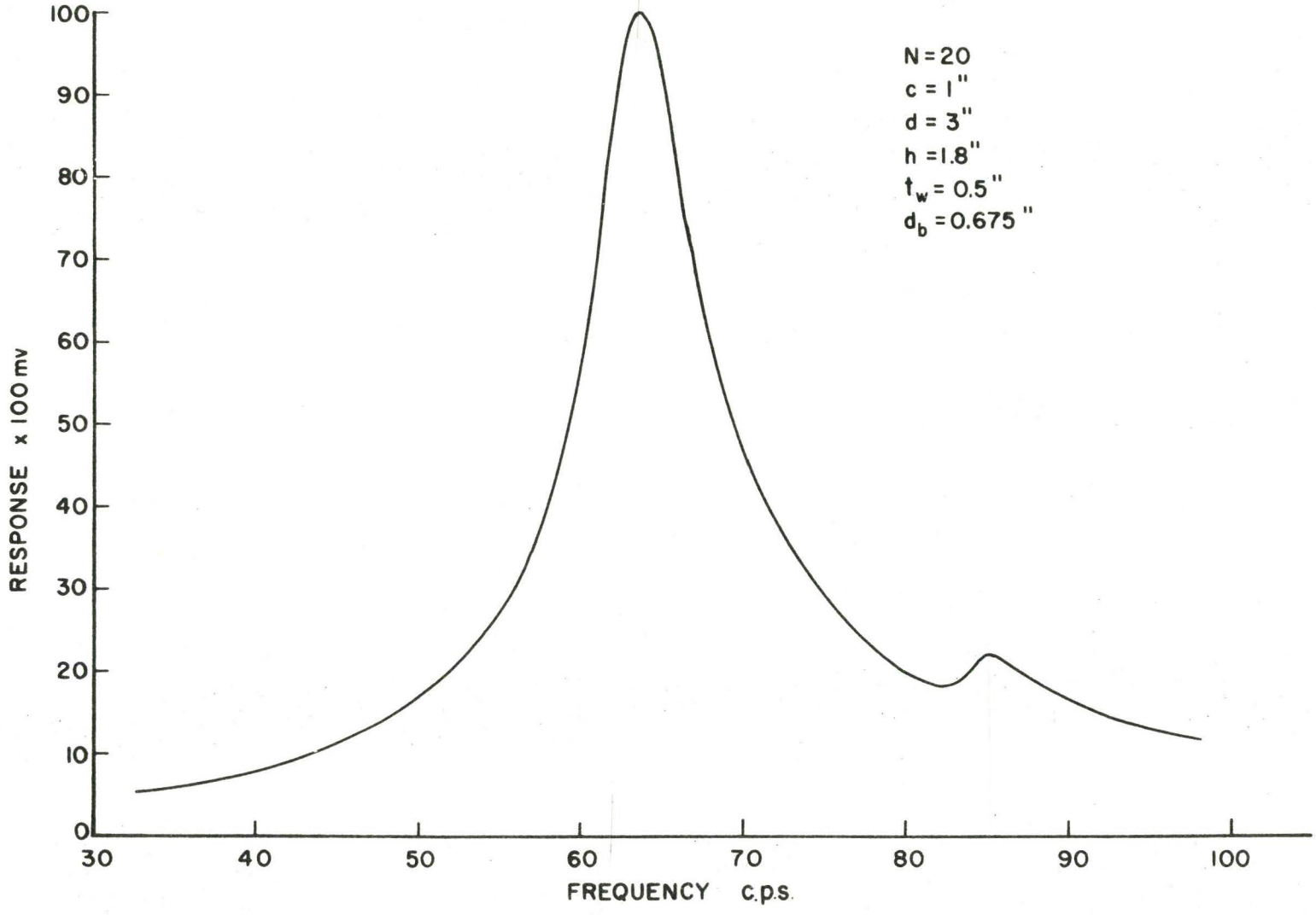

FIGURE 40. TYPICAL EXPERIMENTAL FREQUENCY-RESPONSE PLOT

3.7.3 Experimental Results and Observations

The experimental results plotted as a function of d_b are shown in Figure 41 for Model I and Figure 42 for Model II. Additional curves shown in the two figures are calculations based on the "equivalent" connecting beam concept. As pointed out by Michael (12), there are local wall deformations where the connecting beams join the piers. The condition of built-in ends for the connecting beams is not satisfied in general. One method of correction is to regard the connecting beam as having a span longer than the actual length c. The equivalent length c* is taken to be

$$c^* = c + 2\delta \tag{3.117}$$

Also, the stiffnesses of the piers are reduced such that the equivalent pier widths are taken to be d_j^* where

$$d_j^* = d_j - \delta \qquad (j = 1,2) \tag{3.118}$$

The corrective measure δ is then taken to be proportional to the depth of the connecting beam as follows

$$2\delta = K\, d_b \tag{3.119}$$

Shown in Figure 41, in addition to the idealized theoretical curve where K = 0 are curves with the equivalent beam length equal to the actual length plus 50% (K = 0.50) and 90% (K = 0.90) of the depth of the connecting beam respectively. Shown in Figure 42, in addition to the K = 0 curve, are the three K = 0.50 curves. The first one (3/1 curve) has the end of the beam connecting to pier 1 accounted for 75%

of the total correction. The second one (1/1 curve) represents an equal sharing of the correction by the two ends (as shown in Equation (3.118)) and the last curve (1/3 curve) has the end connecting to pier 2 accounted for 75% of the total correction.

It can be seen that the comparison between theoretical predication and the experimental points is reasonable. For K = 0, theoretical calculation gives a higher value of fundamental frequency than that obtained experimentally. However, the maximum difference for both models is less than 5%. This order of accuracy is sufficient in the application of spectrum technique for seismic design. For the other values of K, which are impirical, the theoretical prediction is more accurate (than for K = 0) for low values of beam depth; but when the beam is sufficiently thick, hence stiff, the prediction becomes an academic exercise. This is particularly shown in Figure 42.

Theoretically, the fundamental frequency of the coupled shear wall increases with the increase of the depth of the connecting beams up to a point. Further increase of the depth of the connecting beams then leads to a slight decrease in fundamental frequency. The explanation for this trend is that an increase of the depth of connecting beams increases both the stiffness and the mass of the coupled shear walls. The gain in stiffness outweighs the gain in mass when the depth of connecting beams is small.

After the "optimal" depth is reached, further increase of d_b only increases the stiffness of the coupled shear wall slightly. Thus, the gain in mass outweighs the gain in stiffness, in this range, resulting in a slight decrease in natural frequency. However, this slight decrease in frequency was not observed experimentally.

An important observation from Figures 41 and 42 is that by increasing the depth of connecting beams, a rapid increase in natural frequency results if the depth of the connecting beam is less than approximately a quarter of the storey height. By increasing the depth of connecting beams over a quarter of the storey height does not effectively increase the stiffness of the coupled walls to any great extent. This fact is illustrated from both the theoretical calculations and the experimental results.

Although damping is not treated in the present analysis, it is of interest, whenever possible, to determine the magnitude of this dynamic characteristic, not only for the realization of its existence but also for future research purposes. Figure 43 lists the values of the percentage of critical damping for the various sizes of wall openings for the symmetric and asymmetric models respectively. The percentage of critical damping is obtained by the "half-power point" method applied to the experimental frequency-response plots. An average of 5.1% is obtained for the symmetric models and 4.4% for the asymmetric models,

giving an overall average of about 5%, which is not unusual for most mechanical and structural systems.

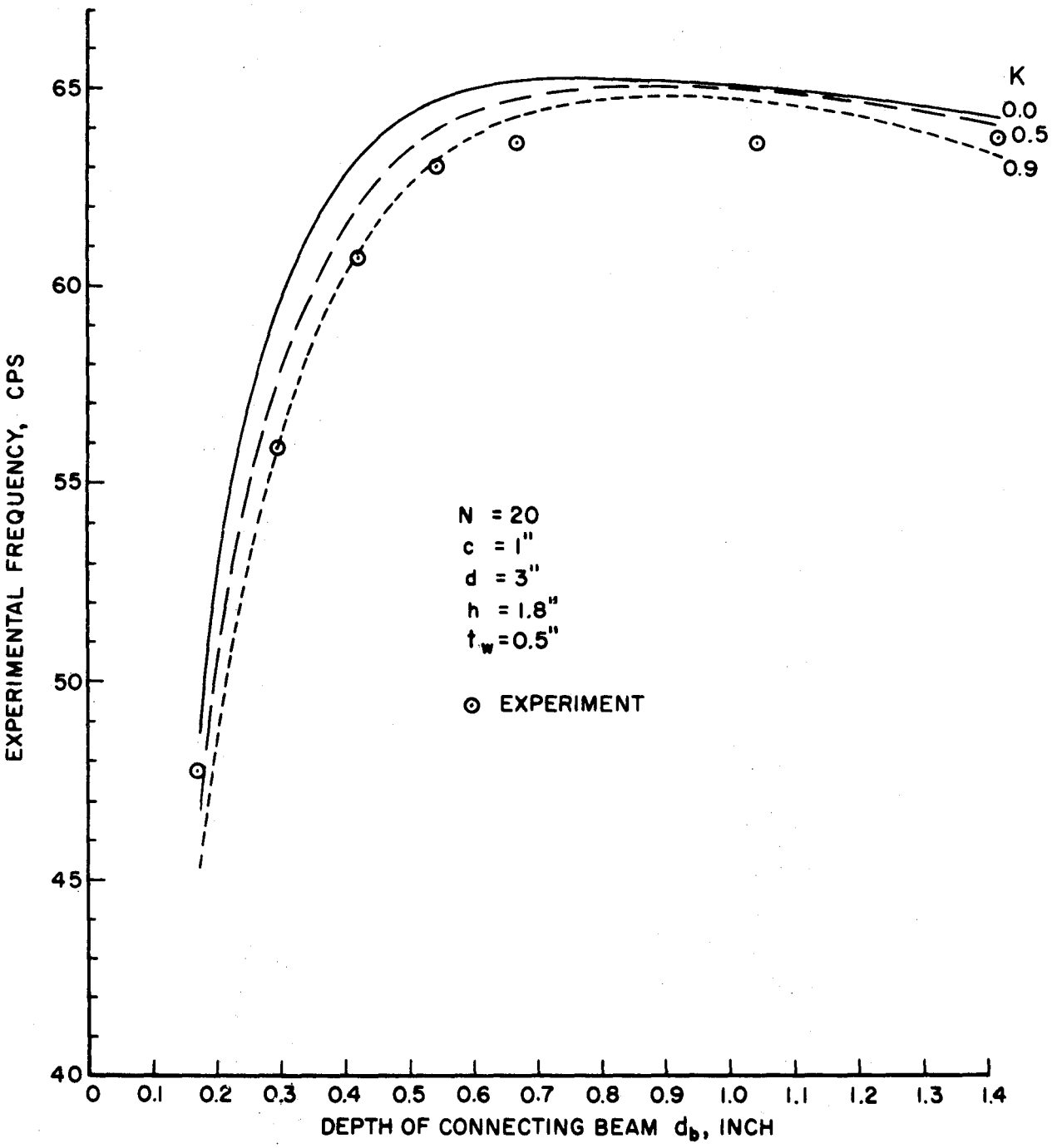

FIGURE 41. FUNDAMENTAL FREQUENCY OF SYMMETRIC COUPLED SHEAR WALL

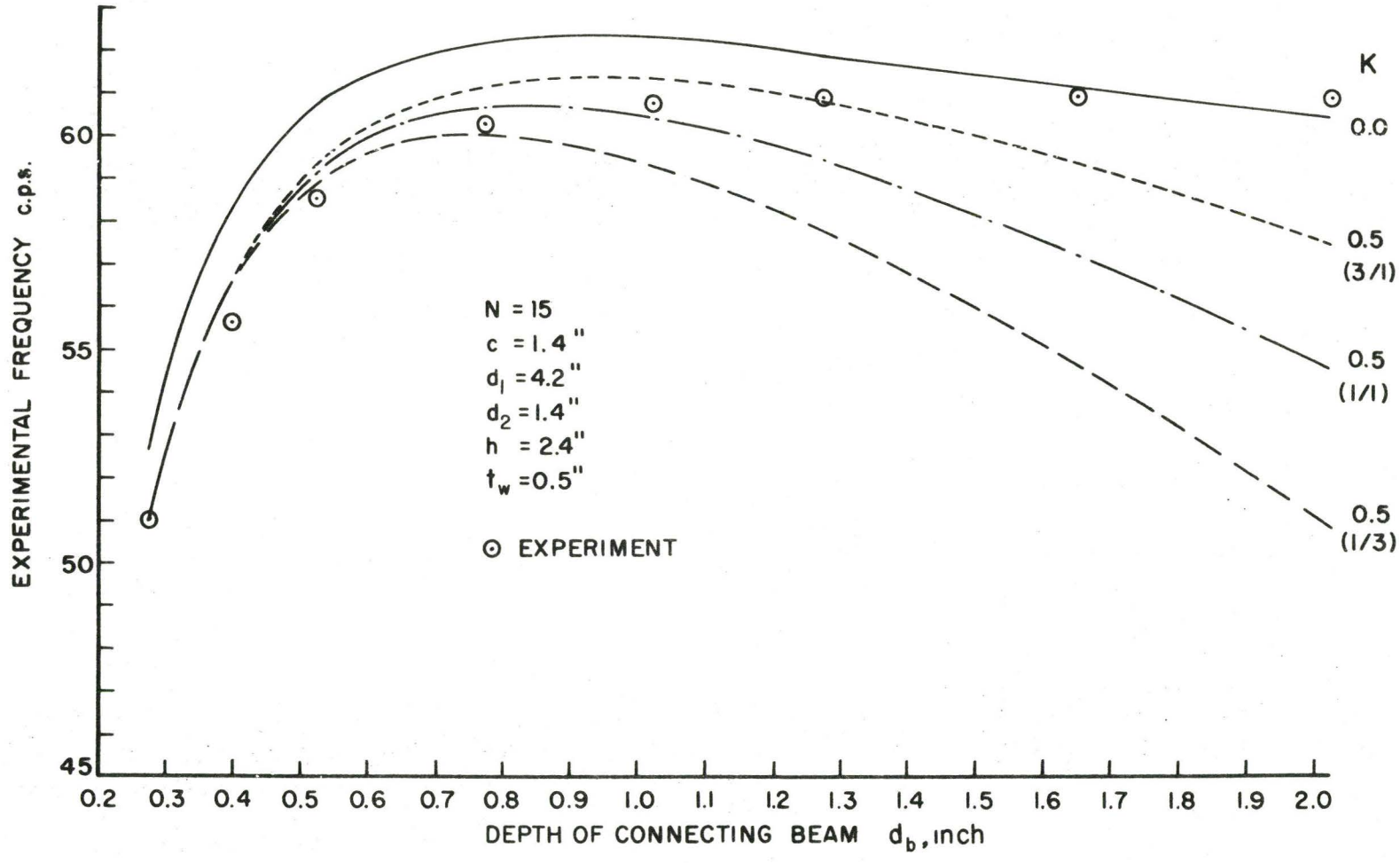

FIGURE 42. FUNDAMENTAL FREQUENCY OF ASYMMETRIC COUPLED SHEAR WALL.

SYMMETRIC MODEL		ASYMMETRIC MODEL	
Depth of Connecting Beam, Inch	% of Critical Damping	Depth of Connecting Beam, Inch	% of Critical Damping
0.175	4.8	0.275	4.3
0.30	6.0	0.40	4.2
0.425	4.7	0.525	4.0
0.55	5.0	0.775	4.4
0.675	4.6	1.025	4.3
1.05	6.2	1.275	3.8
1.425	4.8	1.65	4.3
		2.025	5.7
Average	5.1	Average	4.4

Figure 43. Experimentally Determined Percentage of Critical Damping

CHAPTER 4

Conclusions and Suggestions

In this study, the problem of the statics and dynamics of a plane coupled shear wall is considered. The "continuous" method of coupled shear wall analysis is used. However, no assumption is made in the formulation that the mid-points of the connecting beams are points of contraflexure. Removal of this assumption implies that the two piers may have different deflections. In this respect, the present formulation is a generalization of the "continuous" method of coupled shear wall analysis. The problem is formulated in terms of the deflection variables of the piers. Such a formulation has the advantage that it is readily adaptable for dynamic analysis by taking into account the inertia of the piers.

The conditions under which the mid-points of the connecting beams are points of contraflexure are established. For a symmetric wall, the pier deflections are equal only if there is an equal proportioning of the lateral load on the piers. For an asymmetric wall, even if the lateral loads on the piers are proportional to their respective stiffnesses, the pier deflections need not be the same. From a practical point of view, the assumption of contraflexure points is usually admissible since it is the antisymmetric mode of

deformation z_1 of the shear wall that is of interest. However, there exists practical instances where the symmetric mode of deformation z_2 may be of interest. A case in point is the problem of differential foundation settlement and rotation. It is shown that the symmetric mode of deformation is independent of differential foundation settlement, but directly proportional to the differential rotation of the pier foundations. When differential rotation does occur, the symmetric deflection not only is necessary in the calculation of internal stresses in the structure but has significant effect on the total moment of the piers at the bottom fifth of the coupled shear wall.

The dynamic equations of motion of the system subjected to arbitrary distributed dynamic loading are given. The case of free vibrations is studied. The governing equations are reduced to a set of sixth order coupled linear equations subjected to homogeneous boundary conditions. The natural frequency can be found via a trial and error technique. Through a series of non-dimensionalizing procedures, it is shown that the fundamental natural frequency of the coupled shear walls in its normalized form can be related to non-dimensional properties of the structure. The fundamental frequency is normalized with respect to that of lateral vibration of a cantilever beam having the stiffness of a pier and the mass equal to the mass of the pier plus half of the mass of attached connecting beams. The geometry of

the structure is normalized with respect to the length of the connecting beam. Instead of restricting to specific examples, design curves are presented in the form of normalized frequency versus normalized floor height for a wide variety of configuration of couple shear walls with the aid of electronic computation.

The effect on the fundamental frequency by averaging the pier widths and the pier stiffnesses respectively to arrive at a substitutive symmetric system is examined. It is found that in the particular case considered, averaging the pier stiffnesses gives a better estimate of the fundamental frequency.

The actual fundamental natural frequencies were computed for two coupled shear wall models. By decreasing the depth of the connecting beams in a systematic manner, the variation of the fundamental frequency as a function of the depth of connecting beams is shown. It is found that an increase in depth of connecting beams beyond a quarter of the storey height does not provide significant increase in stiffness in the coupled shear wall system. This observation should be useful in design considerations.

Finally, dynamic testing of two coupled shear wall models made of acrylic sheets were carried out. The experimentally determined frequencies were compared with the theoretical results. The agreement between theory and experiment is within 5%. This leads to the conclusion that

the natural frequencies as determined by the proposed theory should be of sufficient accuracy to be used as input in the response spectrum technique of seismic design of coupled shear walls.

It should be pointed out that for future experiments of this nature, because of the size of the experimental models, control is the key to consistent results: control not only in the overall dimensions of the model but particularly those of the openings; control in the manner of attaching the model to the shake table; control in the frequency range of applied excitation and the last but not least, control in the sensitivity of the frequency counter.

REFERENCES

1. Coull, A. and Stafford Smith, B., "Analysis of Shear Wall Structures (A Review of Previous Research)", Proceedings of a Symposium on Tall Buildings, University of Southampton, April 1966, Pergamon Press, pp. 139-155.
2. MacLeod, I.A., "Lateral Stiffness of Shear Walls with Openings", Proceedings of a Symposium on Tall Buildings, University of Southampton, April 1966, Pergamon Press, pp. 223-244.
3. Chitty, L., "On the Cantilever Composed of a Number of Parallel Beams Interconnected by Cross Bars", Philosophical Magazine (London), Series 7, Vol. 38, 1947, pp. 685-699.
4. Beck, H., "Contribution to the Analysis of Coupled Shear Walls", Journal of the American Concrete Institute, Vol. 59, No. 8, August 1962, pp. 1055-1069.
5. Rosman, R., "Approximate Analysis of Shear Walls Subjected to Lateral Loads", Journal of the American Concrete Institute, Vol. 61, No. 6, June 1964, pp. 717-732.
6. Burns, R.J., "An approximate Method of Analyzing Coupled Shear Walls Subjected to Triangular Loading", Proceedings of Third World Conference on Earthquake Engineering, Auckland - Wellington, New Zealand, January 1965.

7. Traum, E.E., "Multistorey Pierced Shear Walls of Variable Cross-section," Proceedings of a Symposium on Tall Buildings, University of Southampton, April 1966, Pergamon Press, pp. 181-204.

8. Barnard, P.R., and Schwaighofer, J., "The Interaction of Shear Walls Connected Solely through Slabs", Proceedings of a Symposium on Tall Buildings, University of Southampton, April 1966, Pergamon Press, pp.157-173.

9. Coull, A. and Choudhury, J.R., "Stresses and Deflections in Coupled Shear Walls", Journal of the American Concrete Institute, Vol. 64, No. 2, February 1967, pp. 65-72.

10. Coull, A. and Choudhury, J.R., "Analysis of Coupled Shear Walls", Journal of the American Concrete Institute, Vol. 64, No. 9, September 1967, pp. 587-593.

11. Coull, A. and Puri, R.D., "Analysis of Pierced Shear Walls", Journal of Structural Division, ASCE, ST1, January 1968, pp. 71-82.

12. Michael, D., "The Effect of Local Wall Deformations on the Elastic Interaction of Cross Walls Coupled by Beams", Proceedings of a Symposium on Tall Buildings, University of Southampton, April 1966, Pergamon Press, pp. 253-270.

13. Jennings, P.C., "Vertical Shear Failure of Coupled Shear Walls in the Alaskan Earthquake", Proceedings of the Japan Earthquake Engineering Symposium, Tokyo, Japan, October 1966, pp. 379-384.

14. Osawa, Y., "Seismic Analysis of Core-Wall Buildings", Proceedings of Third World Conference on Earthquake Engineering, Auckland-Wellington, New Zealand, Vol. II, January 1965, pp. 458-475.

15. Tani, S., Sakurai, J. and Iguchi, M., "An Approximate Method of Static and Dynamic Analyses of Core-Wall Buildings", Proceedings of Fourth World Conference on Earthquake Engineering, Santiago, Chile, 1969.

16. Tso, W.K., "General Analysis of Coupled Symmetric Shear Walls", unpublished manuscript, 1969.

17. Tso, W.K. and Chan, H.B., "Dynamic Analysis of Plane Coupled Shear Walls", to be published in Journal of Engineering Mechanics Division, ASCE.

```
C
C
C
C
C                              APPENDIX 1
C
C
C           COMPUTER PROGRAM FOR THE FUNDAMENTAL NATURAL
C              FREQUENCY OF PLANE COUPLED SHEAR WALLS
C
C
C
C           H B CHAN
C           DEPT OF CIVIL ENGINEERING AND ENGINEERING MECHANICS
C           MCMASTER UNIVERSITY
C
C
C           RESEARCH PROGRAM TO FIND THE NORMALIZED NATURAL
C           FREQUENCY OF A PLANE COUPLED ASYMMETRICAL SHEAR WALL
C
C
      DIMENSION AA(11),XX(10),YY(10)
      COMPLEX B(10),D(10),G(10),C(12,12),AC(12,12)
      COMPLEX SUM,VALDET,VALDET1
      COMPLEX GG
C
C           SPECIFYING VALUES FOR THE VARIABLES
C
      XM=3.52
```

```
      XM2=XM**2
C
C           INPUT THE NUMBER OF STOREYS, S AND THE RATIO OF
C           LENGTH OF CONNECTING BEAM TO WIDTH OF PIER 1, CD1
C           THE CORRESPONDING RATIO FOR PIER 2, CD2 IS KEPT AT
C           UNITY
C
      S=40.0
      CD1=1.0/1.10
      CD2=1.0
      WRITE (6,600) S,CD1,CD2
  600 FORMAT(//1H ,*NO OF STOREYS = *,F10.2/1H ,*RATIO OF C TO
     1 D1 = *,F10.2/1H ,*RATIO OF C TO D2 =*,F10.2)
C
C           THEXX WHERE XX IS 1,2.....16 ARE NON-DIMENSIONAL
C           VARIABLES
C
      THE1=(1.0/CD1)**3 + (1.0/CD2)**3
      THE2=(1.0/CD1)**3 - (1.0/CD2)**3
      THE6=(1.0/CD1) + (1.0/CD2) + 2.
      THE7=(1.0/CD1) - (1.0/CD2)
      THE8=CD1 + CD2
      THE11=CD1*CD1*(1.0+CD1)
      THE12=CD2*CD2*(1.0+CD2)
      THE13=(CD1**3) + (CD2**3)
```

```
      THE15=(CD1**3) - (CD2**3)
C
C           INPUT THE RATIO OF DEPTH TO LENGTH OF CONNECTING
C           BEAM, DBC
C
      DO 700 III=4,4
      DBC=1.0/FLOAT(III)
      WRITE (6,601) DBC
  601 FORMAT(1H ,*RATIO OF DEPTH TO LENGTH OF BEAM = *,F10.3)
C
C           INPUT THE RANGE OF FLOOR HEIGHT TO LENGTH OF BEAM
C           RATIO, HC
C
      DO 700 JJJ=2,30,2
      HC=FLOAT(JJJ)/10.0
      WRITE (6,602) HC
  602 FORMAT(1H0,*RATIO OF FLOOR HEIGHT TO LENGTH OF BEAM = *,
     1F10.3)
      THE3=S*S*HC*(DBC**3)
C
C           ASSUME E/G = 2.60
C           E IS THE ELASTIC MODULUS
C           G IS THE SHEAR MODULUS
C
      THE4=1.0 + 1.2*2.6*(DBC**2)
```

```
      THE5=(S**4)*(HC**3)*DBC
      THE14=(DBC+2.0*HC*(1.0/CD2))/(DBC+2.0*HC*(1.0/CD1))
      THE16=(1.0+THE14)/(1.0-THE14)
      GG=CMPLX(THE16,0.0)
C
C           DESIGNATION OF MATRICES
C
C           P IS THE MATRIX ASSOCIATED WITH THE SIXTH DERIVATIVE
C             OF THE DEFLECTION VECTOR IN THE EQUATION OF MOTION
C             OR WITH THE FOURTH DERIVATIVE OF THE DEFLECTION
C             VECTOR IN THE FIFTH PAIR OF BOUNDARY CONDITIONS OR
C             WITH THE FIFTH DERIVATIVE OF THE DEFLECTION VECTOR
C             IN THE SIXTH PAIR OF BOUNDARY CONDITIONS
C
C           Q IS THE MATRIX ASSOCIATED WITH THE FOURTH DERIVATIVE
C             OF THE DEFLECTION VECTOR IN THE EQUATION OF MOTION
C             OR WITH THE SECOND DERIVATIVE OF THE DEFLECTION
C             VECTOR IN THE FIFTH PAIR OF BOUNDARY CONDITIONS OR
C             WITH THE THIRD DERIVATIVE OF THE DEFLECTION VECTOR
C             IN THE SIXTH PAIR OF BOUNDARY CONDITIONS
C
C           R IS THE MATRIX ASSOCIATED WITH THE SECOND DERIVATIVE
C             OF THE DEFLECTION VECTOR IN THE EQUATION OF MOTION
C             OR WITH THE ZERO DERIVATIVE OF THE DEFLECTION VECTOR
C             IN THE FIFTH PAIR OF BOUNDARY CONDITIONS OR WITH
```

```
C           THE FIRST DERIVATIVE OF THE DEFLECTION VECTOR IN
C           THE SIXTH PAIR OF BOUNDARY CONDITIONS
C
C         S IS THE MATRIX ASSOCIATED WITH THE ZERO DERIVATIVE
C           OF THE DEFLECTION VECTOR IN THE EQUATION OF MOTION
C
C         U IS THE MATRIX ASSOCIATED WITH THE FIRST DERIVATIVE
C           OF THE DEFLECTION VECTOR IN THE THIRD PAIR OF
C           BOUNDARY CONDITIONS
C
C         V IS THE MATRIX ASSOCIATED WITH THE DOUBLE INTEGRAL
C           OF THE DEFLECTION VECTOR IN THE THIRD PAIR OF
C           BOUNDARY CONDITIONS
C
C
C         FORMING THE COMPONENTS OF COEFFICIENT MATRICES P,Q,U
C
      P11=THE1
      P12=THE2
      P21=THE2
      P22=THE1
      Q11=-(3.0*THE6*THE6+THE1*THE8)*THE3/THE4
      Q12=-(3.0*THE6*THE7+THE2*THE8)*THE3/THE4
      Q21=-(3.0*THE6*THE7+THE1*THE8*THE7/THE6)*THE3/THE4
      Q22=-(3.0*THE7*THE7+THE2*THE8*THE7/THE6+4.0*THE4)*THE3/
```

```
     1THE4
      U11=-3.0*(THE11+THE12)*(0.5*THE6+THE1*THE8/(6.0*THE6))*
     1THE3/THE4
      U12=-(3.0*(THE11+THE12)*(0.5*THE7+THE2*THE8/(6.0*THE6))+
     1(THE4*THE15))*THE3/THE4
      U21=-3.0*(THE11-THE12)*(0.5*THE6+THE1*THE8/(6.0*THE6))*
     1THE3/THE4
      U22=-(3.0*(THE11-THE12)*(0.5*THE7+THE2*THE8/(6.0*THE6))+
     1(THE4*THE13))*THE3/THE4
C
C          INPUT THE TRIAL RANGE OF EEM
C          EEM IS THE NORMALIZED NATURAL FREQUENCY OF PIER 2
C          EM IS THE NORMALIZED NATURAL FREQUENCY OF PIER 1
C
      DO 700 MMM=3000,3800,10
      EEM=FLOAT(MMM)/1000.
      EM=EEM/SQRT(THE14*((CD2/CD1)**3))
      EM2=EM**2
      THE9=EM2*(1.0+THE14)/(CD1**3)
      THE10=EM2*(1.0-THE14)/(CD1**3)
C
C          FORMING THE COMPONENTS OF COEFFICIENT MATRICES R,S,V
C
      R11=-XM2*THE9
      R12=-XM2*THE10
```

```
      R21=-XM2*THE10
      R22=-(XM2*THE9-48.0*THE5)
      S11=THE9*THE3*XM2*THE8/THE4
      S12=THE10*XM2*THE3*THE8/THE4
      S21=THE7*(THE9/THE6)*XM2*THE3*THE8/THE4
      S22=THE7*(THE10/THE6)*XM2*THE3*THE8/THE4
      V11=(THE11+THE12)*XM2*THE9*THE3*THE8/(2.0*THE4*THE6)
      V12=(THE11+THE12)*XM2*THE10*THE3*THE8/(2.0*THE4*THE6)
      V21=(THE11-THE12)*XM2*THE9*THE3*THE8/(2.0*THE4*THE6)
      V22=(THE11-THE12)*XM2*THE10*THE3*THE8/(2.0*THE4*THE6)
C
C           FORMING THE COEFFICIENTS OF THE TWELVE DEGREE
C           CHARACTERISTIC EQUATION
C
      AA(1)=P11*P22-P12*P21
      AA(2)=0.0
      AA(3)=P11*Q22+Q11*P22-P21*Q12-Q21*P12
      AA(4)=0.0
      AA(5)=P11*R22+Q11*Q22+R11*P22-P21*R12-Q12*Q21-R21*P12
      AA(6)=0.0
      AA(7)=P11*S22+Q11*R22+R11*Q22+S11*P22-P21*S12-Q21*R12-R2
     11*Q12-S21*P12
      AA(8)=0.0
      AA(9)=Q11*S22+R11*R22+S11*Q22-Q21*S12-R21*R12-S21*Q12
      AA(10)=0.0
```

```
      AA(11)=R11*S22+S11*R22-R21*S12-S21*R12
C
C           SOLVING THE POLYNOMIAL BY SUBROUTINE BAIRST
C           AA IS THE COEFFICIENT OF THE POWERS ARRANGED AS
C           AA(1)....Y**N
C           XX IS THE REAL PART OF THE ROOT
C           YY IS THE IMMAGINARY PART OF THE ROOT
C           N IS THE HIGHEST POWER OF THE POLYNOMIAL
C
      CALL BAIRST(AA,XX,YY,10)
      DO 100 I=1,10
      X=XX(I)
      Y=YY(I)
      B(I)=CMPLX(X,Y)
      D(I)=CEXP(B(I))
      G(I)=-(((P11*B(I)**2+Q11)*B(I)**2+R11)*B(I)**2+S11)/(((P
     112*B(I)**2+Q12)*B(I)**2+R12)*B(I)**2+S12)
  100 CONTINUE
C
C           POPULATING THE MATRIX OF THE BOUNDARY CONDITIONS
C
      DO 200 J=1,10
      C(1,J)=(1.0,0.0)
      C(2,J)=G(J)
      C(3,J)=B(J)
```

```
      C(4,J)=B(J)*G(J)
      C(5,J)=D(J)*(B(J)**2)
      C(6,J)=D(J)*(B(J)**2)*G(J)
      C(7,J)=D(J)*(B(J)**3)+(U11+U12*G(J))*B(J)*D(J)+(V11+V12*
     1G(J))*(0.5*D(J)*B(J)*B(J)-D(J)*B(J)+D(J)-1.0)/(B(J)**3)
      C(8,J)=D(J)*G(J)*(B(J)**3)+(U21+U22*G(J))*B(J)*D(J)+(V21
     1+V22*G(J))*(0.5*D(J)*B(J)*B(J)-D(J)*B(J)+D(J)-1.0)/(B(J)**3)
      C(9,J)=(P11+P12*G(J))*D(J)*(B(J)**4)+(Q11+Q12*G(J))*D(J)
     1*(B(J)**2)+(R11+R12*G(J))*D(J)
      C(10,J)=(P21+P22*G(J))*D(J)*(B(J)**4)+(Q21+Q22*G(J))*D(J
     1)*(B(J)**2)+(R21+R22*G(J))*D(J)
      C(11,J)=B(J)*C(9,J)
      C(12,J)=B(J)*C(10,J)
  200 CONTINUE
      DO 205 II=1,12
      DO 205 JJ=11,12
      C(II,JJ)=(0.0,0.0)
  205 CONTINUE
      C(1,11)=(1.0,0.0)
      C(2,11)=GG
      C(3,12)=(1.0,0.0)
      C(4,12)=GG
      C(7,11)=(V11+V12*GG)/6.0
      C(7,12)=(U11+U12*GG)+(V11+V12*GG)/8.0
      C(8,11)=(V21+V22*GG)/6.0
```

```
      C(8,12)=(U21+U22*GG)+(V21+V22*GG)/8.0
      C(9,11)=R11+R12*GG
      C(9,12)=R11+R12*GG
      C(10,11)=R21+R22*GG
      C(10,12)=R21+R22*GG
      C(11,12)=R11+R12*GG
      C(12,12)=R21+R22*GG
C
C           EVALUATING THE DETERMINANT OF THE BOUNDARY CONDITIONS
C           MATRIX BY SUBROUTINE DETER
C           OUTPUT THE NORMALIZED NATURAL FREQUENCIES OF PIERS 1
C           AND 2 AND THE VALUE OF THE DETERMINANT
C
      CALL DETER(C,12,VALDET)
      WRITE (6,1700) EM,EEM,VALDET
 1700 FORMAT(10X,2F10.4,10X,E20.8,10X,E20.8)
  700 CONTINUE
      STOP
      END
      SUBROUTINE DETER(A,MM,VALDET)
C
C           THE SUBROUTINE CALCULATES THE VALUE OF THE
C           DETERMINANT BY GAUSS ELIMINATION PROCESS
C
      COMPLEX A(12,12)
```

```
      COMPLEX VALDET
      COMPLEX SIG,T1,T2,DIV
      NN=MM-1
      DO 220 J=1,NN
      J1=J+1
      BIGA=CABS(A(J,J))
      SIG=(1.,0.)
      K=J
C
      DO 230 JMAG=J1,MM
      IF(CABS(A(JMAG,J))-BIGA) 230,230,225
  225 BIGA=CABS(A(JMAG,J))
      K=JMAG
      SIG=(-1.,0.)
  230 CONTINUE
C
      DO 240 N=J,MM
      T1=A(K,N)
      T2=A(J,N)
      A(J,N)=T1*SIG
      A(K,N)=T2
  240 CONTINUE
C
      DO 250 N=J1,MM
      DIV=A(N,J)
```

```
      DO 250 MULT=J,MM
  250 A(N,MULT)=A(N,MULT)-A(J,MULT)/A(J,J)*DIV
  220 CONTINUE
      VALDET = (1.,0.)
C
      DO 260 I=1,MM
      VALDET=VALDET*A(I,I)
  260 CONTINUE
      RETURN
      END
```

APPENDIX 2

LIST OF SYMBOLS

a_1, a_2 - distance from the mid-points of laminas to the centroidal axis of the left and right pier respectively

$a = a_1 + a_2$

$\tilde{a} = a_1 - a_2$

a_s - distance between the centroidal axes of the piers of a symmetric coupled shear wall

c - length of the connecting beam

$c^* = c + 2\delta$ equivalent length of the connecting beam

d_1, d_2 - width of the left and right pier respectively

$d_j^* = d_j - \delta$ $(j = 1,2)$ equivalent width of the pier j

$d_{av.} = \frac{1}{2}(d_1 + d_2)$

d_b - depth of the connecting beam

d_s - width of a pier of a symmetric coupled shear wall

h - storey height (spacing between centerlines of connecting beams)

$i^2 = -1$

m - bending moment distribution along the mid-points of laminas

$m_o = q_o \frac{c}{2}$

n - axial force distribution along the mid-points of laminas

$n_o = \frac{w}{2}$

q - shear force distribution along the mid-points of laminas.

$q_o = \frac{wH}{a_s} \frac{1}{\gamma_s} K_3'$ maximum unit shear induced when the symmetric coupled shear wall is subjected to uniform lateral load w

$n_1 = D_1^3 + D_2^3$

$n_2 = D_1^3 - D_2^3$

$n_3 = N^2 \bar{H} D_b^3$

$n_4 = 1 + 1.2 D_b^2 (\frac{E}{G})$

$n_5 = N^4 \bar{H}^3 D_b$

$n_6 = D_1 + D_2 + 2$

$n_7 = D_1 - D_2$

$n_8 = \frac{1}{D_1} + \frac{1}{D_2}$

$n_9 = \Omega_1^2 D_1^3 - \Omega_2^2 D_2^3$

$n_{10} = \Omega_1^2 D_1^3 - \Omega_2^2 D_2^3$

$r_b^2 = I_b / A_b$

t - time variable

t_w - thickness of the coupled shear wall

w_1, w_2 - lateral load distribution on the left and right pier respectively

$w = w_1 + w_2$

$\tilde{w} = w_1 - w_2$

x - coordinate along the height of the shear wall

y_1, y_2 - deflection of the left and right pier respectively

$z_1 = \frac{1}{2}(y_1 + y_2)$ antisymmetric mode of deflection

z_2 = $\frac{1}{2}(y_1 - y_2)$ symmetric mode of deflection

A_1, A_2 - cross-sectional area of the left and right pier respectively

A = $\frac{A_1 A_2}{A_1 + A_2}$

A_b - cross-sectional area of the connecting beam

A_b^* - effective cross-sectional area of the connecting beam to be considered for shear deformation

A_s - cross-sectional area of a pier of a symmetric coupled shear wall

D_j = $\frac{d_j}{c}$ $(j = 1,2)$ normalized width of the pier j.

D_b = $\frac{d_b}{c}$ normalized depth of the connecting beam

D_s = $\frac{d_s}{c}$ normalized width of a pier of a symmetric coupled shear wall

E - Young's modulus

G - shear modulus

H - height of the coupled shear wall

$\bar{H}$ - $\frac{h}{c}$ normalized storey height

I_1, I_2 - second moment of area of the left and right pier respectively

I - $I_1 + I_2$

$\tilde{I}$ - $I_1 - I_2$

$I_{av.}$ = $\frac{1}{2}(I_1 + I_2)$

I_b - second moment of area of the connecting beam

I_s - second moment of area of a pier of a symmetric coupled shear wall

K_3' - shear stress factor from Figure 4, Reference (9)

M_1, M_2 - bending moment due to external lateral loading on the left and right pier respectively

$M = M_1 + M_2$

$\tilde{M} = M_1 - M_2$

M_{E1}, M_{E2} - total bending moment of the left and right pier respectively

$M_o = \frac{1}{4}wH^2$

N - number of storeys

$\alpha^2 = \frac{12H^2 I_b}{hc^3\beta^2}$

$\bar{\alpha}^2 = \frac{6H^2 I_b a_s^2 \gamma_s}{hc^3\beta^2 I_s}$

$\beta^2 = 1 + \frac{12EI_b}{c^2 GA_b^*}$

$\gamma_j = 1 + \frac{I_j}{a_j aA} \qquad (j = 1,2)$

$\gamma_s = 1 + \frac{4I_s}{a_s^2 A_s}$

$\delta = \frac{1}{2}Kd_b$ correction applied to the length of the connecting beam to account for local wall deformations where the connecting beams join the piers.

δ_1 - relative displacement at the mid-points of laminas due to bending of the piers

δ_2 - relative displacement at the mid-points of laminas due to bending of the laminas

δ_3 - realtive displacement at the mid-points of laminas due to shear deformation of the laminas

δ_4 - relative displacement at the mid-points of laminas due to axial deformation of the piers

$\xi = \frac{x}{H}$ normalized spatial coordinate

ρ_1, ρ_2 - mass of the left and right pier respectively plus half the mass of the connecting beams, per unit height of the shear wall

$\rho = \rho_1 + \rho_2$

$\tilde{\rho} = \rho_1 - \rho_2$

ρ_s - mass of a pier of a symmetric coupled shear wall plus half the mass of the connecting beams, per unit height of the shear wall

$\mu^2 = \frac{2H^2 I_b}{hcI_s}$

ω - natural frequency of the coupled shear wall

ω_a, ω_s - natural frequency of an asymmetric and a substitutive symmetric shear wall respectively

$\omega_o = \frac{3.52}{H^2}\sqrt{\frac{EI_s}{\rho_s}}$ fundamental frequency of lateral vibration of a cantilever beam having the stiffness of a pier of a symmetric coupled shear wall and the mass equal to the mass of the pier plus half the mass of attached connecting beams

$\omega_{oj} = \frac{3.52}{H^2}\sqrt{\frac{EI_s}{\rho_j}}$ $(j = 1,2)$ fundamental frequency of lateral vibration of a cantilever beam having the stiffness of the pier j and the mass equal to the mass of the pier plus half the mass of attached connecting beams

θ - differential foundation rotation

Δ - differential foundation settlement

$\phi = \frac{\mu}{2}\sqrt{\frac{2H}{\mu r_b} + 1}$

$\chi = \frac{\mu}{2}\sqrt{\frac{2H}{\mu r_b} - 1}$

$\Omega_j = \frac{\omega}{\omega_{oj}}$ normalized natural frequency of the pier j

$\Omega_s = \frac{\omega}{\omega_o}$ normalized natural frequency of a pier of a symmetric coupled shear wall